Crees, Owen Lloyd (1988) ***The flocculation of cane sugar muds in Australian raw sugar factories*****. PhD thesis, James Cook University.**

THE FLOCCULATION OF CANE SUGAR MUDS IN AUSTRALIAN RAW SUGAR FACTORIES

A thesis submitted by
Owen Lloyd CREES, B. Sc. (Hons) (James Cook), M.Sc. (Bristol)
in August, 1988

as partial fulfillment for
the Degree of Doctor of Philosophy
in the Department of Chemistry and Biochemistry
at the James Cook University of North Queensland

I, the undersigned, the author of this thesis, understand that James Cook University of North Queensland will make it available for use within the University Library and, by microfilm or other photographic means, allow access to users in other approved libraries. All users consulting this thesis will have to sign the following statement:

> "In consulting this thesis I agree not to copy closely paraphrase it in whole or in part without the written consent of the author; and to make proper written acknowledgement for any assistance which I have gained from it."

Beyond this, I do not wish to place any restrictions on access to this thesis.

O.L. Crees.
20 September 1988

SUMMARY

The flocculation of cane muds in the factories of the Australian raw sugar industry has been investigated under factory operating conditions, in laboratory simulations of factory operations and with model particle systems.

The polymers employed as flocculants in Australian sugar mills are exclusively polyelectrolytes of the acrylamide/acrylic acid copolymer type. The effectiveness of a wide range of these polymers in flocculating muds has been found to depend primarily upon their molecular weights and on the relative amounts of the two comonomers. For a series of polymers of any given composition, the flocculating ability increases approximately linearly with molecular weight. No evidence has been found to indicate a limiting molecular weight although the practical problems associated with the large scale use of such large molecules increase as their size increases.

There was a very pronounced dependence on the copolymer composition, with a definite optimum composition for any given cane mud. The optimum composition was found to depend on the zeta potential of the mud particles, with a higher proportion of ionic monomer required as the zeta potential tended towards higher negative values.

It has been shown that the adsorption of the flocculating polymer occurs under conditions where both the polymer and the particle carry negative charges. Adsorption occurs through the acrylate functional group of the polymer, probably by the formation of a cation bridge with another carboxylic acid group at the particle surface. Adsorption is favoured in the presence of calcium ions which are the predominant multivalent ions in cane juice.

On the basis of the results presented here, a mechanism has been postulated for the flocculation of cane muds, consistent with the generally established principles of bridging flocculation but with some novel features. The optimum conditions for flocculation represent a compromise between the proportion of acrylate groups available for adsorption and the energy of adsorption of the individual ionic groups. When the product of these two parameters is less than the optimum value, polymer absorption is weak and reversible with the result that the aggregates formed are also weak and easily broken, even by the shear forces encountered during sedimentation. The settling rate is low and the supernatant turbidity high. When the product is higher than the optimum, adsorption is irreversible although some subsequent rearrangement of adsorbed molecules can occur. The growth rate of the aggregates is limited by the lack of mobility of the adsorbed polymer. The settling rate is low due to the smaller size of the aggregates but the supernatant turbidity remains low. The optimum value therefore represents the condition where adsorption is strong enough to resist the shear forces and to collect and hold all of the particles while still allowing the adsorbed polymer to retain its solution conformation and flexibility. The growth of the aggregates is not limited by either desorption or mobility of the polymer so the settling rate is maximized and the supernatant turbidity minimized.

Investigations of the solution properties and the monomer sequence distributions of commercial copolymers have shown that flocculation is favoured by a regular distribution of ionic groups along the chain. Random distributions, block copolymers and branching or crosslinking are all deleterious to flocculation.

A very important consequence of this research, and one of its main aims, has been its rapid and successful application to the industrial environment of all Australian sugar mills. Through this application and the cooperation of several of the world's major manufacturers of polyacrylamide flocculants, the industry has been able to effect substantial improvements in process operations and in product quality.

DECLARATION

I declare that this thesis is my own work and that it has not been submitted in any form for another degree or diploma at any University or other Institute or Tertiary Education. Information derived from the work of others, whether published or unpublished, has been duly acknowledged in the text and a list of references is given.

O.L. Crees.
20 September 1988

ACKNOWLEDGEMENTS

It is my pleasure to thank my supervisor, Dr. E. Senogles for his continued support, advice and encouragement throughout this work. I am grateful also to the staff of the Department of Chemistry and Biochemistry of James Cook University for making available their NMR facilities and for their assistance in obtaining spectra.

I wish to record my thanks to the Board of Directors of Sugar Research Limited for their support of this project; to the staff of the Institute, particularly Dr. E. Whayman for many hours of stimulating discussions and advice, and Mr. A.L. Willersdorf for his willing technical assistance.

Much of this work was carried out in sugar mills throughout Australia and I thank them all for their cooperation. I acknowledge also the cooperation received from Allied Colloids Ltd., Cyanamid Australia Pty. Ltd., The Dow Chemical Company, Catoleum Pty. Ltd., who willingly supplied many samples of special polymers in addition to their normal commercial products.

Most importantly, I wish to acknowledge the great contributions made by my wife, Sue, and my children, Rachel and Peter, for whom this has been a long and trying project. Their patience and understanding, support and encouragement over many years is greatly appreciated.

CONTENTS

ERRATA

Following comments made by the external examiners, the following minor alterations should be made:

p.26: In equation 1.20, change "-" to " + ".

p.26, l.13: after "acrylate" add "(with η in dL/g)".

p.27: In equation 1.26, change "η" to "n".

p.28, l.22: should read " > 200 nm".

p.50, l.17: "ϒ/20" should read "λ/20".

p.67, l.2: Change "electrophonetic" to "electrophoretic".

p.79, l.19: Delete "as" at beginning of line.

p.90, l.34: Change "Heidi" to "Hidi".

p.90, l.6: Change "Heidi" to "Hidi".

p.107, l.7: Change "extention" to "extension".

p.140, Table 4.1: Change r1 for sodium acrylate from 0.35 to 1.10.

p.140, l.10: Insert "instantaneous" before "copolymer composition".

p.151, Figure 4.9: Change units of pore size to μm.

p.159, l.14: Change "alternativem" to "alternative".

p.188, l.9: Change "discreet" to "discrete".

p.193, l.29: Delete "and".

p.209, l.1: Change "Bysterbosch" to "Bijsterbosch".

p.214, l.20: Delete "Ed.".

LIST OF FIGURES

LIST OF TABLES

CHAPTER 1

The use of high molecular weight synthetic polymers as flocculants to enhance solid/liquid separations is now common practice in a great many chemical process industries. In the Australian raw sugar industry their importance is such that all factories are now completely dependent on the continuous, controlled addition of low doses of carefully selected polymers. The progress made in recent years in the commercial production of high molecular weight polymers and the parallel development of specialized process equipment has resulted in substantial savings in operating and capital costs, as well as reductions in sucrose losses during processing. However, whilst the literature abounds with references to innumerable applications, much of the work is commercially oriented and therefore provides only limited data, particularly with regard to the properties of the polymers used. There is a singular lack of reported systematic investigations of the effects of specific polymer properties on the flocculation reaction, although their importance is widely recognised. This thesis therefore addresses directly the intimate relationship between the properties of a select group of synthetic polymers and the chemical and electrokinetic properties of sugar cane muds, as well as their mutual interactions under both laboratory and factory conditions.

1.1 THE EFFECT OF POLYMERS ON THE STABILITY OF CHARGE STABILIZED COLLOIDS.

Many polymers adsorb readily onto colloidal particles and can profoundly affect the interaction between particles. Colloid stability may be either increased or decreased, depending on the type and amount of polymer present.

1.1.1 STABILIZATION BY ADSORBED POLYMERS

The stabilization or protection of colloidal particles by polymer adsorption can be achieved by increasing the electrostatic repulsion between particles, by decreasing the van der

Waals' attraction or by introducing a steric component of repulsion. Electrical effects are usually observed when the adsorbing polymer is ionized. If it carries an opposite charge to the particles, electrical repulsion is decreased and stability is reduced. When the polymer and particles have like charges, repulsion is increased and the particles are stabilized. Both of these effects can be readily explained by the DLVO theory[1]. Non-ionic polymers can also increase electrostatic repulsion between particles by displacing counter-ions from the Stern layer, causing the diffuse layer to extend further from the particle surface[2].

The effect of adsorbed layers on van der Waals' forces has been discussed by Vold[3], using the simple Hamaker approach. If the centre-to-centre distance of the particles is held constant, then the effect of the adsorbed layer is almost always to increase the attraction since it effectively increases the size of the particles. Similar conclusions were reached by Langbein[4] using the more exact Lifshitz theory.

The concept of steric stabilization has been widely used to explain the many cases of protection which cannot be adequately explained by either of the above mechanisms. Napper[5] has shown that when the adsorbed layers interpenetrate, the concentration of polymer segments between the particles increases. If the dispersion medium is a good solvent for the adsorbed polymer, mixing of segments is not favoured. The interpenetration thus leads to an increase in free energy and hence a repulsive force between the surfaces.

1.1.2 DESTABILIZATION OF CHARGED PARTICLES BY ADSORBED POLYMERS

The decrease in colloid stability due to the adsorption of polymers is often referred to as 'sensitization'. When very high molecular weight polymers form bridges between particles and promote the formation of large aggregates, the effect is referred to as 'flocculation' or 'bridging flocculation' and the polymers are called 'flocculants'. Some authors use the terms 'flocculant' and 'flocculation' in a more general sense to include other destabilizing agents such as surface active agents and inorganic coagulants. However, in this thesis, 'flocculation' will refer specifically to destabilization by high molecular weight polymers.

The earliest examples of polymeric flocculants were natural polymers such as starches and alginates and these are still used in some applications. Generally, though, they have been superceded by a wide range of synthetic polymers. Depending on the particular application, good flocculants may be anionic, cationic or non-ionic. They are, however, almost always linear polymers of very high molecular weight. Table 1.1 lists some common examples.

By far the most common and most successful flocculants are the polyacrylamides and their derivatives. Non-ionic polyacrylamide can be readily prepared in aqueous or organic solvents by direct polymerization of acrylamide monomer to give molecular weights in excess of 10^7. Anionic and cationic derivatives can be prepared either by subsequent reaction of the homopolymer or by direct copolymerization of acrylamide with a range of other monomers.

Anionic character can be incorporated by partial or complete alkaline hydrolysis of amide groups:

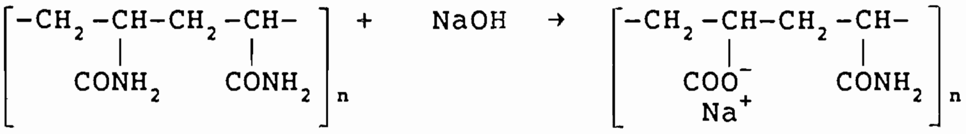

$$\left[-\mathrm{CH_2}-\underset{\mathrm{CONH_2}}{\underset{|}{\mathrm{CH}}}-\mathrm{CH_2}-\underset{\mathrm{CONH_2}}{\underset{|}{\mathrm{CH}}}-\right]_n + \mathrm{NaOH} \rightarrow \left[-\mathrm{CH_2}-\underset{\substack{\mathrm{COO^-}\\ \mathrm{Na^+}}}{\underset{|}{\mathrm{CH}}}-\mathrm{CH_2}-\underset{\mathrm{CONH_2}}{\underset{|}{\mathrm{CH}}}-\right]_n$$

More commonly, acrylamide is copolymerized with various amounts of acrylic acid or its sodium salt. Either way, the relative proportions of ionic and non-ionic monomer can be readily controlled.

ANIONIC	CATIONIC	NON-IONIC
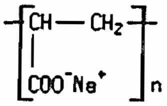 $\left[\begin{matrix}CH - CH_2\\ \vert \\ COO^-Na^+\end{matrix}\right]_n$ Sodium polyacrylate	$\left[CH_2 - CH_2 - {}^{+}NH_2\right]_n$ Polyethyleneimine	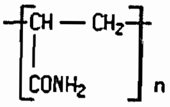 $\left[\begin{matrix}CH - CH_2\\ \vert \\ CONH_2\end{matrix}\right]_n$ Polyacrylamide
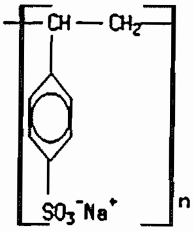 Sodium polystyrenesulphonate	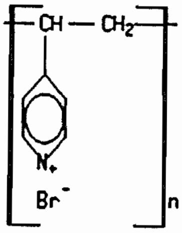 Polyvinylpyridinium bromide	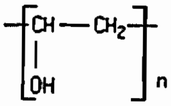 $\left[\begin{matrix}CH - CH_2\\ \vert \\ OH\end{matrix}\right]_n$ Polyvinylalcohol
		$\left[CH_2 - CH_2 - O\right]_n$ Polyethyleneoxide

Table 1.1 Examples of Common Polymeric Flocculants.

Cationic flocculants can also be prepared from polyacrylamide but the procedure is more difficult and generally results in molecular weights considerably below those of the anionic polymers. Although they can be prepared by reactions with the homopolymer, cationic polyacrylamides are usually prepared commercially by copolymerization of acrylamide with a suitable comonomer. Examples of all three groups of polyacrylamides are given in Table 1.1.

1.2 BRIDGING FLOCCULATION

Ruehrwein and Ward[6] first proposed the concept of bridging by adsorbed polymer chains in 1952 when they recognised that the solution dimensions of flocculant molecules may be similar to those of colloidal particles. A polymer molecule could therefore be adsorbed by a number of particles simultaneously.

La Mer[7] and his co-workers[9] carried out extensive studies on flocculation by both natural and synthetic polymers and attempted to develop a quantitative theory of bridging flocculation. The basic concept of the theory was that there exists an optimum in the fractional coverage (θ) of the particle surface by polymer. If bridging requires free segments of an adsorbed polymer to be adsorbed at vacant sites on other particles, then the effect should be greatest when the product $\theta(1-\theta)$ reaches a maximum. Clearly this must occur at the half coverage condition, i.e. $\theta = 0.5$. Although the precise definition of surface coverage is difficult when the adsorbed species is polymeric, it is nonetheless clear that an understanding of polymer adsorption phenomena is essential to any study of bridging flocculation. Adsorption must be strong enough to be irreversible whilst still allowing a high proportion of segments to remain in loops and tails. It is therefore often assumed that adsorption is complete and that there is no free polymer left in solution. However, much of the experimental support for this is based on equilibrium adsorption isotherms. Adsorption during bridging flocculation usually occurs too rapidly to reach or even approach a stable equilibrium state, so the equilibrium isotherms may be of little relevance.

If charged particles are to be bridged by adsorbed polymers, the dimensions of the latter must be greater than the effective range of the double layer repulsion. For charged particles in electrolyte solutions, the distance of closest approach, d, can be assumed to be of the order of $2/\kappa$, where κ is the Debye-Huckel reciprocal length parameter. Since this is the interparticle separation at which substantial overlap of the diffuse layers occurs, the dimensions of the adsorbed polymer must be at least of the same order. This concept is illustrated in Figure 1.1 where the dotted lines represent the extent of the diffuse double layers. It is supported by work by Fleer[8] on the flocculation of silver iodide sols by non-ionic polyvinyl alcohol, and by Vincent[2].

1.2.1 POLYMER AND PARTICLES WITH OPPOSITE CHARGE

Polyelectrolytes interact very strongly with particles of opposite charge and are quantitatively adsorbed, at least up to the point of charge neutralization. Destabilization may therefore be by charge neutralization, as with simple electrolytes, by bridging flocculation or by some combination of the two, although it is sometimes difficult to establish the relative importance of each mechanism. Furthermore, destabilization usually occurs at relatively low concentrations of polymer. The addition of more polymer can lead to re-stabilization as a result of charge reversal or steric effects. Because of the strong electrostatic interactions, adsorbed polymers tend to adopt relatively flat configurations which are not conducive to bridging.

The relative importance of charge neutralization and bridging can be assessed experimentally by comparing the electrokinetic properties of the particles with the stabilization/destabilization behaviour. The electrophoretic mobilities or zeta potentials at which flocculation and restabilization occur, can be compared with values predicted by the DLVO theory. If charge neutralization is the dominant effect, flocculation occurs only when the zeta potential is low

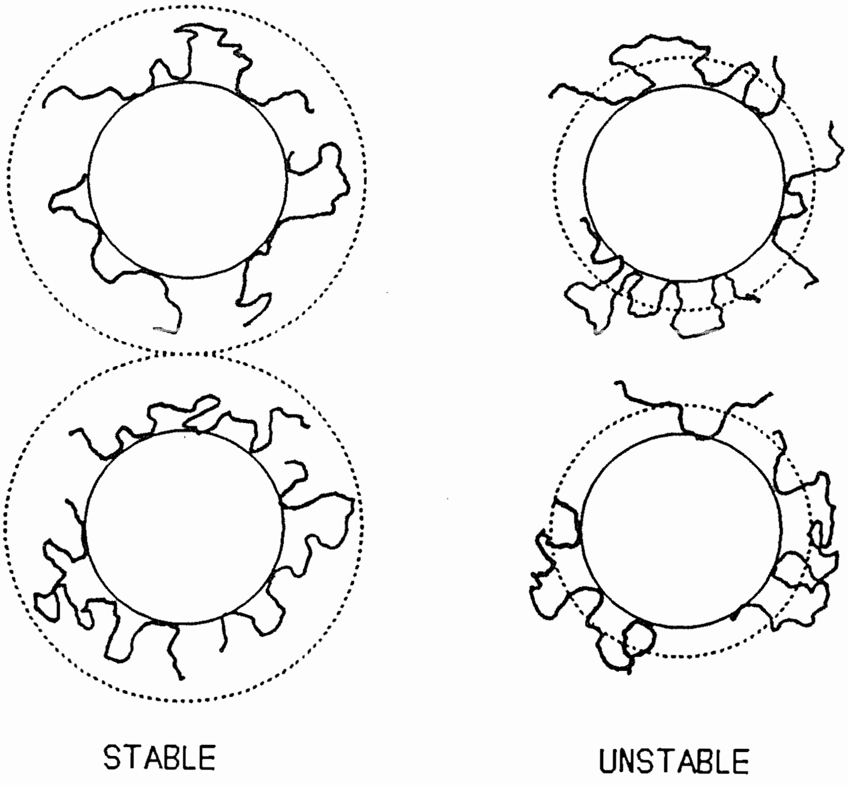

Figure 1.1 Effect of Double Layer Thickness on Bridging.

enough to effectively eliminate the electrostatic repulsion between particles. The onset of flocculation at high zeta potentials indicates bridging through the repulsion barrier as described above.

Work by La Mer et al.[9] on the flocculation of silica dispersions with low molecular weight polyethyleneimines (<35 000) showed a good correlation between the concentration of polymer producing maximum flocculation and that required to reduce the zeta potential to zero. As molecular weight increases, however, maximum flocculation occurs at concentrations well below that required to achieve zero zeta potential.[10] Increasing molecular weights also lead to increases in the rate of flocculation and extension of the zeta potential range over which flocculation occurs. Thus charge neutralization is the dominant effect with low molecular weight polymers, with the bridging mechanism assuming increasing importance as the molecular weight increases. Williams and Ottewill[99] found that, for the flocculation of positively charged silver iodide dispersions with poly(acrylic acid), there was an optimum polymer concentration, C*, which was related to the viscosity average molecular weight, $\bar{M}_v$, by an empirical equation of the form:

$$C^* = a.\bar{M}_v^{-b} \qquad (1.1)$$

where a, b are constants.

In contrast, Gregory[11] found little effect of molecular weight on either the optimum concentration or the rate of flocculation in studies of polystyrene latices with polyethyleneimine. He also found that increasing the electrolyte concentration broadened the polymer concentration range in which flocculation occurred but decreased the rate. Gregory has explained this effect in terms of an 'electrostatic mosaic' model in which there are regions of bare surface with a negative charge and regions of excess positive charge where polymer is adsorbed. There would thus be an additional electrostatic attraction between particles which may cause collisions to occur faster than predicted by Smoluchowski theory. Increasing the ionic strength would decrease the attractive force and the rate enhancement would be reduced.

Black[12] has reported that the optimum polymer concentration was inversely proportional to particle size in the flocculation of polystyrene latices up to 3.49 μm with cationic polyelectrolytes. Iler[13] found similar results for particles below 40 nm but for larger particles, the optimum concentration varied inversely with the square of the diameter. He suggested that one polymer molecule may be attached to several small particles whereas larger particles may require several molecules to bridge between a pair. Iler also reported that, below the optimum polymer concentrations, only large aggregates of roughly similar dimensions and single particles with no adsorbed polymer were present. No free polymer existed in solution. As the polymer concentration increased, the number of single particles decreased and eventually reached zero at the optimum polymer concentration. Increasing the concentration further led to saturation of the particle surface and the appearance of free polymer in solution.

1.2.2 POLYMER AND PARTICLES WITH LIKE CHARGES

Many of the earlier systems in which bridging flocculation was found to occur fall into this category[14], as do many of the applications in modern chemical processing industries. The role of added salts is rather more difficult to interpret as various combinations of three principal effects may be possible.

With any flocculant, whether ionic or not, added electrolyte may enhance bridging flocculation simply by increasing the ionic strength of the dispersion medium and reducing the range of the electrostatic repulsive forces. Eventually, the distance of closest approach becomes less than the dimensions of an adsorbed polymer molecule and bridging can occur. Simultaneously, the increased ionic strength may also cause the polymer chain to become less extended by screening its charges and reducing the repulsion between them. This effect tends to hinder bridging by reducing the size of the flocculant molecules. In addition to these effects, added electrolyte may enhance adsorption of polyelectrolytes on surfaces of like charge.

The role played by various simple ions in flocculation has been investigated by a number of workers. In the flocculation of negative silver bromide particles by anionic polyelectrolytes, Sommerauer et al.[15] concluded that polymer adsorption involved the formation of a complex between counter-ions and the ionic groups of the polyelectrolyte, either carboxylate or sulphate. The fact that divalent ions are much more effective than monovalent ions supports this concept. Miller and Grahame[16] showed similar effects of the importance of anions in the adsorption of cationic polyelectrolytes onto positively charged mercury surfaces. Nemeth and Matijevic[14] argued that the destabilization observed by Sommerauer was due to a reduction in surface charge due to adsorbed polymer although work by Vincent[17] has suggested that this is unlikely.

The effect of multivalent cations on the flocculation of polystyrene latices by sodium polystyrene sulphonate has been studied by Sarkar and Teot[18]. They suggested that the flocculant is actually a neutral complex of the cation and the polyelectrolyte and that a minimum excess cation concentration is needed before flocculation can occur. They also suggested that bridging was not the dominant mechanism. With lanthanum, which formed an insoluble complex with the polymer, heterocoagulation occurred between the latex particles and the insoluble lanthanum/ polyelectrolyte complex. However, the complexes with divalent cations were soluble and there seems little doubt that bridging occurred.

Slater et al.[19] have suggested that there may be no specific effects. Rather, the electrolyte serves simply to screen the electrostatic repulsion between the particle surface and the polymer. They showed that the adsorption of 30 per cent hydrolysed polyacrylamide onto freshly dispersed quartz in water could be activated over a narrow range of pH and Cu^{2+} concentration. Copper ions may form complexes with the carboxylate groups of the flocculant and may also ion exchange with the quartz surface. No such activation occurred with aged quartz even though copper ions are still adsorbed by the particles. In this case, adsorption is probably due to hydrogen bonding between hydroxyl groups at the quartz surface and the polyelectrolyte. The effect of the Cu^{2+} is purely one of charge screening.

Michaels[20] considered the effects of charge density and molecular weight in the action of polyacrylamide flocculants on various silts and clays. Using polymers whose charge density was controlled by hydrolysis, he found that high molecular weight was essential and that there was an optimum charge density for maximum effectiveness. Best results were obtained at 30 per cent hydrolysis. The effect was explained by suggesting that the increased charge density caused the polymer to expand and become a more effective bridge but also tended to reduce the tendency to adsorb on the negatively charged surface, so the optimum hydrolysis represented a compromise between the two effects.

Somasundaran <u>et al</u>.[56] have also investigated the effect of polymer charge density on the flocculation of kaolinite with anionic polyacrylamides. They found that increasing the charge density decreased the flocculating ability of the polymer and suggested the retardation was due to the increased electrostatic repulsion between the polymer and the particle. However a number of other workers (28,57,58) have reported results similar to Michaels and it seems unlikely that all of these observations could have been similarly influenced by variations in water chemistry, as Somasundaran has suggested.

Despite the importance of charge density on flocculation in many industrial processes, it has received scant attention in the literature.

1.3 FLOCCULATION KINETICS

The Smoluchowski[21] theory of rapid coagulation neglected long-range particle interactions and considered that aggregation was purely a diffusion controlled process. His theory has since been modified by Fuchs[22] to accommodate particle interactions and by Spielman[23] and Honig[24] to allow for reductions in the diffusion coefficients of particles as they approach neighbouring particles.

All these theories predict second order kinetics for the rates of disappearance of both primary particles and all particles:

$$\frac{d\ N_1}{dt} = -k\ N_1^{\ 2} \tag{1.2}$$

and

$$\frac{d\ \Sigma\ N_1}{dt} = -k'(\Sigma_i\ N_i)^2 \tag{1.3}$$

where N_1 = number of primary particles,

$\Sigma_i\ N_i$ = total number of particles, and

$k,\ k'$ = rate constants.

The applicability of Smoluchowski's theory to the aggregation of particles by simple coagulation has been demonstrated directly by particle counting methods[25] and indirectly by light scattering[25] and turbidity techniques[26].

When bridging flocculation, rather than coagulation, occurs, equations (1.2) and (1.3) no longer apply. In experiments where particles with adsorbed polymer were mixed with bare particles, Fleer[8] found that equation (1.2) could be modified to the form:

$$\frac{d\ N_1}{dt} = -2\ \phi\ (1 - \phi)\ k\ N_1^{\ 2} \tag{1.4}$$

where ϕ = fraction of particles with adsorbed polymer.

Since only collisions between bare particles and covered particles should be successful, the rate of flocculation should be a maximum at $\phi = 0.5$. Walles[27] considered that, for systems of this type, the ratio of the rate of collisions between bare and covered particles, Z, to the rate of collisions between bare particles, Z_o, increased with increasing adsorbed layer thickness:

$$\frac{Z}{Z_o} = \frac{(2 + \delta/a)^2 (1.6c^{-1/3} - 2)^4}{4(1.6c^{-1/3} - 2-\delta/a)^4} \qquad (1.5)$$

where δ = adsorbed layer thickness,
a = particle radius, and
c = particle concentration.

Where polymer adsorption and flocculation are initiated in a single step, the kinetics are much more difficult to analyse. Smellie[28] and Healy and La Mer[29] used an equation similar to (1.3) for the limiting case where polymer adsorption reaches a steady state very rapidly compared to the rate of particle collision:

$$\frac{d\, N_1}{dt} = -\theta(1 - \theta)\, k\, N_1^{\,2} \qquad (1.6)$$

where θ = fraction of surface covered by polymer. The maximum rate of flocculation should therefore occur at $\theta = 0.5$.

Somasundaran _et al._[56] have investigated the adsorption of polyacrylamides by kaolinite in simultaneous adsorption/flocculation tests. They found that flocculation exhibited a maximum response with respect to surface coverage and estimated the maximum to be at a coverage of 0.1 to 0.2. However, in estimating the coverage, they assumed that saturation adsorption corresponded to monolayer coverage and that the configuration of the adsorbed molecules remained unchanged as coverage increased. In practice, neither of these assumptions is valid.

The rate of adsorption of polymer molecules may also have an enormous influence on the kinetics of flocculation. At the moment of addition of polymer to a dispersion, several rate processes occur:

(i) mixing of polymer among the particles
(ii) polymer adsorption
(iii) rearrangement of adsorbed polymer chains
(iv) collisions between particles

Gregory[30] has considered the case where the added polymer is instantly distributed uniformly through the suspension. Although an ideal case, perfect mixing can be closely approached in practice with proper techniques. The relative rates of the remaining three processes will then control the flocculation reaction.

Gregory treated the adsorption of polymer molecules as a case of heteroflocculation. Assuming that every collision between polymer and particles results in adsorption, the rate of adsorption is given by the equation:

$$\frac{d\,N_2}{dt} = -k_A\,N_1\,N_2 \qquad (1.7)$$

where N_1 = number of particles,
N_2 = number of polymer molecules, and
k_A = collision rate constant.

Integrating equation (1.7) at constant particle concentration gives:

$$\ln\left(\frac{N_2^{\circ}}{N_2}\right) = k_A\,N_1^{\circ}\,t \qquad (1.8)$$

where N_1°, N_2° = initial number of particles and polymer molecules respectively,

N_2 = number of unadsorbed polymer molecules,

t = time.

If it is then assumed that a certain fraction, x, of the added polymer must adsorb before bridging can occur, the time required for bridging to commence, t_A, can be determined from equation (1.8):

$$t_A = \frac{-\ln(1 - x)}{k_A N_1^\circ} \qquad (1.9)$$

The characteristic flocculation time, t_f, which is the average interval between collisions is:

$$t_f = \frac{1}{k_f N_1^\circ} \qquad (1.10)$$

where k_f = flocculation rate constant.

The ratio between these times is:

$$\frac{t_A}{t_f} = -\ln(1 - x) \frac{k_f}{k_A} \qquad (1.11)$$

If the particles and polymer molecules are considered to be spheres of radii a_1 and a_2 respectively, the rate constants can be calculated from Smoluchowski theory:

$$k_f = - 4 \pi D a_1 \qquad (1.12)$$

and

$$k_A = - 4 \pi D a_1 (a_1 + a_2)(\frac{1}{a_1} + \frac{1}{a_2}) \qquad (1.13)$$

where D = diffusion coefficient of particles.

Thus, equation (1.11) becomes:

$$\frac{t_A}{t_f} = \frac{-4\, a_1\, a_2\, \ln(1 - x)}{(a_1 + a_2)^2} \qquad (1.14)$$

For particles and polymer molecules of equal size and x = 0.5, t_A/t_f is approximately 0.7. If the values of a_1 and a_2 are very different, Smoluchowski's theory predicts that the adsorption step would become faster. Nonetheless, adsorption may well be slow enough to significantly affect the flocculation process. In practice, there is often an appreciable delay between polymer addition and the onset of flocculation, particularly in dilute systems.

There is very little information available on the kinetics of rearrangement of adsorbed polymers. Clayfield and Lumb[31] used an entropic repulsion model in a computer simulation of the stabilising action of random copolymers containing polar and non-polar groups, with adsorption occurring at the polar groups. Their results showed that the behaviour of adsorbed molecules was influenced by surface coverage, the frequency of polar groups in the polymer, and the energy of adsorption of each polar group. Molecules which adsorbed flat on the surface did not do so immediately. They exhibited an induction period during which their dimensions fluctuated for some time before suddenly collapsing onto the surface. Chains which adsorbed flat at low surface coverage could be prevented from collapsing by increasing the surface coverage. At high coverage, the adsorbed molecules retained an average size approximating to their original solution dimensions.

Whilst flat adsorption and/or high surface coverage may be desirable for dispersant action, neither condition is appropriate for bridging flocculation. Non-flattening molecules tended to rapidly achieve a metastable state in which no further fluctuations in size occurred, although they retained a high degree of surface mobility. Whereas in flat adsorption, nearly all polar groups were bound to the surface, only about one third were bound in the non-flattening case. Fontana and Thomas[32] previously had assumed that the bound fraction of one-third necessarily denoted a flat configuration. However Clayfield and Lumb suggested it was compatible with an adsorbed film having a thickness comparable with the solution dimensions of the chain. Furthermore, the smaller the proportion of polar groups in a chain and the lower the energy of adsorption of individual polar groups, the smaller the tendency of the chain to collapse flat onto the surface but the greater its tendency to desorb. A clearer picture of the relationship between adsorption behaviour and molecular structure was obtained by considering the product of the fractional frequency of polar groups (f) and the adsorption energy per polar group (q) as a measure of the strength of adsorption of the polymer molecule as a whole. This can be seen from Figure 1.2, which shows the effect of the product f.q on the fractions of polymer molecules which desorb or which collapse onto the surface. It is clear that there is only a very narrow range of (f.q) where the adsorbed molecule does not collapse but retains its solution dimensions and remains mobile on the particle surface without excessive desorption.

It seems reasonable to suggest that bridging is more likely to occur when the adsorbed polymer is in an extended, non-equilibrium state rather than in a flatter, equilibrium configuration. Not only would the chain extend further from the surface but there should also be more unoccupied surface available to adsorb other molecules. Particle collisions would need to occur rapidly enough to take advantage of the opportunity presented by the extended polymer chains and this should be entirely a function of particle concentration. At low concentrations, collisions are infrequent and there may be sufficient time for the adsorbed polymer to approach its equilibrium conformation before many collisions have occurred. In many practical applications, this 'non-equilibrium' flocculation is probably common.

In addition to the above effect, the influence of adsorbed polymer on the collision radius of particles must be considered. Walles[27] examined the effect of increasing the collision radius by adsorbing thick layers of polymer and showed the particle concentration and adsorbed layer thickness were the most

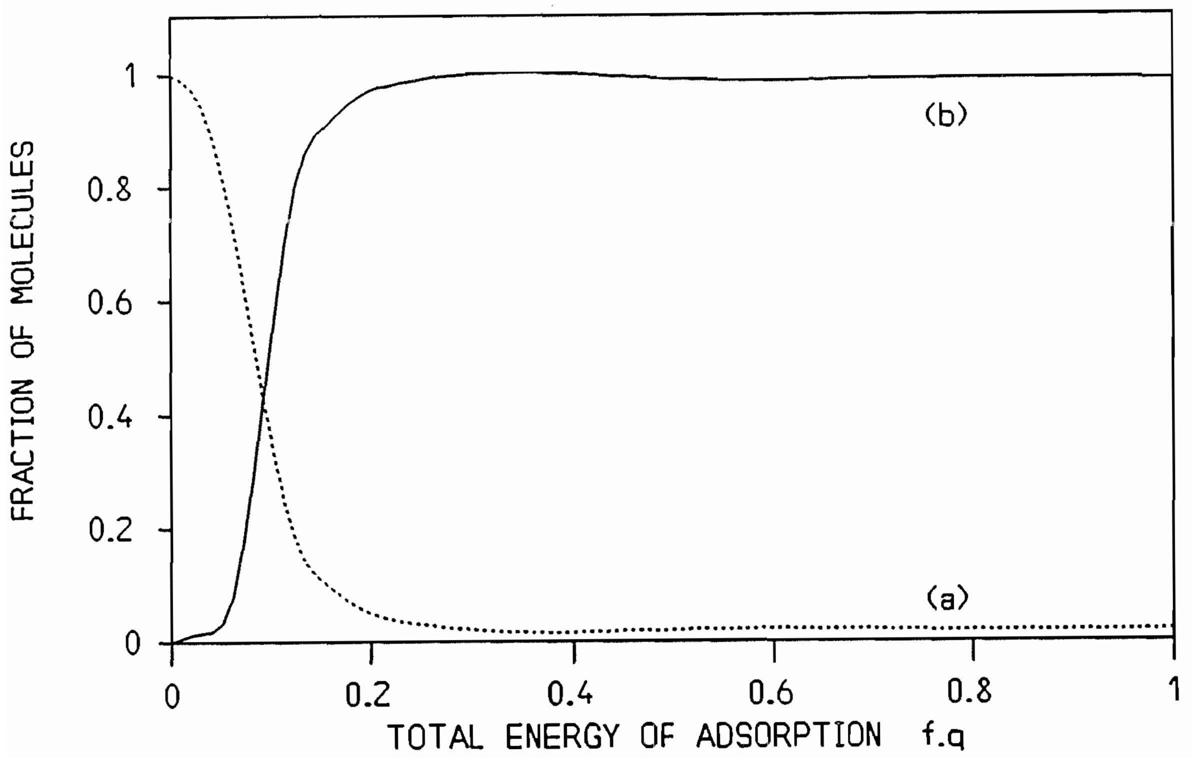

Figure 1.2 Effect of Total Energy of Adsorption on Adsorption of Copolymers[31].

(a) fraction of adsorbed molecules desorbing

(b) fraction of adsorbed molecules collapsing onto particle surface important parameters. His calculations indicated that the collision rate could be markedly enhanced with thick layers and high concentrations.

1.4 POLYMER ADSORPTION

Polymer adsorption is obviously the key to performance of polymers as stabilizers and flocculants. There has been a considerable amount of work, both theoretical and experimental, in this field in recent years. However, much of the work has been directed towards stabilizing action and it is doubtful whether much is relevant to the phenomenon of bridging flocculation.

1.4.1 THEORETICAL ASPECTS

Two principal approaches have been used in the theoretical study of polymer adsorption. Frisch, Simha and Eirich[33] used a random walk approach to determine the changes in conformation which occurred when a Gaussian coil was placed in contact with a reflecting wall. They then calculated the thermodynamic properties of the adsorbed layer and deduced an adsorption isotherm. Similar methods have been used by other workers[36,37] but Silberberg[38] and Dimarzio[39] claimed that the number of distinguishable conformations was overcounted. Dimarzio[39] and Clayfield[31] have used Monte Carlo methods to overcome the problem.

Silberberg[38] used the concept of two energy states for a polymer segment at an interface, with 'trains' of segments lying in the layer immediately adjacent to the interface and 'loops' of segments extending into the bulk solution. By calculating the most probable conformation of the molecule at the interface, he was able to establish a partition function for the system and so calculate the necessary thermodynamic functions. Silberberg originally assumed that the loop size was uniform for a given molecule but others have extended the approach to include loop size distributions[40].

Most of the early work was restricted to isolated molecules at an interface (low coverage) but the theory has been extended to account for high coverage[41], multilayer adsorption[42] and adsorption of polyelectrolytes[43]. There is, however, no satisfactory theory of the kinetics of polymer adsorption.

The principal aim of most theories has been to predict how parameters such as the adsorbed mass per unit area (Γ), the fraction of segments in trains (p) and the adsorbed layer thickness (w) depend on the various properties of the system. They generally refer to the equilibrium adsorption isotherms for homopolymers and thus, as described previously, frequently are not directly relevant to bridging flocculation. The inability to predict kinetics adds a further restriction.

Most theories agree that, as the polymer concentration increases, Γ should initially rise sharply then level off although it may not actually reach a plateau. At the same time, p should decrease while w should increase. Both Γ and w should increase as polymer molecular weight (M) increases. Various relationships have been predicted, e.g.

$$\left[\frac{d\Gamma}{d\,C_2}\right]_{C_2 \to 0} \propto M \qquad (1.15)$$

$$\log\left[\frac{d\Gamma}{d\,C_2}\right]_{C_2 \to 0} \propto M \qquad (1.16)$$

and, for θ-solvents,

$$\Gamma \propto M^{1/2} \qquad (1.17)$$

Both Γ and p should increase as the flexibility of the polymer molecule increases, suggesting that w should decrease. However there are other variables which, though difficult to accommodate in theoretical analyses, are likely to have profound effects. These include branching, tacticity and, for copolymers, monomer sequence distribution.

The main influence of the adsorbent is in the difference in adsorption energy (E) between solvent molecules and polymer segments. Of course, p must depend strongly on E and it might be expected that, as E increases, Γ should also increase. However, at higher E, the adsorbed molecule will tend to adopt a flatter configuration so there may well be a maximum in Γ. It is presently suggested[36,37,41] that there is a critical value of E below which no adsorption occurs. Above this limit, p initially rises sharply and levels off at higher values of E.

1.4.2 EXPERIMENTAL STUDIES

In principle, polymer adsorption isotherms and kinetics should be readily determined. However there are two major experimental problems. Firstly, the time required to reach equilibrium may be considerable, sometimes as much as several days[51]. Secondly, except in the plateau region where the polymer concentration is relatively high, there are frequently practical problems associated with quantitative, or even qualitative, measurements of trace amounts of polymer in bulk solutions. Furthermore, deductions about the state of the adsorbed layer made solely from adsorption isotherms may be both difficult and misleading. Additional information can be obtained by a number of means. Hydrodynamic techniques such as viscometry, ultra-centrifugation, electrophoresis and light scattering techniques have all been used to measure adsorbed layer thicknesses. Although the hydrodynamic thickness is usually less than the total thickness, it can be argued that the hydrodynamic thickness is actually a better approximation of the real condition. Microcalorimetry has been used to measure adsorption energies and, in non-aqueous systems, infrared spectroscopy has been employed to estimate p.

In general experimental observations agree, at least broadly, with the theoretical predictions in the plateau region. Most workers have used polymers of relatively low molecular weight ($<10^6$) by comparison with modern bridging flocculants. However, some results are of particular interest.

The adsorbed mass (Γ) generally increases as polymer molecular weight increases, reaching a plateau at high molecular weights[44] although the dependence is strongly influenced by solvent effects. In good solvents, molecular weight has little effect[45] on Γ, which agrees with the theoretical predictions. There is a similar dependence of w on molecular weight[46]. In many cases, the value of w in the plateau region is similar to the dimensions of the free polymer molecule in bulk solution[47]. However p appears to be largely independent of molecular weight.

The influence of polymer properties such as tacticity, flexibility and monomer sequence distribution in copolymers has received little attention. Fleer[49] reported that increasing the proportion of vinyl acetate groups in samples of poly (vinyl alcohol) led to stronger adsorption onto silver iodide and paraffin surfaces. This is expected since vinyl acetate groups are more strongly adsorbed than alcohol groups. Howard et al.[50] examined the adsorption of styrene/methyl methacrylate copolymers from benzene onto silica surfaces. They found that Γ in the plateau region was constant up to 90 per cent styrene but fell sharply at higher styrene contents. ABA block copolymers (where A represents methyl methacrylate and B, styrene) were more strongly adsorbed than random copolymers. For both random and block copolymers, p for all groups remained constant at about 0.25 up to high styrene levels although up to 50 per cent styrene, the fraction of bound methyl methacrylate groups increased since they are more strongly adsorbed. However, Howard[52] also found that, for the adsorption of propylene oxide-ethylene oxide copolymers on charcoal, there was no difference between block and random copolymers, at least up to molecular weights of 11,300.

1.5 POLYMER ADSORPTION AND THE DLVO THEORY

The essence of the DLVO theory is that the stability of lyophobic colloids can be described in terms of the contributions of repulsive and attractive forces between particles. The presence of an adsorbed polymer layer may alter the structure of the electrical double layer and thus also affect the electrical repulsion. The long range Van der Waals' attraction may also be affected. In addition, the adsorbed layer may produce other forces of attraction and repulsion.

The effects of adsorbed layers on the energy of attraction between particles has been analysed by Vold[3] and Vincent[53] using the Hamaker approach. Ninham and Parsegian[54] have used the Lifschitz continuum approach. The analysis is complicated by the fact that the adsorbed layer will be a composite layer containing polymer segments and solvent molecules. Furthermore, the segment density will not be uniform throughout the layer. Some density distribution must be assumed and the results are often vastly different from those obtained with an homogeneous distribution.

The adsorption of a neutral homopolymer may alter the structure of the electrical double layer in a number of ways, not all of which are independent. It may alter the surface charge by changing the ionization state of surface groups or by the adsorption of potential determining ions. Specifically adsorbed counter-ions and oriented water dipoles may be displaced. The dielectric constant and the thicknesses of both the inner and outer double layers may also change. Vincent[55] has examined some of these effects and shown that, for negative silver iodide particles, strong displacement of specifically adsorbed ions can lead to an increase in the potential at the outer Helmholtz plane. At constant surface charge, the displacement of water dipoles should tend to decrease the outer Helmholtz potential.

Vincent also indicated that, for high molecular weight homopolymers, the segment density in the diffuse layer should be small and there should thus be no first-order effect. However, the plane of shear may well be shifted away from the surface so that the usual assumption that zeta potential is equivalent to the outer Helmholtz potential may no longer be valid. It then becomes necessary to assume some relationship between the two before the electrical repulsion energy term can be calculated.

There are at least three conditions where the segment distribution in the diffuse layer cannot be assumed to be small and where the above analyses therefore cannot be applied. They are: adsorbed polyelectrolytes; polymers adsorbed only at their end groups; and adsorption where bridging flocculation occurs. A new model of the double layer is required but, as yet, no satisfactory model has been developed.

1.6 THE PROPERTIES OF POLYACRYLAMIDE FLOCCULANTS

The anionic polyacrylamides are the most widely used class of compounds by far in bridging flocculation. Advances in production technology in the past 10 years have seen a vast improvement in their performance which has been parallelled by similar advances in user technology. Despite their economic importance to both producers and consumers, there has been little reported work on the chemical and physical properties which are of importance in understanding their role in bridging flocculation. The combination of very high molecular weight and electrostatic effects due to the presence of ionized carboxyl groups means that even very dilute solutions have high viscosities, making experimental work very difficult. Most of the published work, apart from simple reports of various applications, has therefore been restricted to low molecular weight polymers for reasons of convenience. There is a real need for reliable data on the properties of typical commercial polymers.

1.6.1 METHODS OF MANUFACTURE

Copolymers of acrylamide and sodium acrylate can be prepared either by direct copolymerization of the two monomers or by polymerization and subsequent hydrolysis of acrylamide. Although both methods are used, almost all of the successful latest generation polymers are manufactured by free radical copolymerization[59-61]. Some details of the process are available from patents but most of the important information remains as closely guarded secrets within each company.

1.6.2 MOLECULAR WEIGHT

The viscosities of dilute solutions of polyelectrolytes in ionizing solvents display a unique dependence on concentration which distinguishes them from non-ionic polymers. For the latter the reduced viscosity (η_{sp}/c) increases linearly with concentration (c) and the intrinsic viscosity, [η], can be readily determined by extrapolating η_{sp}/c to $c = 0$. Molecular weights can then be determined using the appropriate Mark-Houwink equation.

$$[\eta] = K M^{a} \qquad (1.18)$$

For the polyacrylamide homopolymer in water at 25°C, Collinson <u>et al.</u>[63] have determined values of $K = 6.8 \times 10^{-4}$ and $a = 0.66$ when M is the number average molecular weight with η in dl/g. For polyelectrolytes, η_{sp}/c increases markedly with dilution, reaching values many times higher than would be expected for non-ionic polymers. This behaviour occurs because the electrostatic interactions between ionized groups in the polymer cause the molecule to expand. At moderate concentrations, the molecules are in close contact, often overlapping, and expansion is restricted. As the solution is diluted, they no longer fill all the space and are able to expand fully, thus causing the viscosity to increase. Fuoss[64] has shown that the viscosity of such solutions can be described by an empirical equation:

$$\eta_{sp}/c = \frac{A}{1 + B\sqrt{c}} \qquad (1.19)$$

where $A = 1/[\eta]$
B = constant.

A more appropriate method, however, is to eliminate the expansion due to electrostatic effects by the addition of a sufficient quantity of neutral salt, usually about 0.5 M depending on polymer molecular weight. A simple linear equation has been proposed by Huggins[101]:

$$\frac{\eta_{sp}}{c} = [\eta] - k[\eta]^2 c \tag{1.20}$$

where k = Huggins' constant.

In the derivation of this equation, Huggins introduced the constant k to accommodate the interactions between solvent molecules and the segments of the polymer molecule. As such, it is an arbitrary parameter whose molecular significance has not been elucidated, except for uncharged solid spheres where it is approximately 2.0 both in theory[102] and in practice[103]. For flexible linear polymers in good solvents[101], k is often near 0.35 and should be constant for a series of polymer homologues. A number of equations have been derived to relate weight average molecular weight to intrinsic viscosity for polyacrylamide and poly/sodium acrylate:

$$[\eta] = 3.73 \times 10^{-4}\ \bar{M}_w^{0.66} \tag{1.21}$$

for polyacrylamide in 1 M $NaNO_3$ at 30°C[62]

$$[\eta] = 12.4 \times 10^{-4}\ \bar{M}_w^{0.50} \tag{1.22}$$

for poly (sodium acrylate) in 1.50 M NaBr at 15°C[65]

$$[\eta] = 10.5 \times 10^{-4}\ \bar{M}_w^{0.54} \tag{1.23}$$

for poly (sodium acrylate) in 2.0 M NaOH at 25°C[66].

In addition, for copolymers of acrylamide with sodium acrylate, equations have been proposed to relate $[\eta]$ to $\bar{M}_w$ and the ratio of comonomers. However, Klenina and Lebedeva[67] have shown that, at high ionic strength, the intrinsic viscosities of fully neutralized copolymers are not affected by the proportion of sodium acrylate, at least up to 50 per cent. It is therefore possible to determine molecular weights using a single Mark-Houwink equation.

Light scattering techniques can also be used to determine molecular weights of polyelectrolytes, provided account is taken of the Donnan effect. Strauss *et al.*[68] has shown that extrapolation of the Debye plot to infinite dilution will lead to an apparent molecular weight for charged polymers. They derived a relationship between the true and apparent molecular weights which requires the separate measurement of the Donnan equilibrium between the polyelectrolyte solution and the supporting electrolyte. A simpler procedure was devised by Vrij and Overbeek[69] which avoids the necessity of carrying out actual chemical analysis of supporting electrolyte to determine the Donnan equilibrium. This is achieved by measuring both the Rayleigh ratio and the refractive index gradient at constant chemical potential rather than at constant concentration of supporting electrolyte. In effect, the three component systems of polyelectrolyte, supporting electrolyte and solvent is reduced to a pseudo two component system by allowing a Donnan equilibrium to be established betweep the polyelectrolyte solution and a solution of the supporting electrolyte. The true molecular weight can then be determined from equations similar to the Debye equations:

$$\left(\frac{K^{*}C}{R^{*}_{\theta}}\right)_{\theta\to 0} = \frac{1}{M} + 2B.C + \ldots. \qquad (1.24)$$

and $$\left(\frac{K^{*}C}{R^{*}_{\theta}}\right)_{C\to 0} = \frac{1}{M}\left(\frac{1}{P(\theta)}\right) \qquad (1.25)$$

where $$K^{*} = \frac{2\pi^{2} n_{o}^{2}}{N\lambda^{4}} (\partial\eta/\partial c)_{\mu}^{2} \qquad (1.26)$$

M = molecular weight of polyelectrolyte

C = polyelectrolyte concentration

R^{*} = Rayleigh ratio at constant chemical potential

θ = scattering angle

N = Avogadro's number

n_o = refractive index of supporting electrolyte

λ = wavelength of light

$\left(\frac{\partial n}{\partial c}\right)_{\mu}$ = refractive index gradient constant chemical potential

The function $P(\theta)$ can be related to the radius of gyration of the polymer (Rg) by the equation:

$$\frac{1}{P(\theta)_{\theta \to 0}} = 1 + \frac{16\,\pi^2\ Rg^2\ \sin^2\left(\frac{\theta}{2}\right)}{3\lambda^2} \qquad (1.27)$$

Experimental data can thus be treated by conventional methods such as that of Zimm[70] to determine molecular weight, second virial coefficient and radius of gyration.

The effect of polydispersity on the Zimm plot is to introduce some curvature to the plot at the limit of infinite dilution. The Zimm plot then leads to the weight average molecular weight (M_w) and the z-average radius of gyration $(R_g^2)_z^{\frac{1}{2}}$.

In principle, the curvature observed should also furnish some information regarding the distribution of molecular weights. Benoit[71] has demonstrated that, for a randomly coiled polymer, there is a useful asymptotic result at large values of the parameter $W = \frac{1}{2}(4\pi \operatorname{Sin}(\frac{\theta}{2})\ R_g)^2$. The low angle asymptote leads to M_w and $(R_g^2)_z$ while the large angle asymptote leads to twice the number average molecular weight ($2M_n$) and the number average radius of gyration $(R_g^2)_n^{\frac{1}{2}}$. When measurements are carried out in the range $\theta = 30°$ to $135°$ with wavelengths of 300 to 400 nm, only the low angle asymptote is observed for $(R_g^{2\frac{1}{2}})_z < 80$ nm. For $(R_g^2)_z^{\frac{1}{2}} >$ nm, only the large angle asymptote is accessible. At intermediate sizes, the curvature is such that neither is accessible and consequently there may be substantial errors in estimating the molecular weight.

1.6.3. POLYDISPERSITY

Commercial polyacrylamides would be expected to exhibit both chemical and molecular weight heterogeneity. A number of workers have reported using various forms of exclusion chromatography to examine the molecular weight distributions of a range of acrylamide based polyelectrolytes[72-74]. Unfortunately, they all refer to polymers whose molecular weights are considerably lower than those of interest to this work and very few refer to commercial products. Similar comments apply to the method of Bain et al.[75] in which polyacrylic acid was fractionated by adsorption onto barium sulphate crystals. Furthermore, it is likely that in any technique there will inevitably be some overlap of chemical and molecular weight effects but chemical heterogeneity appears to have been largely ignored. However, there is evidence to show that during the commercial polymerization process, the proportion of acrylamide in the polymer decreases as the reaction proceeds[76].

1.6.4. MONOMER SEQUENCE DISTRIBUTION

It has generally been recognised that the sequence distribution of the acrylamide and sodium acrylate monomers may have a profound effect on the flocculating ability of polymers. However, the complete absence of any information in this area has made it necessary to use tacit assumptions in interpreting results. The development of carbon-13 nmr as a technique for determining monomer sequences has recently provided an opportunity to rectify this deficiency. The only reported work on acrylamide polymers has been carried out on low molecular weight molecules and serves mainly to assist in making peak assignments[77-79]. There are major practical problems which must be overcome to obtain reasonable spectra from any high molecular weight polymers and it appears that most workers have chosen to avoid this area.

1.6.5 STABILITY OF POLYACRYLAMIDE IN AQUEOUS SOLUTION

The stability of polyacrylamides in aqueous solutions has been extensively studied by a number of workers. Muller et al[80] have demonstrated that the anionic character of polyacrylamides could be increased from 30 per cent to almost 60 per cent in solutions held at pH 4 and 100°C for 24 hours due to hydrolysis of amide groups. The rate of hydrolysis depends on both pH and temperature to the extent that, in neutral solutions at ambient temperature, there is no measurable change in anionic character over periods of several days.

Molecular weight degradation, which results in losses of both solution viscosity and flocculating ability, can occur in two ways. Mechanical degradation occurs from the direct application of shearing stress. Photolysis under ordinary laboratory illumination, sunlight or UV radiation also cause degradation. Basedow et al.[81] have shown that mechanical degradation is a first order reaction in which the rate constant is proportional to the molecular weight and to the shearing stress. The molecules are broken preferentially near the centre of the chain. There is a critical molecular weight, inversely proportional to the shear stress, below which chain breakage does not occur[82]. Photodegradation occurs through a radical process which frequently involves reaction between dissolved oxygen and metal ions to form OH° radicals[83]. In both mechanical and photolytic degradation, the rates of reaction increase directly with temperature and inversely with solution concentration.

As the technology of polymer manufacture has improved, the molecular weights of commercially available polymers has increased. Increasing attention must therefore be paid to the preparation and use of solutions in both laboratory and industrial work to avoid degradation. Unfortunately, there are many examples in the literature of apparently anomolous results which can be readily explained if degradation has occurred.

1.7 PROPERTIES OF SUGAR CANE MUDS

The process used universally in Australian sugar mills for the extraction and clarification of juice from sugar cane is shown schematically in Figure 1.3.

Raw juice at pH 5.5 and 30 - 35°C is extracted from cane by mechanical crushing. It is immediately heated to 76 ± 1°C at which a voluminous precipitate of plant protein is produced. After 30 to 45 minutes at 76°C, the pH is adjusted to 7.5 - 8.0 by the addition of lime which has been partially or completely dissolved in juice or syrup. The juice is boiled briefly and polymeric flocculant is added as it enters a clarifier where insoluble solids are separated from clear juice by gravity sedimentation. The clarified juice is subsequently concentrated by evaporation to produce crystal sucrose.

The cold raw juice from the crushing station is a solution of sucrose containing both soluble and insoluble impurities. Soluble impurities comprise approximately 10 per cent of the total dissolved solids and include both organic and inorganic components. Approximately 33 per cent are inorganic, primarily K_2SO_4 with lesser quantities of other salts including Na^+, Ca^{2+}, Mg^{2+}, PO_4^{3-}, Cl^- and other essential plant components. Glucose and fructose represent a further 33 per cent with the remainder being a complex mixture of plant proteins, polysaccharides, amino acids, organic acids etc.

The insoluble impurities are variable in both quantity and type, depending on cane variety, climatic conditions and field and factory practices. Typically however, they include minor quantities of starch granules, and variable quantities of plant fibre and field soil.

The aim of the clarification process is to remove the maximum amount of impurities, both soluble and insoluble, and to raise the pH sufficiently to minimize sucrose losses due to acid or alkaline hydrolysis during subsequent processing. In its simplest form, the juice is first heated to prevent bacterial attack and to precipitate plant proteins. The pH is then adjusted by the addition of lime which simultaneously precipitates phosphates as calcium salts. The juice then carries a suspension comprising the original insolubles together with precipitated proteins and phosphates. Despite the complexity of the mixture, Bennett[84] has shown that it behaves electrophoretically as a homogeneous dispersion in which the particle surfaces are characteristically proteinaceous and carry a nett negative charge due to the ionization of carboxylic acid groups. The influence of the carboxylic acid groups is greater than expected for a purely proteinaceous surface and Bennett has attributed this to the adsorption of acidic polysaccharides containing more carboxylic groups.

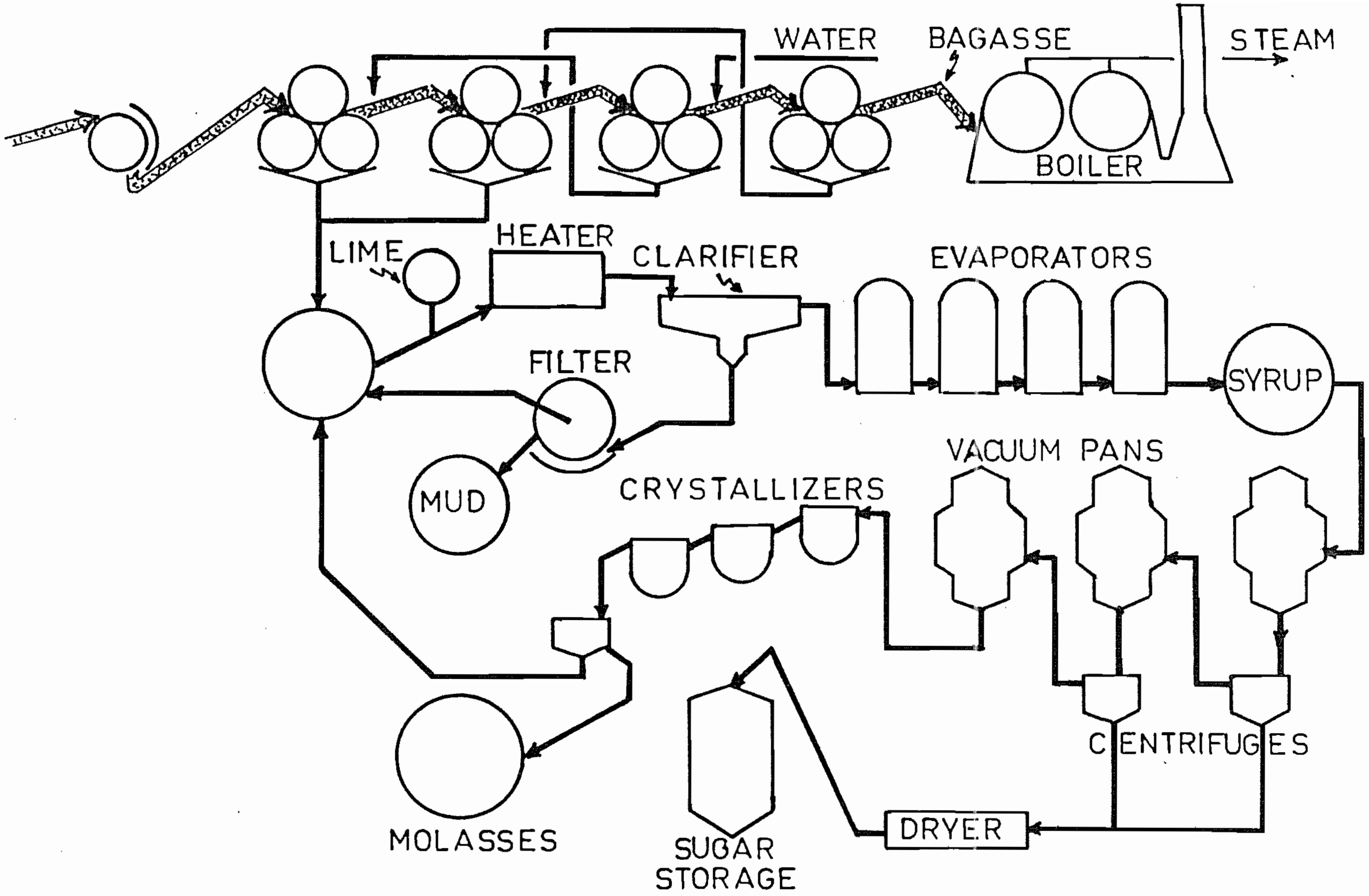

Figure 1.3 Simplified Raw Sugar Process Flowsheet.

The surface charge of the particles is influenced by cane variety through variations in both the type and quantity of inorganic salts, proteins and other ionic species. It is also affected by the method of lime addition. When added to cold juice prior to heating, relatively high particle charges result. Much lower charges are found when lime is added after heating[85]. In Australian factories lime is usually added not as a slurry (milk of lime) but dissolved in concentrated sucrose solution (calcium sucrate or calcium saccharate) since this procedure is known to lead to a marked reduction in the turbidity of clarified juice. Whatever the procedure, the nett particle charge is usually small enough for the dispersion to be unstable. Rapid coagulation, as defined by Smoluchowski[86], occurs and the particles settle spontaneously to leave a clear supernatant.

The role of calcium and phosphate ions in the process has been examined by Bennett and Ragnauth[87] who suggested that precipitated calcium phosphate acts as a primary flocculant by bridging between adjacent particles, being attached to the particles through Ca^{2+} ions which are already adsorbed at the protein/polysaccharide surface. The number of particles flocculated in this manner depends on the quantity of phosphate precipitated. Thus the turbidity of clarified juice improves as the amount of phosphate precipitate increases. So important is this aspect that it is common practice in Australian sugar mills to add phosphate, as either phosphoric acid or superphosphate, to juices to improve the efficiency of clarification when product quality standards are not being met. The effects of Ca^{2+} ions are not associated with charge reversal phenomena within the pH range 7.0 - 9.0 at which clarification is normally practised.

1.7.1. SYNTHETIC FLOCCULANTS IN SUGAR MANUFACTURE

The use of synthetic polyelectrolytes to enhance juice clarification in sugar factories was reported more than 30 years ago[88]. Laboratory trials conducted in Australia soon after showed that it was possible to improve dramatically both the settling rate of solids and the turbidity of the supernatant juice. Despite the obvious potential advantages, it was some time before the industry adapted to their use. However, by the late 1960's all Australian sugar factories were using polyelectrolytes to improve both the rate and the efficiency of solid/liquid separation in their clarifiers. In fact, the improvements in equipment capacity and raw sugar quality were so dramatic that factories rapidly became completely dependent on them.

The product quality standards in the sugar industry are such that the principal aim of the clarification stage is to produce clarified juice of the lowest possible turbidity at all times. Other parameters such as the settling rate of solids and the final volume of sediment are of secondary importance. However the advent of polyelectrolytes made possible vast improvements in all areas of clarification. When it was realized that high settling rates could be maintained without sacrificing turbidity, it became apparent that the potential benefits of synthetic polyelectrolytes could not be fully realized with existing equipment which had been designed to operate without added flocculants. New equipment was developed[90] specifically to capitalize on the high settling rates which could be achieved.

As polyelectrolyte usage by the industry grew, so too did the number of products offered for sale. Although there is an almost bewildering array of products available, the anionic polyacrylamides are by far the most successful and the polymers used in Australian sugar factories are exclusively in this class. As in any commercial enterprise, there is a strong financial incentive to minimize the quantity used. Unlike most other process industries, however, sugar factories are further constrained by the severely detrimental effects of excess polymer on product quality and by health and safety considerations. In fact, the National Health and Medical Research Council of Australia has followed the ruling of the United States' Food and Drug Administration[91] and imposed a limit of not more than five grams of polyacrylamide per tonne of cane processed, and then only if the polymer contains less than 0.05 per cent residual monomers.

Despite the absolute dependence of the Australian industry on these polymers and their obvious potential in sugar factories throughout the world, there has been no other systematic study of their properties or of the mechanism of their flocculation reactions. Indeed the same could be also said of practically all other applications. Most of the published literature can be readily classified into two distinct groups. There are a great many reports which do nothing more than describe applications in which a number of polymers of unspecified character have been compared. Too often, simple laboratory tests are used, which frequently bear little relation to the actual process considered. Alternatively, careful laboratory studies have been made of various properties of polymers and particles which are important to the flocculation reaction. Because of the practical problems encountered with very high molecular weight polymers, properties such as adsorption isotherms, molecular weight distributions, ion binding etc. have generally been examined using polymers whose molecular weights are far below those of commercially important flocculants. Extrapolation of the results thus obtained to much higher molecular weights often cannot be justified. In addition, there are differences in the conditions under which polymerizations are carried out so that specific properties of commercial polymers, such as molecular weight distribution and monomer sequence distribution, are rarely duplicated in laboratory samples.

The work in this thesis is primarily a detailed examination of the parameters which influence and control the flocculation of cane muds under actual process conditions. A closer understanding of the mechanism should automatically enable the process to be optimized by ensuring that the polyelectrolyte used is the best available for the prevailing conditions. Equipment capacity, product quality and operational costs should all improve as a result. The work thus has important commercial significance to the sugar industry in particular and generally to all similar processes where flocculation is important.

CHAPTER 2

MATERIALS, APPARATUS AND EXPERIMENTAL PROCEDURES

2.1 MATERIALS

2.1.1 GENERAL REAGENTS

Potassium poly(vinylsulphate) was obtained from Eastman and used without further purification. However, the purity of each new batch was determined before use. The potassium content of a small sample was determined gravimetrically and the equivalent weight of the sample calculated.

Methyl glycol chitosan was obtained from ICN Pharmaceuticals and used without further purification.

Acrylamide (BDH Laboratory Reagent) was recrystallized twice from chilled acetone, dried under vacuum at 20°C and stored for up to two weeks in a dark bottle at 4°C. Samples held for longer periods were repurified before use.

Styrene (BDH), chlorostyrene (Merck) and acrylic acid (BDH) were purified by distillation at reduced pressures (<1 kPa) under an atmosphere of nitrogen and stored in a refrigerator for not more than 24 hours before use. Itaconic acid (BDH) was recrystallised twice from ethanol and kept in a desiccator.

Calcium saccharate (lime sucrose reagent) was prepared in the manner normally employed in Australian sugar mills[130]. 150 g of refined sugar was dissolved in approximately 60 mL of hot water. 15 g of CaO was added slowly, with constant stirring, to 100 mL of hot water then mixed thoroughly with the hot sucrose solution. The hot solution was filtered under vacuum through a Whatman No. 54 filter paper using Supercel filteraid and stored in a refrigerator. Fresh reagent was prepared every four weeks.

Other reagents were A.R. grade and were used without further purification.

2.1.2 COMMERCIAL POLYMERS

An extensive range of commercial polyacrylamides from a number of the major manufacturers was used throughout this investigation. A list of the companies who provided samples and relevant details of their products is contained in Table 2.1. All samples used were characterized by estimation of molecular weight, copolymer composition and flocculating ability. Other properties examined on selected polymers included molecular weight distribution, chemical heterogeneity, solution dimensions and monomer sequence distributions. Experimental details are described later.

In addition to the commercial samples, a number of special samples were kindly provided by both Allied Colloids Pty. Ltd. and Cyanamid (Australia) Pty Ltd at various times. Details of these samples are given in the relevant sections of subsequent chapters.

Overall, the polymers used covered the molecular weight range 3 - 28 × 10^6 daltons and varied from zero to 60 mol % acrylic acid.

Table 2.1 Sources of Commercial Polyacrylamides

Company	Product	Physical Form
Allied Colloids Pty Ltd	Magnafloc	granular
BASF	Sedipur	powder
Catoleum Pty Ltd	Alfloc	emulsion
Cyanamid Aust. Pty Ltd	Superfloc	granular
Dow	Separan	powder
Daiichi Kogyu Seiyaku	Hiset	granular

2.1.3 PREPARATION OF HYDROLYSED POLYACRYLAMIDES

A range of low molecular weight polymers was prepared by polymerization and subsequent controlled hydrolysis of acrylamide to provide reference samples for monomer sequence distribution studies by C^{13} nmr.

Acrylamide (25 g) was dissolved in 150 g of distilled water and thoroughly purged with nitrogen. The solution was heated to 40°C and 60 mg each of potassium metabisulphite and potassium persulphate added as initiator. The reaction was allowed to proceed for four hours with N_2 purging, after which the polymer was recovered and purified by reprecipitation with methanol. A series of hydrolysed polymers was prepared from this sample of homopolymer by reaction in 0.25 M NaOH at 50°C. Using the kinetic data of Higuchi and Senju[92], the reaction time required to achieve the desired hydrolysis was calculated. The reactions were stopped by neutralization with HCl and the polymer recovered by methanol precipitation. The extent of hydrolysis was determined by conductometric titration. A set of six samples was obtained, covering the range from zero to 44 per cent hydrolysis.

2.2 ANALYSIS OF ACRYLAMIDE POLYMERS

2.2.1 MOISTURE CONTENT OF POLYMERS

The moisture contents of both commercial and experimental polymers were determined by drying in an air oven at 105°C for 24 hours. Figure 2.1 shows that the rate of water loss from a typical commercial copolymer was relatively slow. At least 16 hours was required for the sample to reach constant weight. Drying under vacuum at or above 60°C increased the drying rate slightly but the improvement was not sufficient to warrant a change in the method.

It was found that polymers dried to constant weight were difficult to redissolve. Drying at 60°C under vacuum did not appear to affect the solubility as such but rather altered the surface properties of the polymer particles making them difficult to wet. The effect was more pronounced in polymers which were dried at 105°C and there was occasionally evidence of cross-linking leading to some insolubility. Samples which had been freeze-dried from aqueous solution redissolved readily. However, for all quantitative work, solutions were prepared from polymer powders as received and the actual concentration calculated from the moisture content which was determined separately.

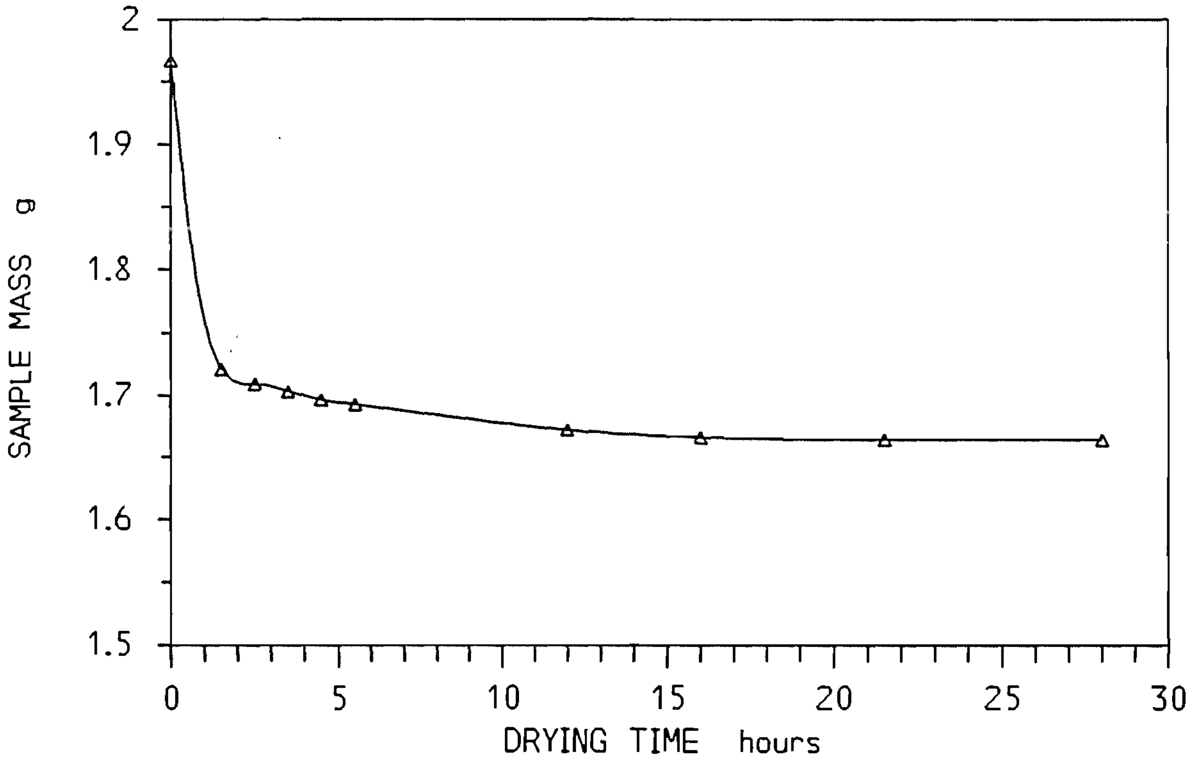

Figure 2.1 Drying Curve for Typical Commercial Flocculant.

2.2.2 COPOLYMER COMPOSITION

The relative amounts of acrylamide and sodium acrylate monomers in a polymer can be determined in a number of ways. All of the available methods can be readily applied to low molecular weight polymers but the extremely high viscosities of solutions of typical commercial polymers has precluded all but a very few for this work.

Methods used by other workers to determine the copolymer composition include potentiometric[93] and conductometric[94] titrations, infra-red spectroscopy, colloid titration and elemental analysis. The potentiometric titration of partially hydrolysed poly-acrylamides has been discussed by Fenyo, Laine and Muller[95] using an extended linear Henderson-Hasselback equation of the form:

$$pH = pK_a^{\alpha=0.5} - n \log \frac{1-\alpha}{\alpha} \qquad (2.1)$$

where α = degree of dissociation

$pK_a^{\alpha=0.5}$ = dissociation constant at $\alpha=0.5$

$n = 1 + 0.575\ (a+b)$

The values of a and b are obtained from the equation:

$$pK_a^{\alpha} = pK_o + a\alpha + b\alpha^2 \qquad (2.2)$$

where pK_o = intrinsic ionization constant

They showed that the values of pK_o, a and b were all functions of the degree of hydrolysis, the concentration of polymer in solution and the nature of the cation in the titrant. Consequently, the pH change during titrations occurs only gradually without the sharp change normally observed at the end point. A clear end point cannot be obtained either by potentiometric or conductometric means except at low molecular weights ($<10^6$ daltons). The experimental problems are further exacerbated with high molecular weight polymers where the extremely high viscosities of aqueous solutions mean that solutions must be very dilute. Even so, several hours are required for the system to reach equilibrium after each addition of titrant. Thus, whilst these methods are satisfactory for low molecular weight polymers, they have proved to be of little value in any investigation involving polymers of commercial significance.

Throughout this investigation, copolymer composition was determined either by elemental analysis or by colloid titration. When elemental analysis was used, the sodium content of a sample was determined gravimetrically as anhydrous sodium sulphate[96] and the nitrogen content measured using the Kjeldahl method for plastics, resins and resin solutions[97]. After correcting for the moisture content, the molar ratio of the three monomers acrylamide, acrylic acid and sodium acrylate was then calculated and the ionic content expressed as the total mole per cent of acrylic acid plus sodium acrylate.

The colloid titration technique was based on a procedure described by Terayama[98] and relied on the rapid, stoichiometric reaction between anionic polyacrylamides and the cationic polymer methyl glycol chitosan in dilute solution. The polyacrylamide was reacted with a known quantity of the chitosan polymer and the excess cationic polymer determined by titration with another anionic polymer, potassium polyvinylsulphate (PVSK), using toluidine blue indicator.

Approximately 0.5 g of PVSK which had been previously analysed (2.1.1) was accurately weighed and dissolved in one litre of distilled water in a volumetric flask to give a stock solution of PVSK of whose equivalent concentration was calculated from the previous analysis. Approximately 50 mg of the polymer to be analysed was accurately weighed and dissolved in about 750 mL of distilled water. After stirring for at least two hours, the solution was made up to one litre in a volumetric flask. A 20 mL aliquot of this solution was then added to a 100 mL beaker together with 20 mL of distilled water and 0.5 mL of 0.1 M NaOH. While stirring vigorously, 20 mL of a 0.02% (W/W) solution of methyl glycol chitosan and 2 drops of 0.1% (W/W) toluidine blue were added and the solution titrated with the PVSK solution until the colour changed from blue to pink. A blank titration was also performed by substituting water for the polyacrylamide solution. The ionic content was then calculated for the equation:

$$\text{Ionic content (mole \%)} = \frac{3.55\times10^{4}\ (B-P)C}{(D.W)-115(B-P)C} \qquad (2.3)$$

where B = titre of blank in mL
P = titre of polymer in mL
C = concentration of PVSK (equivalents/litre)
D = per cent dry solids in polymer sample
W = weight of polymer in 1 litre of water (g)

A comparison of the results obtained by the two procedures is shown in Figure 2.2 for a series of polymers covering the range of ionic contents of interest in this work. Although the correlation is reasonable, it was found that the end point colour change of the titration was somewhat time dependent and therefore not easily reproduced. Considerable practice was required to achieve reproducible results. It was thus decided that the colloid titration procedure was satisfactory for routine analysis of large numbers of samples but was not appropriate in other cases, particularly where improved accuracy was required.

2.2.3 MOLECULAR WEIGHT BY VISCOMETRY

As discussed in Chapter 1, there are several equations available which relate the intrinsic viscosities of polyacrylamides in various solutions to their molecular weights. Throughout this work, intrinsic viscosities were determined at 30°C in 1M $NaNO_3$ and the weight average molecular weight calculated using the equation:

$$[\eta] = 37.3 \times 10^{-5}\ \bar{M}_w^{\ 0.66} \qquad (1.21)$$

where $[\eta]$ = intrinsic viscosity in g/dL
$\bar{M}_w$ = weight average molecular weight.

The viscosities of polymer solution prepared under a variety of conditions have been examined throughout this work. Specific aspects of the procedures and results are discussed in detail in Chapter 4. As a result of that work, however, the following procedure was adopted for routine molecular weight

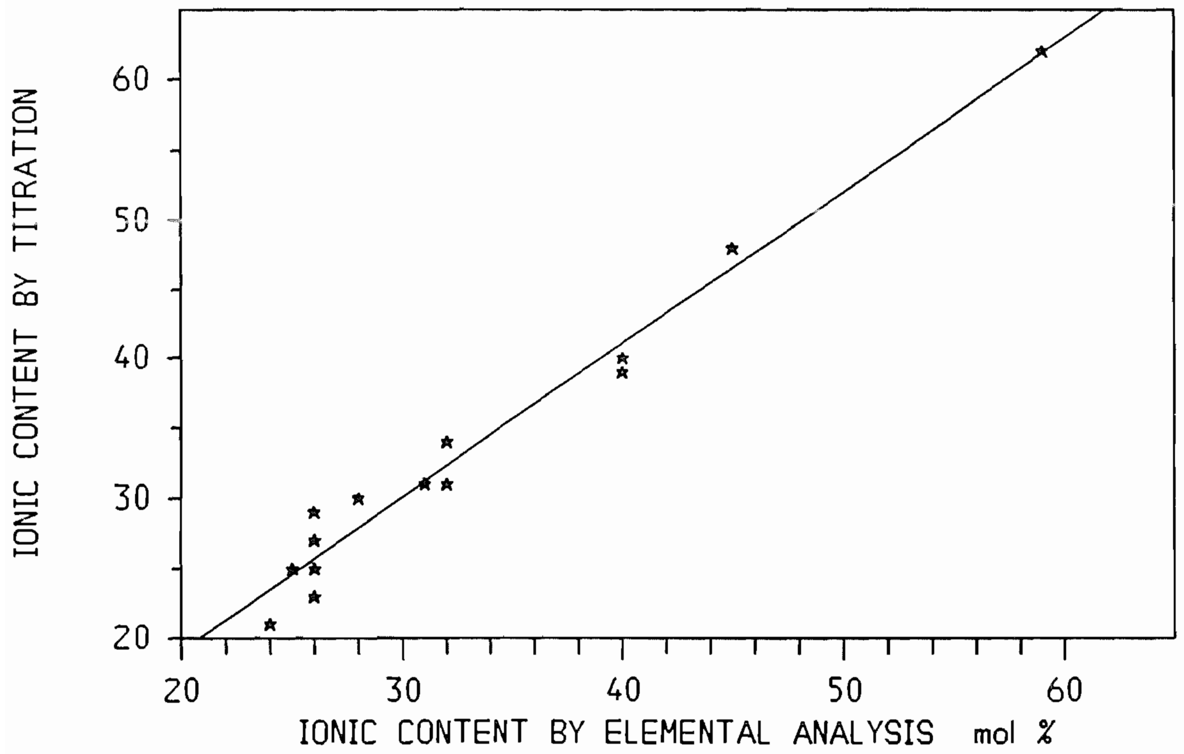

Figure 2.2 Comparison of Analytical Methods for Copolymer Composition.

determinations. The required amount of polymer (generally 0.1-0.2 g) was accurately weighed and added slowly to about 75 mL of distilled water with vigorous stirring in a covered glass beaker which had been painted black to obscure light. An aliquot of 0.1 cm^3 of 1.00 M NaOH was also added to the water prior to the addition of polymer. This quantity was calculated to be sufficient to completely neutralize any of the polymers examined without the risk of inducing further hydrolysis during the time period of the measurements. Within a few minutes, the viscosity increased sufficiently to prevent the particles from settling. The stirring rate was then reduced to 30 ± 10 Hz. Stirring was continued for four hours after which 100 mL of 2.00M $NaNO_3$ was added by pipette. After further stirring for one hour, the solution was transferred to a 200 mL volumetric flask. Considerable care was needed to ensure quantitative transfer of the solution from the beaker. The flask was made up to the mark with distilled water. A separate gravi-metric determination of the moisture content of the polymer was required (see 2.2.1) to enable the final concentration to be calculated.

Viscosity measurements were performed in a suspended level Ubbelohde dilution viscometer at 30.00 ± 0.02°C. The viscometers used had working volumes of 15-75 mL and solvent flow times of 70-90 s. They were cleaned by soaking in chromic acid followed by thorough rinsing with distilled water each day before use. The viscometer was thoroughly rinsed with a filtered solution of 1.00 M $NaNO_3$. Approximately 20 mL of the filtered $NaNO_3$ solution was then added and the system allowed to equilibrate in a water bath. The solvent flow time was measured and compared with previous values. If the mean of five measurements flow time varied by more than ± 0.1 s from the expected value, the cleaning procedure was repeated until the value was within this range.

The polymer solution was filtered through a stainless steel screen (pore size 75 μm) and some of the filtered solution used to rinse the viscometer. 15 mL of the filtered solution was then added to the viscometer by pipette and, when thermal equilibrium was established, the solution flow time was measured. The polymer solution in the viscometer was diluted progressively with aliquots of 1M $NaNO_3$ until the total volume reached 75 mL.

After each addition of solvent, the solution was thoroughly mixed and allowed to equilibrate before the flow time was measured. At the higher concentrations, this often required periods of up to 30 minutes. The relative viscosity (η_r) and specific viscosity (η_{sp}) were then calcůlated at each concentration using the equations:

$$\eta_r = \frac{t_c}{t_o} \qquad (2.4)$$

$$\eta_{sp} = \eta_r - 1 \qquad (2.5)$$

where t_o, t_c = mean flow times for solvent and solution

The intrinsic viscosity is defined[100] as:

$$[\eta] = (\eta_{sp}/c)_{c \to 0} \qquad (2.6)$$

where c = concentration in g/dL.

and is usually determined by extrapolation to zero concentation of a plot of η_{sp}/c against c which, according to the Huggins' equation (1.20), should be linear at low concentrations.

It has been suggested[100] that, using the series expansion for the natural logarithm, the intrinsic viscosity can also be defined as:

$$[\eta] = (\ln \eta_r/c)_{c \to 0} \qquad (2.7)$$

It should therefore be possible to determine the intrinsic viscosity from a plot of ($\ln \eta_r/c$) against c. However, with the polymers considered in this work, the values of η_{sp} are usually greater than unity so the essential approximation in equation (2.7) viz:

$$\ln \eta_r = \ln (1 + \eta_{sp}) \approx \eta_{sp} \qquad (2.8)$$

is not valid. This can be clearly seen in Figure 2.3 in which the data for a typical commerical polymer plotted by both procedures is shown. The plot of ($\ln \eta_r/c$) against c shows a distinct curvature, except at the lowest values of concentration where the approximation of equation (2.8) becomes valid. Fitting a smooth curve through the data (Figure 2.3) gives an improved correlation and closer agreement with the conventional plot. However, in view of the linearity of the plot of η_{sp}/c against c and the ease of data handling, this method has been used throughout.

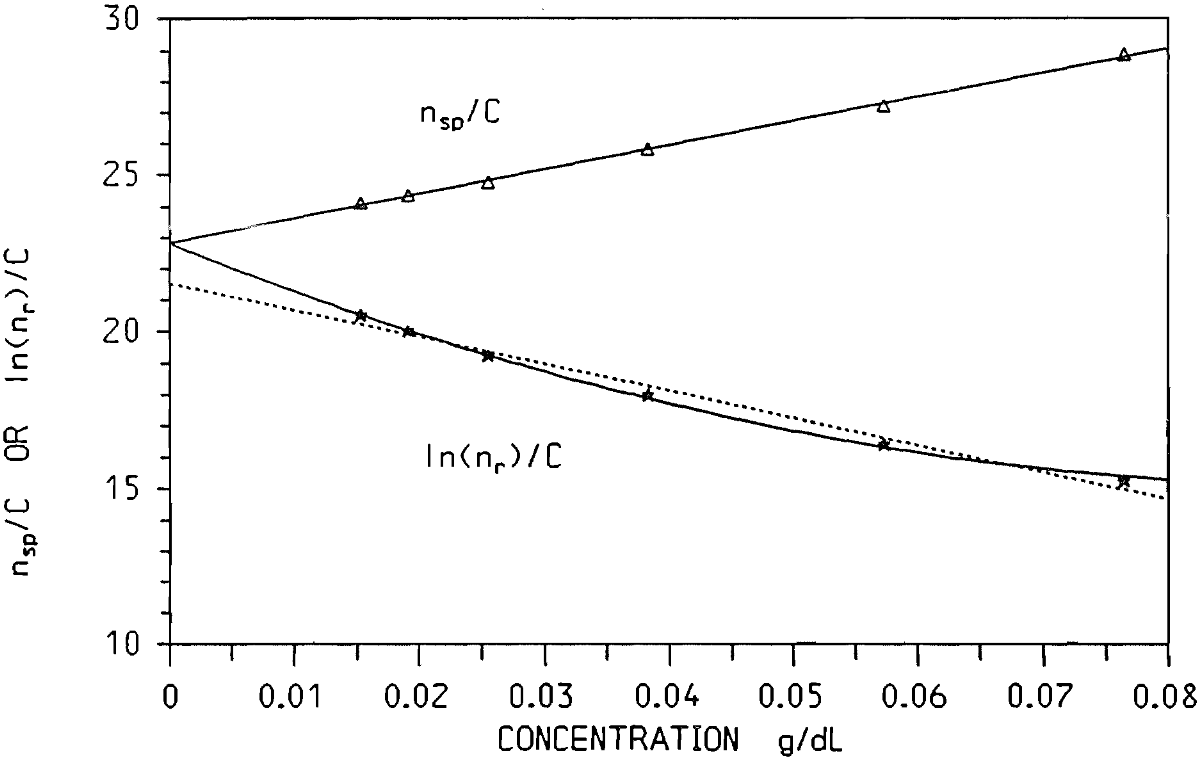

Figure 2.3 Alternative Plots of Viscosity Data.

The Huggins' constant k as defined in equation (1.20) was also determined from this graph since the slope of the graph is equivalent to $k\,[\eta]^2$.

The effect of shear rate on specific viscosity and intrinsic viscosity was examined using viscometers with different solvent flow times. The maximum rate of shear obtained with any viscometer was 75 s^{-1} and the minimum 25 s^{-1}. Within this range, no change in viscosity was observed.

2.2.4 MOLECULAR WEIGHT BY LIGHT SCATTERING

In many ways, light scattering appears to be an ideal technique for the determination of polymer molecular weights. The contribution from small solvent molecules is small and, when properly extrapolated to infinite dilution and zero scattering angle, it gives an absolute measure of molecular weight. Furthermore, the angular dependence of scattering intensity yields information about molecular dimensions and the concentration dependence is related to thermodynamic interactions.

For molecules whose dimensions are less than $\lambda/20$, where λ is the wavelength of incident light, light scattering by a solute in a two component system can be treated in the same way as was used by Rayleigh to calculate the scattering for a gas.[105]

An incident light beam will induce an oscillating dipole in any particle in its path. The induced dipole is itself a source of electromagnetic radiation and this new radiation is the scattered light whose intensity is measured. Rayleigh derived the following expression for the scattering of unpolarized incident light by a dilute, isotropic gas:-

$$\frac{i_\theta r^2}{I_o} = \frac{8\pi^4 C\alpha^2}{\lambda^4}(1 + \mathrm{Cos}^2\theta) \qquad (2.9)$$

where i_θ = intensity of light scattered at an angle θ to the direction of the incident beam

I_o = intensity of incident beam

λ = wavelength of incident beam

r = distance from scatterers to detector

α = polarizability of scattering molecules

C = number of molecules per unit volume (taken as $1\ cm^3$)

The polarizability α, which occurs in this equation, is related to the refractive index by the equation:-

$$\alpha = \frac{Mn_o(dn/dc)}{2\pi N} \qquad (2.10)$$

where M = molecular weight

n_o, n = refractive index of solvent and solution respectively

c = concentration in $g.cm^{-3}$

N = Avogadro's constant

The number concentration C can be related to the mass concentration, c, by the equation

$$C = Nc/M \qquad (2.11)$$

and if equations (2.10) and (2.11) are substituted into (2.9), then

$$\frac{i_\theta r^2}{I_o} = \frac{2\pi^2 n_o^2 (dn/dc)^2}{\lambda^4 N} (1 + \text{Cos}^2\theta)\ M.c \qquad (2.12)$$

Since the value of r is constant for a particular instrument it is convenient to define a quantity R_θ, known as the Rayleigh ratio:

$$R_\theta = \frac{r^2 i_\theta}{I_o} \qquad (2.13)$$

$$\text{Thus,}\quad R_\theta = \frac{2\pi^2 n_o^2 (dn/dc)^2}{\lambda^4 N} (1 + \text{Cos}^2\theta)\ M.c \qquad (2.14)$$

$$= K.Mc\ (1 + \text{Cos}^2\theta) \qquad (2.15)$$

$$\text{where}\quad K = \frac{2\pi^2 n_o^2 (dn/dc)^2}{\lambda^4 N} \qquad (2.16)$$

An alternative experimental procedure is to measure the diminution of intensity of the incident beam. The turbidity τ of the solution is defined as $-\ln (I/I_o)$ where I is the intensity after passing through a volume of solution in a 1 cm cube. The relation between τ and i_θ is found by integrating over the surface of a sphere of radius r, which gives

$$\tau = \frac{16\pi}{3} R_{90} \tag{2.17}$$

Thus, from (2.15)

$$\frac{Kc}{R_{90}} = \frac{HC}{\tau} = \frac{1}{M} \tag{2.18}$$

where $$H = \frac{16\pi}{3} K \tag{2.19}$$

and τ refers to the excess scattering due to the solute component.

In an alternative treatment, Smoluchowski[110] considered the scattering of light by pure liquids as being the result of local fluctuations in density, and hence in dielectric constant, due to the Brownian motion of the molecules. This method was then adapted to include two-component systems by Einstein[111] and by Debye[112] who considered that the dielectric constant will undergo random variations due not only to fluctuations in density, but also to fluctuations in the concentration of one component with respect to the other. The general result of a treatment along these lines, assuming small, isotropic molecules and considering only concentration fluctuations is:-

$$\frac{Kc}{R_\theta} = \frac{1}{RT\bar{V}_1}\left(\frac{\partial \mu_1}{\partial c}\right)_{T,P} \tag{2.20}$$

where R = universal gas constant

T = absolute temperature

$\bar{V}_1$ = partial molal volume of solvent

μ_1 = chemical potential of solvent

Debye[112] has shown how (2.20) can be used to determine the molecular weight of the solute by relating the chemical potential μ_1 to the osmotic pressure Π. Expansion of the chemical potential term then leads to a virial equation, namely,

$$\begin{aligned}\mu_1 - \mu_1^{\circ} &= -\Pi\bar{V}_1 \\ &= -RT\bar{V}_1 c(1/M + Bc + \ldots.) \qquad (2.21)\end{aligned}$$

where μ_1° = chemical potential of pure solvent.

Thus

$$-\left(\frac{\partial\mu_1}{\partial c}\right)_{T,P} = RT\bar{V}_1(1/M + 2Bc + \ldots.) \qquad (2.22)$$

If the virial expansion is truncated after the second term, combining (2.20) and (2.22) gives the Debye equation:-

$$\frac{Kc}{R_\theta} = \frac{1}{M} + 2Bc \qquad (2.23)$$

In the case of ideal solutions, the virial coefficient B becomes zero and the Debye equation reduces to the Rayleigh equation (2.18).

Most macromolecules have at least one dimension larger than $\tau/20$ and it becomes necessary to use the approximate theory developed by Rayleigh[106-108] and Debye[109]. The physical basis is depicted in Figure 2.4 where a large particle of arbitrary shape is divided into smaller volume elements. Each element is treated as a Rayleigh scatterer and it is assumed that the incident field is not perturbed by the rest of the particle. It is clear that light scattered by A will be out of phase with that scattered from B, resulting in interference and diminution of the scattered intensity. As the scattering angle (θ) decreases, the phase difference and thus the interference also decrease, finally disappearing at $\theta = 0$.

In general, the effect of large size may be described by a function $P(\theta)$,

$$P(\theta) \equiv \frac{\text{scattered intensity for large particle}}{\text{scattered intensity without interference}}$$

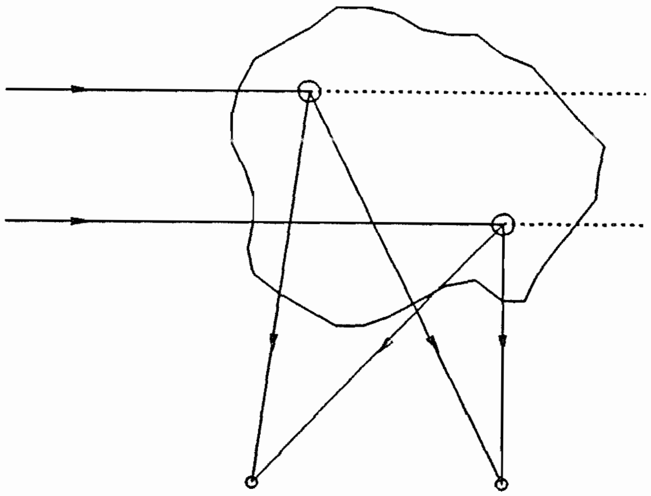

Figure 2.4 Light Scattering by Large Particles.

which may be much less than 1 when θ is large but which will increase as θ decreases until P(θ) = 1 when θ = 0. Thus, all the conclusions of the previous section, in particular equation (2.23), apply to large particles. Experimentally, this means that data must be obtained at several angles and extrapolated to θ = 0.

Debye[109] obtained a general expression for P(θ) which enabled expressions to be derived for particles of certain geometric shapes. A more important result, however, is that P(θ) becomes independent of shape as θ approaches zero and, under these limiting conditions, becomes a measure of the radius of gyration of the particle. This result is unique since no other physical measurement provides a measure of the dimensions of a macromolecule without any assumption regarding its general shape. Guinier[113], who first recognised this feature, derived the following relationship between P(θ) and the radius of gyration R_g :-

$$\lim_{\theta \to 0} \frac{1}{P(\theta)} = 1 + \frac{16\pi^2}{3\lambda^2} R_g^2.\mathrm{Sin}^2 \ (\theta/2) \qquad (2.24)$$

When the expression is combined with the Rayleigh equation (2.18), the result is:-

$$\frac{Kc}{R_\theta} P(\theta) = \frac{1}{M}$$

$$\frac{Kc}{R_\theta} = \frac{1}{M} . \frac{1}{P(\theta)}$$

$$= \frac{1}{M} \{1 + \frac{16\pi^2}{3\lambda 2} R_g^2.\mathrm{Sin}^2(\theta/2)\} \qquad (2.25)$$

Guinier's equation and that of Debye (2.23) provide two ways of determining molecular weight. The two alternative procedures were combined in the method of Zimm[70] in which Kc/R_θ is plotted against $\mathrm{Sin}^2(\theta/2) + kc$ where k is an arbitrary constant chosen to give a convenient spread of the data in the graph. Two types of limiting plot are obtained. Extrapolation to $\theta = 0^0$ gives a plot of Kc/R_θ versus kc which, from equation

(2.23), gives 1/M as the intercept and 2B/K as the limiting slope. Extrapolating to $c = 0$ gives a plot of Kc/R_θ versus $\sin^2(\theta/2)$. From equation (2.25), this gives 1/M as the intercept (the same as the $\theta = 0$ plot) and a limiting slope of $(16\pi^2 R_g^2/3\lambda^2 M)$.

Debye's general equation for $P(\theta)$ can be written as:-

$$P(\theta) = \frac{2}{N^2 u^2}\{Nu - 1 + \exp(-Nu)\} \tag{2.26}$$

where N = degree of polymerization

$$u = \frac{\mu^2 b^2}{6}$$

$$\mu = \frac{4\pi}{\lambda}\sin(\theta/2)$$

b = length of statistical element of chain

If $P^{-1}(\theta)$ is plotted against Nu, this function has an asymptote $y = \frac{1}{2}(Nu + 1)$. When the molecules are such that $R_g/\lambda < 0.5$ (i.e. $R_g < 200$ nm with the mercury arc) the asymptotic behaviour is not observed. Under these conditions a weight average molecular weight and a z-average radius of gyration are obtained. Benoit[71] has shown that at larger values of R_g the asymptotic behaviour is observed and it becomes possible to determine also the number average molecular weight and the number average of R_g. Figure 2.5 illustrates all the information that can be obtained from a Zimm plot for polydisperse systems of linear chains.

Benoit has also shown that for values of $R_g > 300$ nm only the large angle asymptote is accessible. In this instance the values of both molecular weight and radius of gyration will be number averages.

Charged macromolecular particles in a salt solution form a three component system where the fluctuations of macromolecule and salt are interdependent. Zernike[114] was the first person to

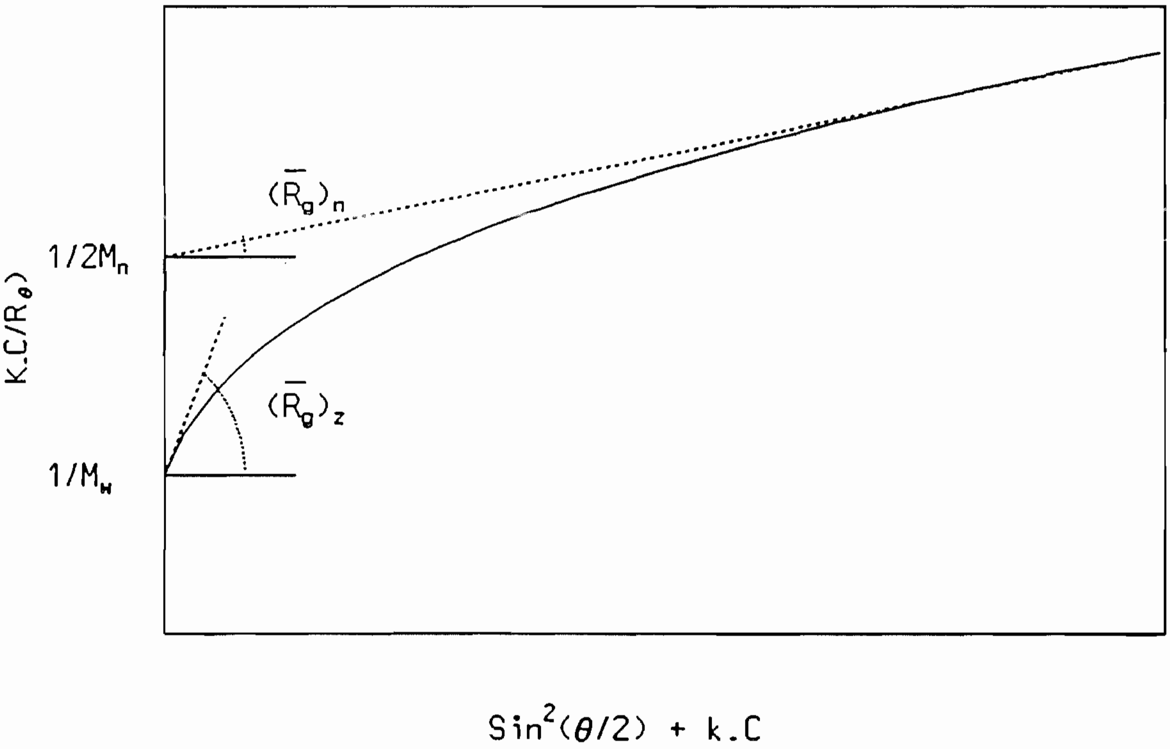

Figure 2.5 Information from Light Scattering.

give a rigorous treatment of light scattering in multicomponent systems. His treatment has been extended subsequently by a number of workers[115,116] and suitable generalizations have been derived for K (containing the refractive index increment) and for $d\Pi/dc$ (related to the free energy of the system). In electrolyte solutions, however, it is hard to find accurate explicit expressions for the free energy because activity coefficients are so difficult to calculate. Mysels[117], in studying light scattering by soap micelles, tried to avoid activity coefficients by ascribing an 'effective charge' to the micelles and further assuming ideal behaviour of the solutions. Vrij and Overbeek, however, consider this approach to be unsatisfactory and have treated the light scattering by charged particles in salt solutions by fluctuation theory[69]. They considered the situation where

$$\frac{2\mathrm{Sin}\ (\theta/2)}{\kappa\lambda} < 0.05$$

This corresponds to the condition that $1/\kappa < 10$ nm which, in aqueous solution, requires an ionic strength of more than 10^{-3} mol/L. Under these conditions, the limiting equations of the Zimm plot described above are valid if the value of H is taken as

$$H = \frac{32\pi^3 n^2}{3\lambda_o^4 N} (dn/dc)_{\mathrm{Donnan}} \tag{2.27}$$

$$\text{and} \quad \tau = \tau_s - \tau^*$$

where $(dn/dc)_{\mathrm{Donnan}}$ is the refractive index increment measured between the salt solution (turbidity = τ^*) in Donnan equilibrium with the polymer solution (turbidity = τ_s). If these requirements are met then the Zimm plot will give the true molecular weight and the true virial coefficient.

An inherent assumption in treatment so far has been that the scattering particle is optically isotropic. If it is not, there arises the possibility of additional scattering due to fluctuations in the orientation of the scattering particles.

When unpolarized incident light is used, the existence of this effect can be detected by measuring the ratio of the intensity of the horizontally polarized component of light scattered at 90°, in the horizontal plane, to the intensity of the vertically polarized component at the same viewing position. If the scattering particle is completely isotropic, then the dipole induced in it is parallel to the electric vector of the incident light. If the light is unpolarized, there will be two independent oscillating dipoles, both perpendicular to the direction of the incident light, one at 90° in the horizontal plane and one at 90° in the vertical plane. The former component will clearly contribute nothing to the radiation in the direction $\theta = 90^\circ$ in the horizontal plane. The light viewed along this line will therefore be completely polarized in the vertical plane, and the ratio of horizontally to vertically polarized scattered light will be zero.

In anisotropic particles, however, the induced moment is generally not parallel to the electric vector of the incident light. The ratio of horizontally to vertically polarized scattered light, with unpolarized incident radiation, will therefore not be zero. This ratio is known as the depolarization ratio, ρ_u and Cabannes[118] has shown how it may be related to the excess scattering due to anisotropy. Thus the value of R_θ due to concentration fluctuations alone is less than the observed value by a factor C(θ) which has been formulated as[119]:-

$$C(\theta) = \frac{1 + \rho_u(90^\circ) + \{1 - \rho_u(90^\circ)\} \operatorname{Cos}^2\theta}{\{1 - (7/6)\ \rho_u(90^\circ)\}\ (1 + \operatorname{Cos}^2\theta)} \qquad (2.28)$$

which, at $\theta = 90^\circ$, reduces to Cabannes' original equation

$$C(90^\circ) = \frac{6 + 6\rho_u(90^\circ)}{6 - 7\rho_u(90^\circ)} \qquad (2.29)$$

All light scattering measurements were made in a SOFICA Model 42 000 PGD at 30°C using special, perfectly cylindrical glass cells. The scattering cell is set in a vat of benzene and the entire interior surface of the vat, except for the entrance windows for the incident beam and an observation port, are blackened. A special light absorbing glass is located opposite the entrance window to serve as a trap for transmitted light without reflection. Part of the scattered light receiver also sits in the vat liquid and the entire receiver assembly is rotated about the scattering cell for angular measurements from 30° to 150°. Extraneous light reflected from internal surfaces should therefore be negligible provided the benzene in the vat is kept clean. The refractive index of the glass of the measuring cell is 1.482 compared to 1.520 for benzene so reflections at the benzene/cell interfaces can be neglected. The refractive index of 1.0 M $NaNO_3$, which was the solvent in most solutions, is 1.3411. As the fraction of light reflected at the glass/solvent interface is only 0.0025, no allowance was made for it in subsequent calculations.

The instrument is supplied with a secondary standard of high density flint glass to avoid the problem of having a fresh supply of dust free benzene at all times. The glass standard was initially calibrated by reference to pure benzene, for which the Rayleigh ratio at 546 nm was taken as[120]:

$$R_{90} = 15.8 \times 10^{-6} \text{ cm}^{-1}$$

Glassware was carefully cleaned in chromic acid followed by thorough rinsing with distilled water and finally flushed with refluxing acetone shortly before use. Solutions were prepared in a manner similar to that used for viscosity measurements. Approximately 0.05 g of polymer was accurately weighed, dispersed in 75 mL of distilled water and dissolved by stirring gently for four hours. 100 mL of 2.000M $NaNO_3$ was added by pipette and the solution stirred for a further hour.

Aliquots of this solution were then diluted with 1.000 M $NaNO_3$ to give five solutions covering the concentration range 0.25 mg/mL to 0.05 mg/mL. All five solutions were placed in dialysis tubes and dialysed overnight in a one litre beaker of 1.000 M $NaNO_3$. The concentration of each solution was calculated from the known weight of polymer, its moisture content and the dilution factors.

Dust removal from solutions prior to the light scattering measurements proved to be an extremely difficult task. As discussed in later sections, filtration through membrane filters was found to be of no value as most of the polymer was retained by the membrane at least up to 3.0 μm membranes. Centrifugation was found to be the most effective procedure for removing dust from both solvent and solutions. For each run, the five solutions and a sample of the solvent from the dialysis were centrifuged simultaneously in a Sorval RC-5 centrifuge for one hour at 20 000 g. After centrifuging, a 25 mL aliquot was removed from the upper section of each tube using a clean pipette and transferred to a clean cell. Considerable care was needed to avoid disturbing the centrifuge tubes in the rotor and to ensure that no dust was collected during the transfer. The SOFICA photometer has a facility which allows each cell to be checked for dust before measurements are taken by viewing the cell directly from the 90° position. Solutions were discarded if any dust particles were present. Such was the difficulty in preparing dust-free solutions that, over the period of this work, at least half of the solutions prepared were discarded.

The Rayleigh ratio of each solution was then determined. A cell was placed in the photometer and set at an observation angle of 30°. The variable slit was adjusted to give a reading of about 80 per cent of full scale. A series of twelve readings were then taken over the range 30° to 150°. The cell was then replaced with the glass standard and the calibration factor noted for the particular slit position. For each solution, three such series of readings were obtained with the cell being rotated through 120° between each series. The depolarization ratio ρ_u was also measured for each solution but, as expected for high molecular weight polymers, was very low (<0.002). The Cabannes' factor calculated from (2.28) was less than 1.004 over the angular range 30°-150° so this correction was ignored.

The Rayleigh ratio for each solution was then calculated from the equation:

$$R_\theta = \frac{R_B}{I_b}\left(\frac{n_s}{n_b}\right)^2 \frac{\sin\theta}{1+\cos^2\theta}\,\frac{1}{t_s^2\,(1-4f_s^2)}\,(I_\theta - 2f_s\, I_{180-\theta}) \qquad (2.28)$$

where θ = angle of measurement

R_B = Rayleigh's ratio for benzene

I_b = relative scattered intensity for benzene

n_s = refractive index of solution

n_b = refractive index of benzene in which the cell is located

f_s = fraction of light reflected at the glass/solvent interface

t_s = $1-f_s$

$I_\theta, I_{180-\theta}$ = measured scattered intensities at forward (θ) and backward ($180-\theta$) angles corrected for solvent scattering and normalized using the calibration factor determined with the glass standard.

In this equation, the term $(n_s/n_b)^2$ represents the refraction correction for the volume viewed by the phototube.

A computer program was developed to calculate the values of $^c/R_\theta$ from the raw data using equation (2.28), and to plot the results according to the method described by Zimm. Details of the program are given in Appendix I. It was found that, whilst a linear extrapolation was satisfactory for data at constant angle, a second order extrapolation was necessary for data at constant concentration. The angular variation of K_c/R_θ frequently showed a sharp downward curvature above 120° so extrapolations to $\theta = 0$ were limited to $\theta < 120°$. The value of $(K_c/R_\theta)_{\substack{c\to 0\\ \theta\to 0}}$ determined Zimm plot was then used to determine the molecular weight, the second virial coefficient (B) and the radius of gyration (R_g) as described previously.

2.2.5 MEASUREMENT OF REFRACTIVE INDEX GRADIENT

An essential parameter in determining molecular weights by light scattering is the refractive index gradient (dn/dc) of the solute. Since the square of this term appears in equation (2.16) for the optical constant K, the accuracy of the molecular weight determination is strongly dependent on the accuracy of the measurement of (dn/dc). Refractive index gradients were therefore measured with a Ziess interference refractometer using a 10 cm cell. The instrument was calibrated using a series of aqueous KCl solutions. Polymer solutions were prepared by the method described in Section 2.2.4.

2.2.6 MONOMER SEQUENCE DISTRIBUTION

Some ^{13}C nmr spectra were obtained on a JEOL spectrometer at 15 MHz. When studying the carbonyl region spectra were obtained at 20°C but it was found that better resolution of the methine and methylene carbons was obtained at 90°C. A 90° pulse was used with a pulse delay of 4.2 seconds and spectral width of 500 Hz for the carbonyl region. For the methylene and methine carbons, the pulse delay was 0.8 seconds with a spectral width of 3 000 Hz. Most carbonyl spectra were obtained on a Bruker 300 at 20°C with a 45° pulse and a pulse delay of 5 seconds, although other values of these parameters were also used at times.

The viscosity of solutions of the commercial polymers is so high that above 0.5% w/w solutions cannot be poured or transferred to standard nmr cells. Test samples were therefore added directly to the cells and carefully dissolved in D_2O containing sufficient NaOH to ensure that the acrylic acid comonomer was completely neutralized. Despite prolonged ultrasonic irradiation for up to 96 hours, they remained as gels and it was found that a concentration of about 5% represented a practical limit. At higher concentration, the gels were visibly heterogeneous and it was extremely difficult to remove most of the air bubbles which appeared as samples were heated to 90°C.

The relatively low concentrations meant that long accumulation times were necessary and spectra were normally run for 16 hours. The resolution was still only fair making direct assignments of peaks difficult. Peak assignments were therefore made by reference to a series of low molecular weight polymers prepared under conditions of controlled hydrolysis. The preparation of these samples has been described in 2.1.2.

The kinetics of hydrolysis of polyacrylamide can be described in terms of three rate constants, as depicted in Figure 2.6, which also shows the six possible triad sequences viz. AAA, ABA, AAB≡BAA, ABB≡BBA, BAB and BBB.

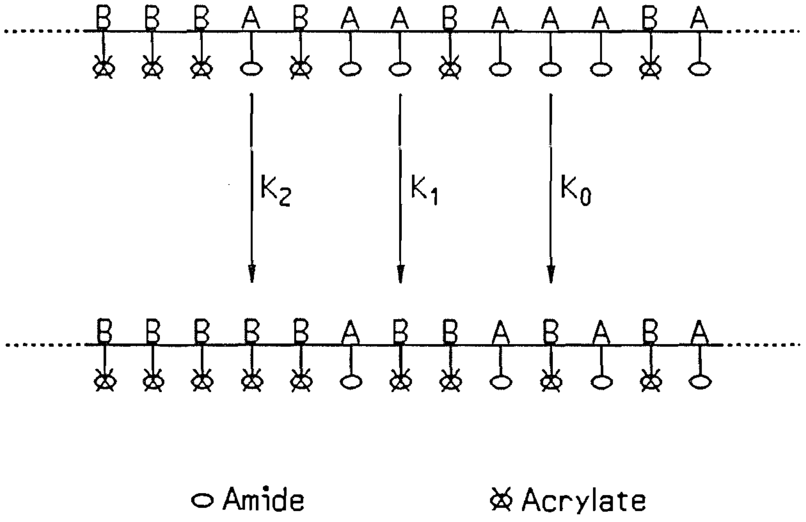

Figure 2.6 Kinetic Scheme for Polyacrylamide Hydrolysis.

Higuchi and Senju[92] have used this simple approach, in which only nearest neighbour effects are considered, to determine the ratios k_2/k_1 and k_1/k_0 under mild alkaline conditions. They found that, at 60°C in 0.5 M NaOH, k_1/k_0 was 0.19 while k_2/k_1 was 0.017 and demonstrated the existence of a conversion limit at approximately 61 per cent. Since the effect of a carboxylate group on the hydrolysis of neighbouring amide groups is considered to be due to the electrostatic repulsion between the ionized group and the hydroxyl group, it should be strongly influenced by ionic strength. Higuchi's results show that the ratios k_1/k_0 and k_2/k_1 decrease as both temperature and ionic strength decrease.

In the early stages of reaction, the rate of hydrolysis can be described by the equation:

$$\frac{dx}{dt} = k_0(a - b.x)(OH^-) \qquad (2.1)$$

where a = initial concentration of amide ($mol.L^{-1}$)
x = concentration of carboxylate ($mol.L^{-1}$)
t = time (s)
b = $3 - 2\ k_1/k_0$

The data obtained during the preparation of hydrolysed polymers were plotted according to this equation to determine k_0 and k_1/k_0. When b = 3, a linear plot was obtained for ln (1-b.x/a) against time, as Figure 2.7 shows. The value of k_0 from the graph is 4.95×10^{-4} mol. L^{-1} s^{-1} which is in good agreement with Higuchi's value of 5.10×10^{-4} mol. L^{-1} s^{-1}. The value of b equal to 3.0 also indicates that k_1/k_0 must be essentially zero. The results further indicate a conversion limit of about 45 per cent hydrolysis.

Since the values of k_1 and k_2 are insignificant at 50°C with 0.25 M NaOH, the formation of ABB and BBB triads should be negligible and the polymer should develop a regular sequence of carboxyl groups tending towards an alternating copolymer as hydrolysis proceeds towards 50 per cent.

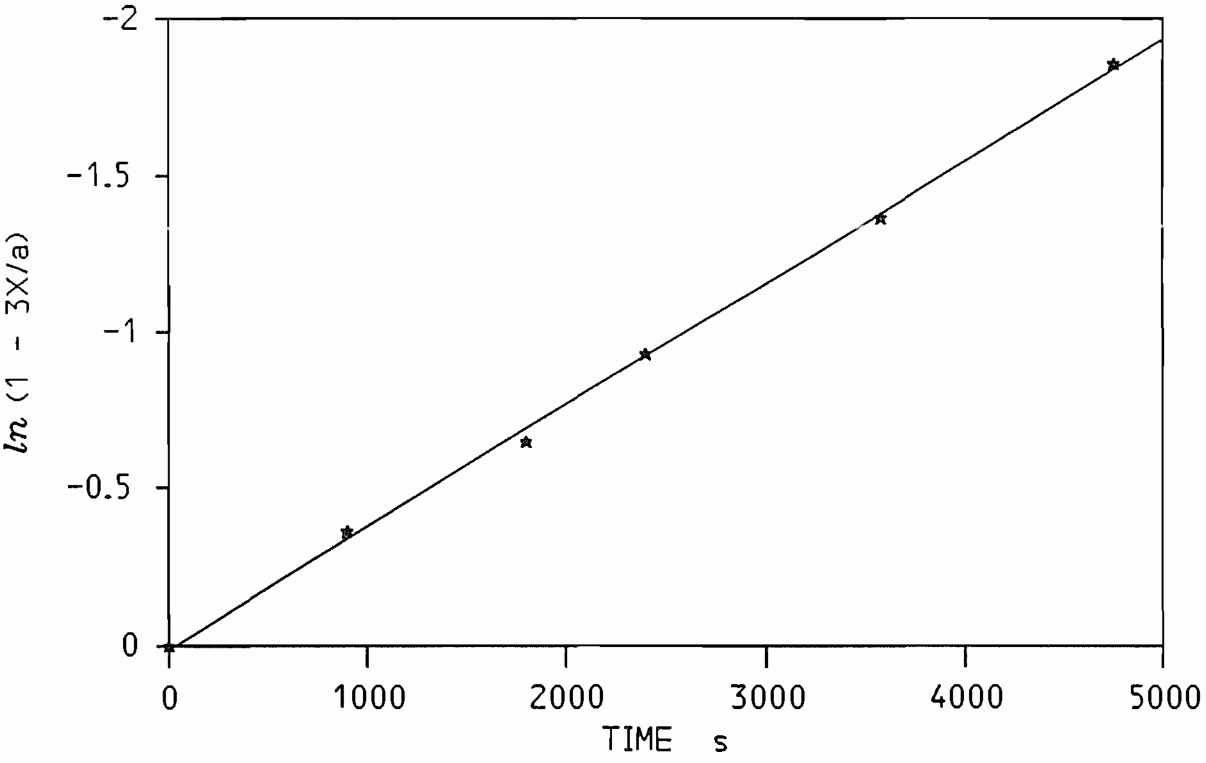

Figure 2.7 Rate of Hydrolysis of Polyacrylamide at 50°C in 0.025 M NaOH.

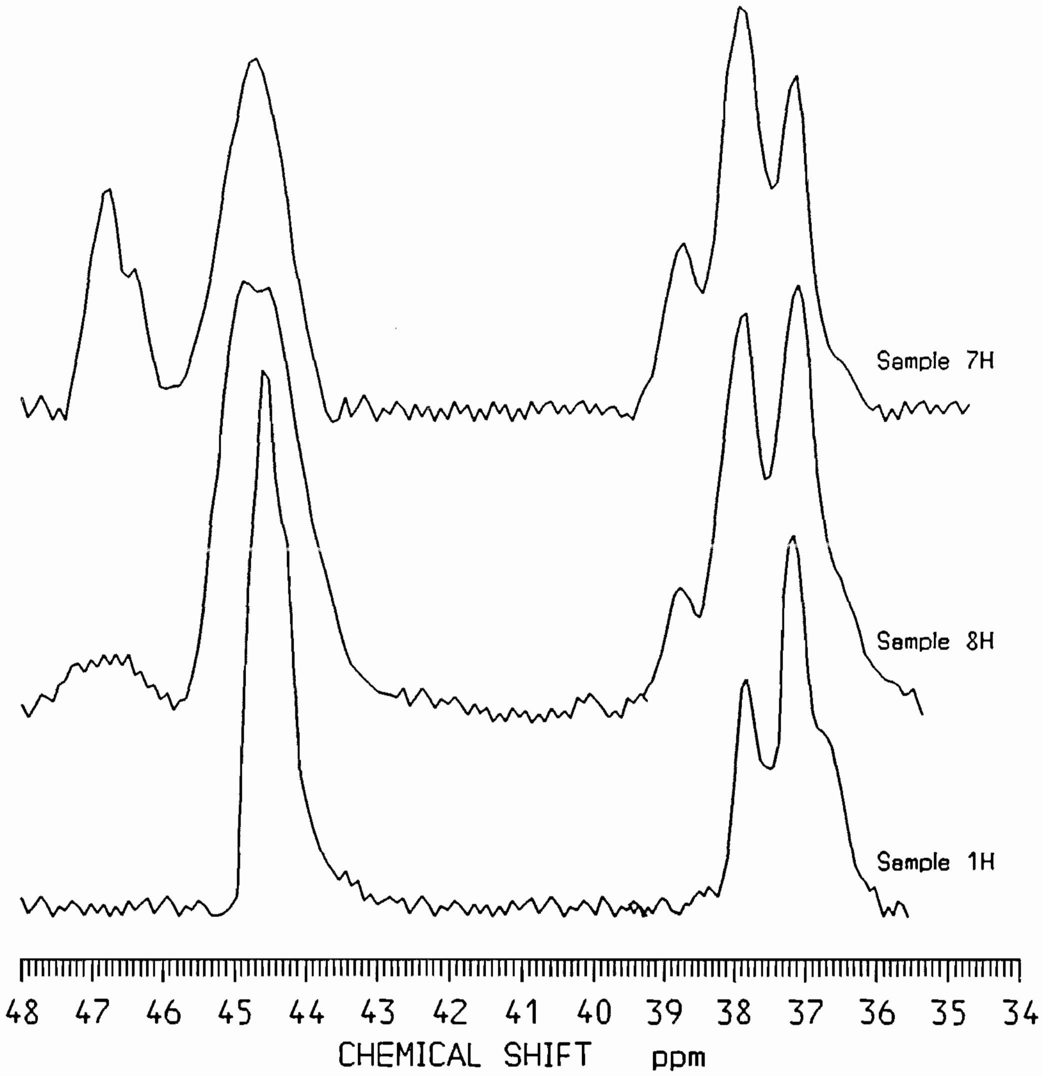

Figure 2.8 Methylene and Methine Spectra of Hydrolysed Polymers.

(a) Sample No. 1H, 0% hydrolysed
(b) Sample No. 8H, 10% hydrolysed
(c) Sample No. 7H, 33% hydrolysed

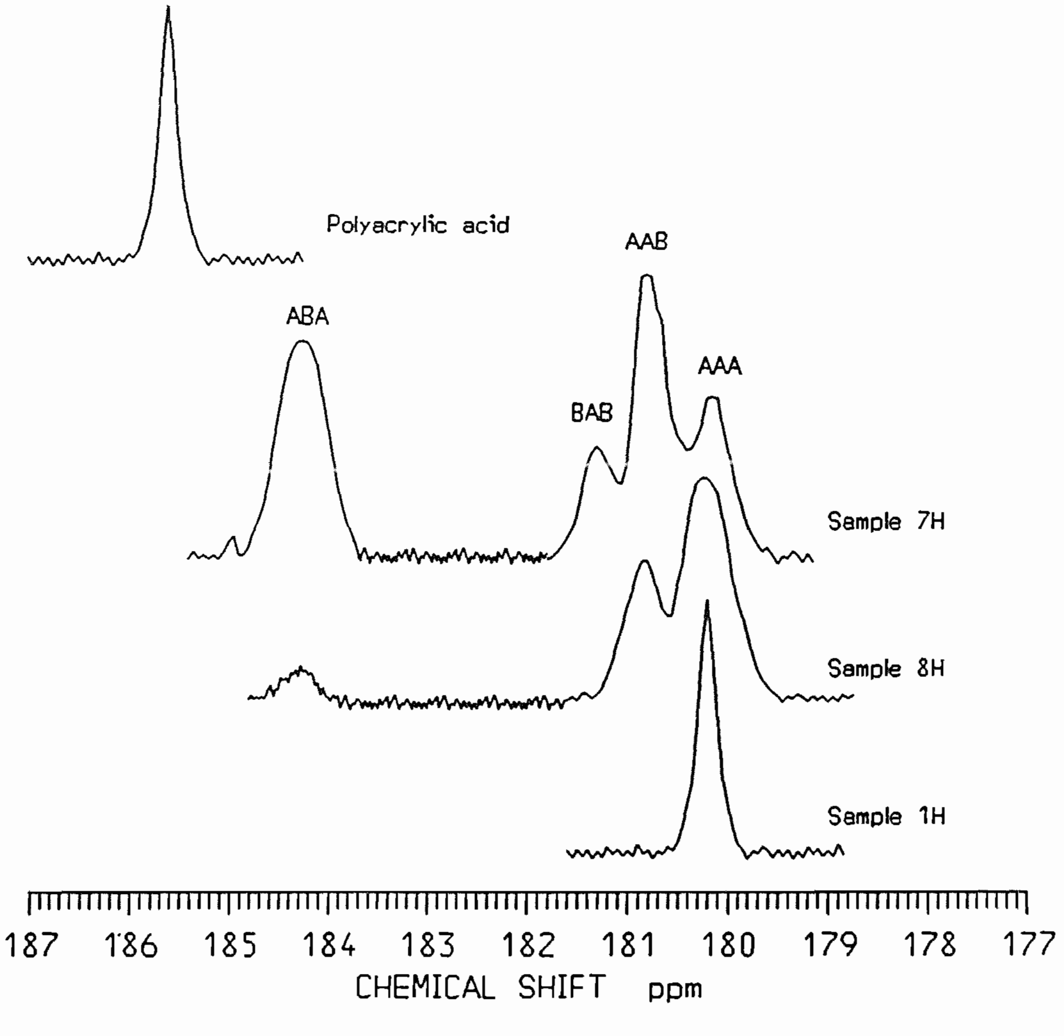

Figure 2.9 Carbonyl Spectra of Hydrolysed Polymers.

(a) Sample 1H
(b) Sample 8H
(c) Sample 7H
(d) Polyacrylic Acid

The spectra for the laboratory prepared, low molecular weight samples were obtained under the same conditions as for the commercial polymers except that solutions were prepared at a concentration of 30% W/W. The methylene and methine spectra for three of the samples are shown in Figure 2.9. The methines of the acrylamide and the acrylate are easily identified and show no splitting. In the methylene region, from 36 to 38 ppm, there is some splitting even in the acrylamide homopolymer, presumably due to tacticity effects. It is obvious that the peak at 46.7 ppm corresponds to the -CH- of the acrylate monomer while the one at 44.3 ppm must correspond to the -CH- of the amide. Although the peaks are influenced by the hydrolysis, the added complication of tacticity makes resolution of sequences difficult. One very useful aspect of this region of the spectrum is that integration of the peaks can provide an internal measurement of the copolymer composition. When the methine peaks are used for this purpose, the results are in good agreement with those obtained by titration, as Table 2.2 illustrates for the three polymers shown in Figure 2.8.

Prospects for determining monomer sequence are better in the carbonyl region. Figure 2.9 shows the carbonyl spectra for the samples referred to above together with a sample of low molecular weight polyacrylic acid kindly supplied by Daiichi Kogyo Seiyaku. Resolution of sequence distributions is possible to triad level and most of the data have been collected in this region. Peak assignments can be made for all triads except ABB, which are not expected from the kinetics of hydrolysis, and which are not evident in Figure 2.9.

Table 2.2 Comparison of Results for Copolymer Composition.

Sample	Ionic content (mol%)	
	by titration	by nmr
1H	0.0	0
8H	10.4	9.4
7H	33.0	32.2

2.3 ZETA POTENTIAL OF CANE MUD PARTICLES

The electrophonetic mobilities of cane mud particles were measured using a Rank Particle Microelectrophoresis Mk 11 instrument manufactured by Rank Brothers, Cambridge, England. In this apparatus, the velocity of charged particles under the influence of an applied electric field is measured by direct observation using dark field illumination. The electrophoretic mobility can be then calculated from the equation:

$$u = \frac{V \cdot l}{E} \qquad (2.29)$$

where u = electrophoretic mobility ($cm^2\ s^{-1}\ V^{-1}$)
V = particle velocity ($cm\ s^{-1}$)
l = electrical length of cell (cm)
E = applied potential (V)

Both $Ag/AgCl/Cl^-$ and blacked platinum electrodes were available although only the platinum electrodes were used in this work. A cell of rectangular cross-section was used to eliminate the effects of particle sedimentation during measurement. For such cells, the electrical length (l) is determined from the equation:

$$l = R \kappa A \qquad (2.30)$$

where R is the electrical resistance of the cell when filled with a solution with a specific conductance of κ, and A is the cross-sectional area. For the cell used throughout this work, the value of l was 7.056 ± 0.006 cm. This value was checked by measuring the electrophoretic mobility of human red blood cells, which is known to be $1.31 \times 10^{-6}\ cm^2\ s^{-1}\ V^{-1}$ in M/15 phosphate buffer at pH 7.3[121]. The value measured on this instrument was $(1.31 \pm 0.06) \times 10^{-6}\ cm^2\ s^{-1}\ V^{-1}$.

The relationship between the electrophoretic mobility and zeta potential for non-conducting spheres has been given as:[122]

$$\zeta = \frac{6 \pi \eta u}{R F D} \qquad (2.31)$$

where ζ = particle zeta potential
η = viscosity of liquid phase
D = dielectric constant of liquid phase
R = relaxation correction
F = correction for distortion of the electric field

For particles with zeta potentials less than 25 mV the relaxation effect is negligible and $R = 1$. Furthermore, when the Debye-Huckel parameter (κ) and the particle radius (a) are such that $\kappa a > 300$, the factor F becomes equal to 3/2. Equation 2.31 then becomes:

$$\xi = \frac{4 \pi \eta u}{D} \qquad (2.32)$$

For a typical Australian cane juice containing 15 per cent sucrose by weight and with an ionic strength of approximately 0.3 m, the value of κ has been calculated to be $1.8 - 1.95 \times 10^7$ cm^{-1}, depending on the temperature. The product κa will therefore be >300 provided the particle radius is >165 nm, a condition which is easily satisfied. Equation 2.32 has thus been used throughout this work to calculate zeta potentials. For typical cane juices encountered in Australia, 2.32 becomes:

$$\xi = 1.90 \times 10^5 \ u \qquad (2.33)$$

with ξ in mV when u has units of $\text{cm}^2 \ \text{s}^{-1} \ \text{V}^{-1}$.

When determining electrophoretic mobilities by direct observation in the Rank apparatus or similar equipment, it is essential to also consider the electro-osmotic movement of the liquid phase relative to the walls of the cell towards one of the electrodes. If the cell is sealed at each end, there must also be a return flow so that the nett transport of liquid is zero. When the two effects are combined, the result is a parabolic velocity profile in which there are two points where the velocity of the liquid is zero (Figure 2.10). Measurements of particle velocities are therefore conveniently made at these points, which are referred to as stationary levels. For cells of rectangular cross-section as used here, the locations of the stationary levels are calculated from:

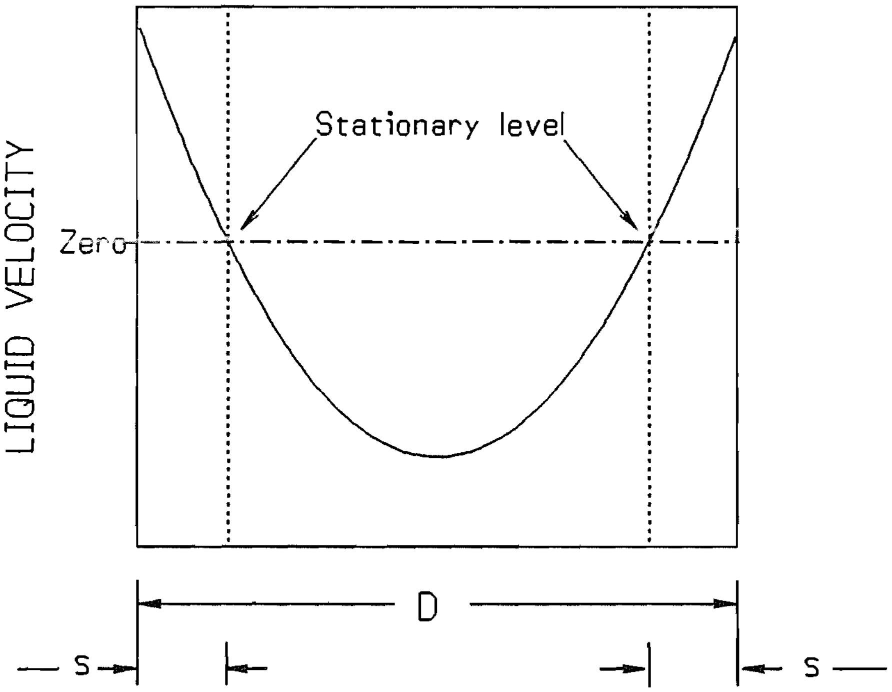

Figure 2.10 Velocity Profile in Rectangular Cells.

$$\frac{s}{D} = 0.500 - \left(0.0833 + \frac{32D}{\pi^5 h}\right)^{\frac{1}{2}} \qquad (2.34)$$

where s and D are defined in Figure 2.10 and h is the vertical height of the cell.

A laboratory procedure which accurately simulates the relevant section of the normal factory operation was used to prepare samples of muds for the electrophoresis experiments. A large sample of juice at 75°C was obtained from the factory and divided into a number of sub-samples which were held at 75°C in a water bath until required. When a sample was removed from the bath, its pH was immediately adjusted by the addition of a predetermined volume of lime saccharate with vigorous stirring for a few seconds before being boiled for three minutes. The laboratory procedure simulating the factory clarification process is described in more detail later.

With both the cane juices and the model particle systems, the particle concentrations were too high for direct observation in the electrophoresis cell. Dilution was achieved by allowing the coagulated particles to settle then decanting the clear supernatant. A few drops of the settled solids were then redispersed in this liquid. Particle numbers were thus reduced to practical levels for observation but were still dispersed in their original liquid phase.

It was found to be impractical to measure particle velocities at elevated temperatures because of the effects of convection due to small variations in temperature and the difficulties in eliminating leaks from the electrode compartments of the cells. The samples were therefore quickly cooled to 30°C and the electrophoretic mobilities measured at the maximum voltage which could be applied without visible gassing at the electrodes. Velocities were determined at both stationary levels of the cell, with the polarity of the applied field reversed between successive readings. Approximately 50 particles were observed in each direction at each stationary level making a total of about 200 measurements for each sample. The mean electrophoretic mobility and zeta potential were then calculated using equations (2.29) and (2.31).

Reversible electrodes are often preferred when gassing is likely to disrupt measurements. A pair of Ag/AgCl electrodes was obtained from Rank Brothers and used for some measurements. However the KCl salt bridge, which consisted of a porous glass frit at the bottom of the electrode chamber, was prone to frequent blocking by waxes in the juice and the electrodes proved to be unsuitable for this application. Blacked platinum electrodes were subsequently used for all other experiments.

2.4 MEASUREMENT OF FLOCCULATION EFFICIENCIES

The rate of a flocculation or coagulation can be studied by direct particle counting techniques or by observation of some indirect property of the state of aggregation of the system. The method employed is usually determined by the aims of the particular process under examination. Particle counting techniques are restricted by the sizes of the particles and aggregates, generally employing either a Coulter counter or a microscopic procedure, and are relatively slow. They are unsuitable for most situations where bridging flocculation occurs because of the large size of the aggregates formed and the rapid rate of reaction. It is more common to use one or a combination of the many indirect techniques available. Slater and Kitchener[123] have compared several empirical procedures including sedimentation velocity, specific sediment volume, supernatant turbidity and refiltration rates and suggested that they all lead to similar conclusions in many instances. However it has also been recognised[124] that these tests are not universally valid and do not necessarily give meaningful information on the effectiveness of flocculation. It is essential that the techniques empolyed are relevant to the specific aims of the process being investigated and the equipment available to achieve those aims. Interpretation of the results must be viewed in a similar context.

In the operation of a sugar factory clarifier, the prime aim is to produce clarified juice of the lowest possible turbidity. At the same time, it is essential to maintain a high rate of sedimentation although not at the expense of any increase in turbidity. These two criteria have therefore been used throughout this work to assess the effectiveness of flocculation.

Ideally, turbidity measurements should be made using a nephelometer or similar instrument in which the intensity of light scattered by the particles is observed at an angle (preferably 90°) to the incident beam. Unfortunately, convenient laboratory instruments capable of accepting samples at or near 100°C are not available. Furthermore, a great number of experiments were conducted on site in factories throughout Queensland where laboratory facilities were often limited and it was necessary to use laboratory spectrophotometers to measure absorbance rather than turbidity. A wavelength of 800 nm is used in Australian sugar mills for this purpose, having been shown[85] to be largely independent of the colour of the juice. In keeping with this practice, throughout this thesis the turbidity of clarified juice has therefore been defined as:

Turbidity = 100 A
where A = the absorbance at 800 nm in 1 cm glass cells with distilled water as the reference.
(2.35)

The particle concentration and extent of flocculation observed in Australian raw sugar factories is such that the aggregates do not settle independently. There is considerable interaction between them with the result that sedimentation is characterised by a clearly defined interface between the mud and the supernatant. This phenomenon has been described[143] as 'hindered settling'.

The settling rate is initially constant but decreases as thickening becomes significant. Since the initial settling rate rather than the thickening rate is the critical variable in the design and operation of factory equipment, the test procedure employed has been designed specifically to determine this parameter. Experience gained during the project has demonstrated that it provides a reliable and quantitative estimate of actual factory performance and can be used to obtain accurate basic data for equipment design purposes.

The sedimentation rate or settling rate of flocculated muds was measured in a batch test procedure using the apparatus illustrated in Figure 2.11. It comprises a perspex fronted

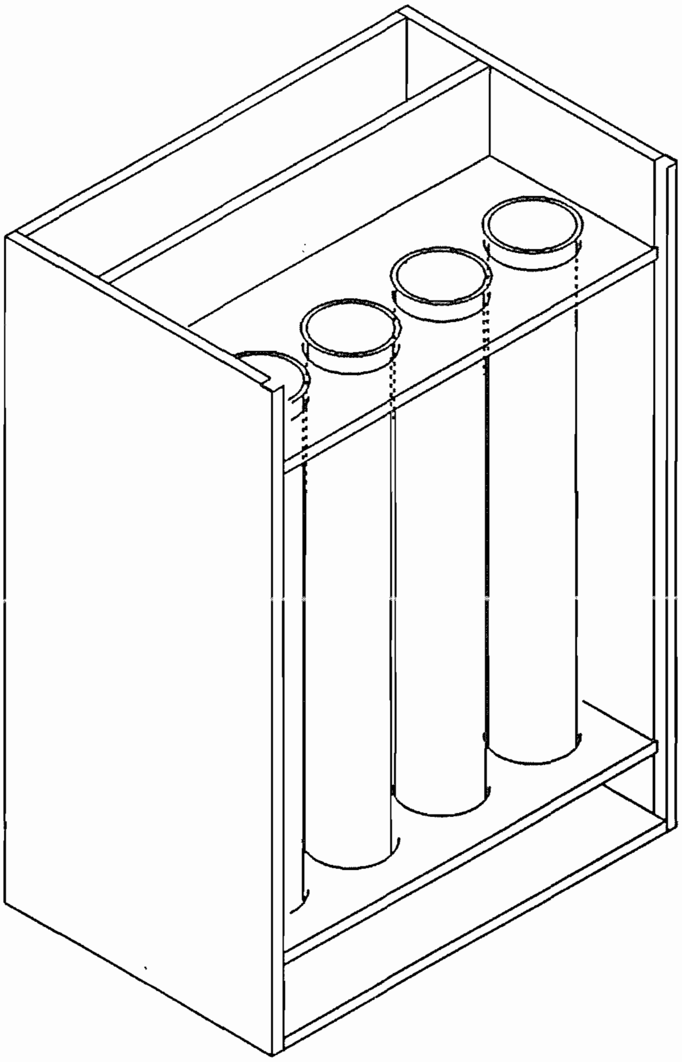

Figure 2.11 Apparatus for Batch Settling Tests.

timber box in which four calibrated glass settling tubes are suspended from perspex inserts. Behind each tube is a 450 mm long 53 watt incandescent lamp which provides illumination. More importantly, the lamps generate sufficient heat to maintain a temperature close to 100°C within the box. Heat transfer to and from the settling tubes is so low that no thermal convection was observed during the tests. Each settling tube is 450 mm long and is calibrated 0 to 100% over a length of 400 mm. Tubes of 56.5 mm internal diameter with a working volume of one litre were used in most experiments. On occasions when the clarifed juice turbidity was high and the interface was difficult to observe, 40 mm diameter tubes were used. In general, however, the flocculated aggregates were so large that they would not settle in the smaller tubes until they had been deliberately broken.

If batch settling tests with juices are to accurately reflect the operation of real factory equipment, it is essential that they are conducted with minimum delays. They were therefore carried out within the factory, as close as possible to the clarifier. Solutions of test flocculants were prepared at 0.1% by weight if they were to be used within 24 hours. For longer series of experiments, stock solutions were prepared at 0.5% and stored in a refrigerator. Fresh solutions at 0.1% were prepared daily by dilution of the stock solutions.

All tests were performed in sets of four (the number of tubes in the apparatus) with a fresh sample of juice for each set. Four one litre polypropylene measuring cylinders and four three litre polypropylene beakers were set in front of the test apparatus and the required aliquot of 0.1% flocculant solution added to each beaker with a disposable plastic syringe. Syringes were found to be far more accurate than pipettes for this purpose due to the high viscosity of the solutions.

A large sample (approximately six litres) of juice was obtained from a convenient sample point between the mill flash tank and the clarifier (see Figure 1.3). At this point, the juice has been limed, superheated and flashed to atmosphere so that the samples collected were free of dissolved gases, at a constant temperature of 100°C and constant pH (typically 7.6 ± 0.1). The measuring cylinders were quickly filled and the contents of one cylinder poured into the first beaker. After stirring gently for 10 seconds with a broad spatula, the flocculated juice was poured carefully into the first settling tube and a stopwatch started. The procedure was repeated for each of the remaining tubes at intervals of precisely 30 seconds. The level of the mud interface in each tube was noted at 0.5, 1.0, 2.0 and 3.0 minutes after filling. Levels were recorded for longer periods when necessary but this occurred only rarely.

As with most other experimental procedures used to examine flocculation phenomena, some operator experience is required to obtain reproducible results. With practice, a set of four tests could be completed within six minutes of collecting the initial sample with satisfactory reproducibility of results. At the end of each set, aliquots of about 20 mL were withdrawn from the supernatant and their turbidities measured as described previously. When large numbers of experiments were conducted, there were sometimes variations in juice characteristics, generally outside the control of the operators, during the period of the tests. To overcome the effect on experimental results, only one of the set of four parameters was changed for the next test. In this way, a number of comparative results were obtained for each parameter. For each individual test, the initial settling rate was then obtained from a graphical analysis of the data.

2.5 RESIDUAL POLYMER CONCENTRATIONS

The determination of adsorption isotherms for polyacrylamides during the flocculation of cane muds and of the model particle systems requires the determination of polymer concentrations at levels below 5 ppm and frequently below 1 ppm. Except in the model systems, this must be achieved in a process solution which contains a complex mixture of natural polymers and other solutes, many of which contain amide or carboxylic acid functionality at concentrations far in excess of the residual polyacrylamides.

There have been numerous procedures described in the literature for the determination of polyacrylamides in aqueous solutions at concentrations below 10 ppm. Those which rely on the determination of the component elements nitrogen, carbon and oxygen are quite clearly inappropriate for cane sugar juices and no attempt was made to evaluate any of them. Methods in which specific reactants are added to form complexes with either the amide or the carboxylic acid functional groups of the polymer would undoubtedly suffer interference from the naturally occurring polymers present in the juice. Nonetheless, turbidimetric methods based on the reactions of anionic polyelectrolytes with tannic acid, Hyamine 1622 and chitosan were considered.

Tannic acid precipitates only polyacrylamides containing little or no acrylic acid comonomer[125]. Since almost all of the polymers used here contained at least 15 mol % acrylic acid, this method was of no value. The determination of polyacrylamides in distilled water by precipitation with Hyamine 1622 has been described by Crummett and Hummel[126]. Their procedure has been used successfully only in distilled water and suffers severe interference from cations, particularly calcium. Even domestic tap water contains unacceptable levels of calcium. In evaluating this technique, it was found that pretreatment of samples with weak or strong cation exchange resins to remove interfering ions also lead to a variable loss of polyacrylamide. While the loss may be acceptable at high polymer concentrations, it introduced an appreciable error in the concentration range of interest here.

The reaction of hydrolysed polyacrylamides with chitosan has already been described in a procedure to estimate the anionic content of flocculants (see 2.2.2). It should also be possible to employ the reaction to determine polymer concentrations if due allowance is made for the anionic content. As with the Hyamine 1622 procedure, the chitosan method was found to be useful in distilled water at concentrations as low as 0.2 ppm with an accuracy of approximately 7%. Unfortunately, it suffers similar problems with interferences from simple cations. The end-point colour change disappeared completely at a sodium chloride concentration of <0.02M which is well below the ionic strength of cane juices (typically 0.3M).

Other methods which have been reported include scintillation counting of ^{14}C labelled polymer[127], polarography[128], viscometry[128] and flocculation of solids added to the supernatant[129]. None of the methods discussed was considered satisfactory for use with cane juices. Indeed, very few are useful even with simple laboratory systems where bridging flocculation occurs. An alternative method has been devised which is suitable for concentrations below 5 ppm. Although developed specifically for use with cane juices, it has been used with the model systems and can be easily applied to almost any other process stream or laboratory study.

Early in the course of the factory experiments, it became evident that the presence of traces of residual flocculant in raw sugar could be detected by the celite filtrability test which is used by the Australian industry as one of its quality control parameters. In this test, the filtration rate of a concentrated sugar solution through a bed of celite filter aid is compared with the rate for a solution of pure sucrose. In its standard form[130], the test was found to be sensitive to the presence of flocculants containing less than 20 mol % acrylic acid at levels of 0.1 ppm. It was almost completely unaffected by up to 5 ppm of more anionic polymers. However the response was also dependent on pH and a uniform response was achieved at pH 7.0 ± 0.1.

To determine the filtrability of a sample of juice, about 300 mL collected from the top of a settling tube was centrifuged at 3000 g to remove any residual insoluble solids. The supernatant was cooled to 20.0 ± 0.1°C and an aliquot of 200 ± 0.1 g weighed out. The pH was adjusted to 7.0 ± 0.1 with a few drops of 0.10 M HCl. The solution concentration was measured using a refractometer calibrated for sucrose and sufficient pure sucrose added to increase the concentration to 60.0 ± 0.1 % by weight. For experiments on model particle systems, the initial concentration was zero so 300 ± 0.1 g of sucrose was added to each 200 g aliquot of supernatant. The solution was stirred for 30 minutes to dissolve the added sucrose after which 1.15 g of standard celite filter aid was added and the solution stirred for a further 12 minutes. After standing for 15 minutes, the filtration rate was measured by filtering through a Whatman No. 54 filter paper at a pressure of 345 kPa in the standard CSR apparatus[130].

The filtrability of the sample was then expressed as a percentage of the filtration rate of a pure sucrose solution under the same conditions. Since the original procedure is used throughout the Australian sugar industry, the data for pure sucrose solutions is available in reference tables which correspond to previously calibrated batches of celite. Complete details of the standard procedure on which the method is based are given in reference 130.

The filtration rate is sensitive to variations in temperature due to the effect on solution viscosity. Correction factors are available but were not applied here because each series of tests was performed at a constant temperature and separate calibrations curves were prepared for each new sample of juice.

When conducting experiments to measure the adsorption of polymers during bridging flocculation, approximately 10 L juice was collected and the required batch settling tests performed immediately as described in 2.4 above. At the end of each set, samples of supernatant were withdrawn and stored in sealed flasks. The flasks and the remainder of the initial sample were then taken to the factory laboratory for further analysis. The sample of original juice was centrifuged and used to prepare standard curves of filtrability as a function of polymer concentration for each of the flocculants used.

For a constant pressure filtration process such as the filtrability test, the rate of filtration can be described by a form of the Darcy equation[144]:

$$\frac{t}{M} = \frac{\alpha\mu CM}{2pA^2\rho^2} \qquad (2.35)$$

where α = specific cake resistance
μ = filtrate viscosity
ρ = density of filtrate
C = solids concentration
M = mass of filtrate collected
t = time
p = applied pressure
A = area of filter

From this equation, it can be shown that the filtrability (F) as defined above is related to the specific cake resistance by a simple relation:

$$F = M/M_o$$

$$= (\alpha_o/\alpha)^{0.5} \qquad (2.36)$$

from which

$$\alpha = \alpha_o/F^2 \qquad (2.37)$$

The specific cake resistance obtained for pure sucrose solutions (α_o) is constant at constant temperature. It can be readily calculated from tabulated data but its absolute value is as a function of the concentration of flocculant as illustrated in Figure 2.12. Within the errors of the method, the lines obtained for different polymers were the same for a particular juice although different curves were obtained for different juices. To overcome this difficulty, new calibration curves were prepared for each new sample of juice. The concentrations of residual polymer in the samples of supernatants were then determined by reference to the standard graphs.

2.6 MODEL PARTICLE SYSTEMS

The chemical and surface properties of cane muds in the actual factory environment could not be characterised as completely and accurately as many other particle systems. A number of model particle systems were prepared with electrokinetic properties similar to cane mud but with precise chemical compositions and surface properties which could be accurately characterised.

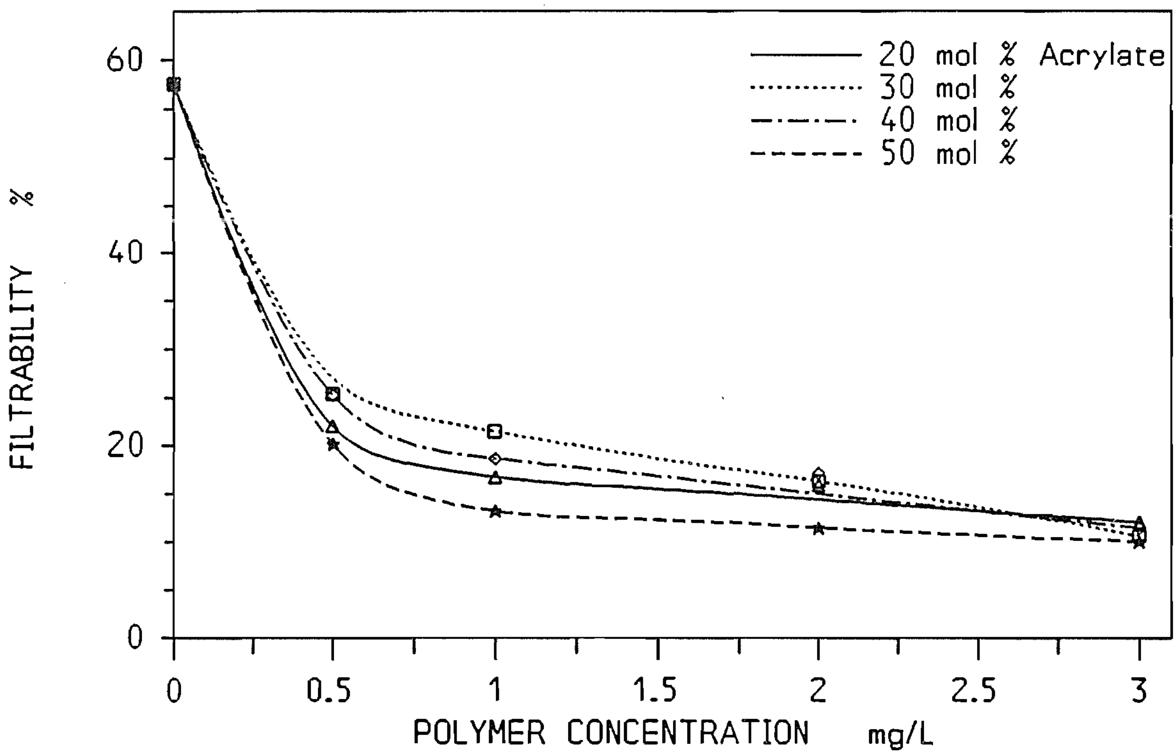

Figure 2.12 Typical Calibration Curves for Polymer Concentration Measurements.

For any model system to provide data which can be compared directly with the behaviour of cane muds, the particle charge must be negative and should result from the dissociation of fixed carboxylic acid groups at the surface[84] rather than from fragments of initiator or the adsorption of surface active agents.

The density and size of the particles should be such that the kinetics of polymer adsorption, bridging flocculation and sedimentation should be of the same order as for cane muds. If not, the interpretation of data is likely to be confused by differences in the rates of one or more of the steps in the reaction.

There are numerous publications which describe methods for the preparation and characterization of homopolymer and copolymer latices of varying sizes and size distributions. However, the bulk of the reports, and certainly most of those where ionic comonomers are included in the latex, refer to latices based on the polymerization of styrene. Preparation of model particle systems based on polystyrene latices would be expected to be a relatively straightforward procedure whereas a novel system which satisfies all of these requirements listed above may well be a major project in itself. Consequently, the model systems prepared and evaluated here were all based on the polymerization of styrene and its derivatives with comonomers containing carboxylic acid functional groups.

2.6.1 PREPARATION OF ANIONIC POLYSTYRENE LATICES

A procedure has been described by Hen[131] for the preparation of styrene/itaconic acid latices of narrow size distribution. Particles of different sizes were obtained when different emulsifiers were used to stabilise the initial dispersion of monomers in an aqueous continuous phase. A latex prepared with sodium dodecylsulphonate as the emulsifier had a mean particle diameter of 68 nm with 60 % of the itaconic acid monomer present as fixed groups at the particle surface. The use of sodium dicyclohexylsulphosuccinate as the emulsifier resulted in larger particles (308 nm) but the proportion of itaconic acid fixed at the surface declined to < 25%.

A number of latices were prepared by a method similar to that described by Hen but using lower concentrations of sodium dicyclohexylsulphosuccinate as emulsifier. The reaction mixture was prepared by adding a predetermined amount of itaconic acid to 200 g of double distilled water containing 0.30 g of potassium persulphate, 20 g of freshly distilled styrene, emulsifier and sufficient dilute sulphuric acid to bring the pH to 1.20 ± 0.05. The mixture was placed in a glass screw-top bottle and purged with nitrogen for 10 minutes after which the lid was screwed on firmly and the bottle shaken vigorously for a further 10 minutes. The bottle was then placed in a water bath at 70°C and rotated at 50 rpm for 20 hours. The proportion of itaconic acid in the mixture was varied in six steps from zero to three per cent by weight of the total monomer. Three levels of emulsifier were used viz. zero, 0.2 and 0.4 g.

At the completion of the reaction, the latex was purified by dialysis against 0.005 M NaOH for seven days with daily changes of solution. The latex was then characterised and evaluated as a potential model for cane muds as described in the following section.

In addition to the variations in experimental procedures described above, a number of polymerizations were carried out in which the styrene was replaced with a molar equivalent amount of chlorostyrene. In a further series, the itaconic acid was also replaced with acrylic acid.

In all, a total of 64 different latex samples were prepared.

2.6.2 CHARACTERIZATION OF MODEL SYSTEMS

The number and nature of the surface charge groups were examined using both potentiometric and conductometric titration curves as described by Hen[131], Homola and James[132] and others[133,134,135]. Conductivity measurements were made with a Phillips PW9501 conductivity bridge using blacked platinum electrodes in a cell with a cell constant of 1.28. Potentiometric titrations were performed automatically using a Radiometer

PH26 pH meter and SBR2c Titrigraph. The use of the automatic titrator, which produced a graph of the progress of the reaction, was a very convenient method of performing titrations slowly and with very small increments to improve endpoint determinations.

The potentiometric method was found to be of little assistance due to the difficulties in determining the end points for the weakly acidic surface carboxylic acid groups[136]. All of the data reported here have therefore been obtained from conductometric titrations of the latices with dilute NaOH or HCl.

The electrokinetic properties were determined using the Rank Particle Microelectrophoresis apparatus described in section 2.3. One or two drops of the purified latex were added to a flask containing 200 mL of supporting electrolyte, shaken well to disperse the particles and allowed to stand for seven days. KCl was used as the supporting electrolyte at ionic strengths from 0.05 to 0.3 m. $CaCl_2$ was added at concentrations from zero to 0.010 m and the pH adjusted over the range 5.0 - 10.0 with HCl or KOH as required.

For the reasons discussed in the following section, approximate estimates of the mean particle sizes were obtained using an optical microscope but detailed particle size analyses were not carried out on any of the latices prepared.

2.6.3 BRIDGING FLOCCULATION OF MODEL SYSTEMS

The flocculation of the model particle systems based on the polystyrene latices was studied by observing the settling rate of the solids interface and the turbidity of the supernatant liquid as described in Section 2.4. The ionic environment employed initially was an aqueous solution containing 0.3 mol KCl and 0.01 mol $CaCl_2$ per litre, which provided an ionic strength and calcium concentration similar to cane juice[85].

In almost all of the latices prepared, it was possible to achieve bridging flocculation in which the final size of the aggregates approached that encountered in raw sugar factories.

However the rate of aggregate growth was invariably slower by at least an order of magnitude. Furthermore, the density of the particles prepared from styrene was obviously very slightly lower than the density of the supporting electrolyte as the aggregates floated very slowly (typically less than 1 mm/min). Particles prepared from chlorostyrene were sufficiently dense to settle rather than float but again the rates were only of the order of 10 mm/min.

In cane mud flocculation, the particle densities were much higher than the juice densities. The rates of flocculation were such that settling rates were generally greater than 20 cm/min and frequently exceed 40 cm/min. The differences between the two situations were so great that there was little to be gained from a detailed study of the sedimentation behaviour of these model particle systems.

Despite the inadequacies of the model systems for sedimentation experiments, they were nonetheless useful in the examination of polymer adsorption behaviour. The well characterised nature of their surfaces was important in the study of the mechanism of polymer adsorption, particularly the role of metal ions and the importance of the number and distribution of ionic groups within the polymer.

2.6.4 OTHER MODEL SYSTEMS

The polystyrene based particle models clearly had some serious deficiencies in this instance and proved to be unsatisfactory for the purposes required. For experiments where data were required on any kinetic, rather than equilibrium, aspects of polymer adsorption and aggregate growth during flocculation, two other model systems were employed. Previous work by the author[137] has shown that carefully prepared bentonite dispersions can be used to model some aspects of the kinetics of aggregate growth.

For experiments in which the specific aim was to study the interaction of metal ions in solution with the ionic functional groups of the polyelectrolyte and the particle surface, the weak cation exchange resin Biorex 70 was used as a model. This resin is a weakly acidic carboxylic acid and is stable up to 100°C. The particle size of the resin sample obtained was nominally 325 mesh (US Standard) and the particle density was sufficient for sedimentation to occur at rates of up to 20 cm/min when flocculated. No attempt was made to further characterize the particle size distribution or to separate the resin into narrow size fractions as this was considered to be irrelevant to the aims of the experiments.

CHAPTER 3

FLOCCULATION OF CANE MUDS

The relationship between the extent of bridging flocculation, the properties of polyacrylamide flocculants and the electrokinetic behaviour of cane muds has been explored extensively in both laboratory and factory experiments. Because of the variable nature of the cane muds entering a cane sugar factory, it has been necessary to perform a very large number of tests in almost all of the factories in Queensland. Nevertheless, a very definite pattern of behaviour has emerged and has been related to the more readily quantifiable properties of both the polymers and the muds.

On the basis of the results obtained in these experiments, a mechanism has been proposed for the action of partially hydrolysed polyacrylamides in flocculating cane muds. The mechanism is consistent with many aspects of other mechanisms previously described and discussed in Chapter 1 but differs from others proposed for bridging flocculation in that it places far greater emphasis on the role of the ionic comonomer. However, it is consistent with and supported by the results discussed in this chapter. Further support for the mechanism is presented in the subsequent chapters which describe the results of laboratory studies of specific polymer properties and of studies with model particle systems.

3.1 ELECTROKINETIC PROPERTIES OF CANE MUDS

The zeta potentials of a number of cane muds were measured as a function of juice pH at 12 different factories spread throughout Queensland using the procedure described in Section 2.3. It was found that, when the pH was adjusted by the addition of lime in the form of calcium saccharate to simulate normal factory operations (see 2.1.1), similar results were obtained at each of the factories within a particular region of the industry. However, there were substantial differences between these regions (Figure 3.1).

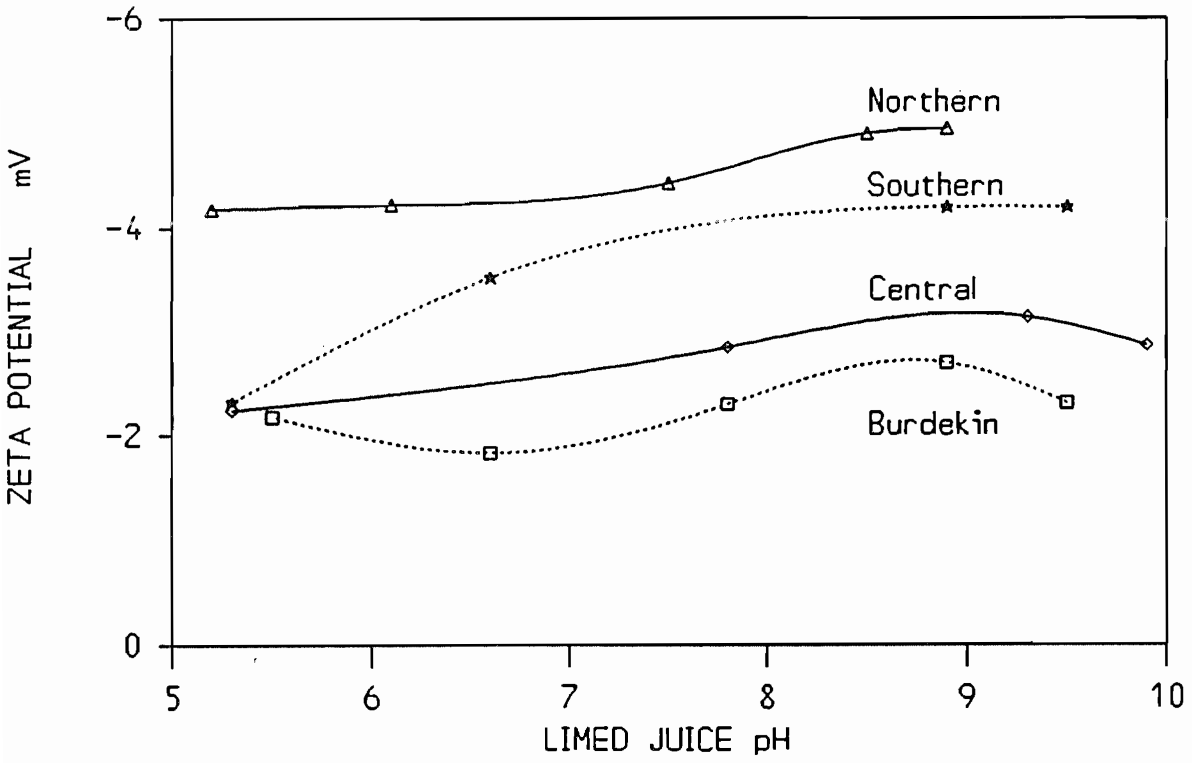

Figure 3.1 Zeta Potentials of Cane Muds in Different Mill Areas.

The values obtained were very low, which is consistent with the observation that the particles normally undergo spontaneous rapid coagulation. The slight increase in the magnitude of the potential with increasing pH may be due in part to the variation in the degree of dissociation of carboxylic acid groups in polysaccharides adsorbed by the calcium phosphate precipitate, and partly to the combined effects of pH and added calcium ions on the composition of the precipitated calcium phosphate. There were also small but significant differences between some factories. The importance of these factors will be discussed later in this chapter in relation to the performance of various flocculants.

No attempts were made to determine the surface charge by other experimental means. Any such measurements would have to be made under experimental conditions so different from those encountered in the remainder of the work that they would have little or no relevance. Although it may be possible to calculate estimates of the surface charge density from the measured zeta potentials, there was little to be gained by doing so.

It has been well known within the sugar industry for many years that adequate concentrations of both calcium and phosphate ions are essential in achieving a high standard of clarification. Their effects on the coagulation of muds have been examined by Bennett[139] but there have been no previous attempts to relate these observations to the electrokinetic properties or to bridging flocculation. The effect of phosphate concentration on zeta potential was examined by adding dilute phosphoric acid to aliquots of juice before heating and liming to the normal factory level of pH 7.6 as above. The results shown in Figure 3.2 were obtained at factories in the Northern and Burdekin regions with juices whose initial phosphate contents varied from 2.35×10^{-3} to 3.90×10^{-3} M as PO_4^{3-}. The juices used in these experiments were not those described in Figure 3.1 so the data cannot be compared directly.

The results suggest that the higher zeta potentials correspond to lower initial phosphate contents. More importantly in this instance, the addition of phosphate to juices with higher zeta potentials leads to a substantial decrease in zeta

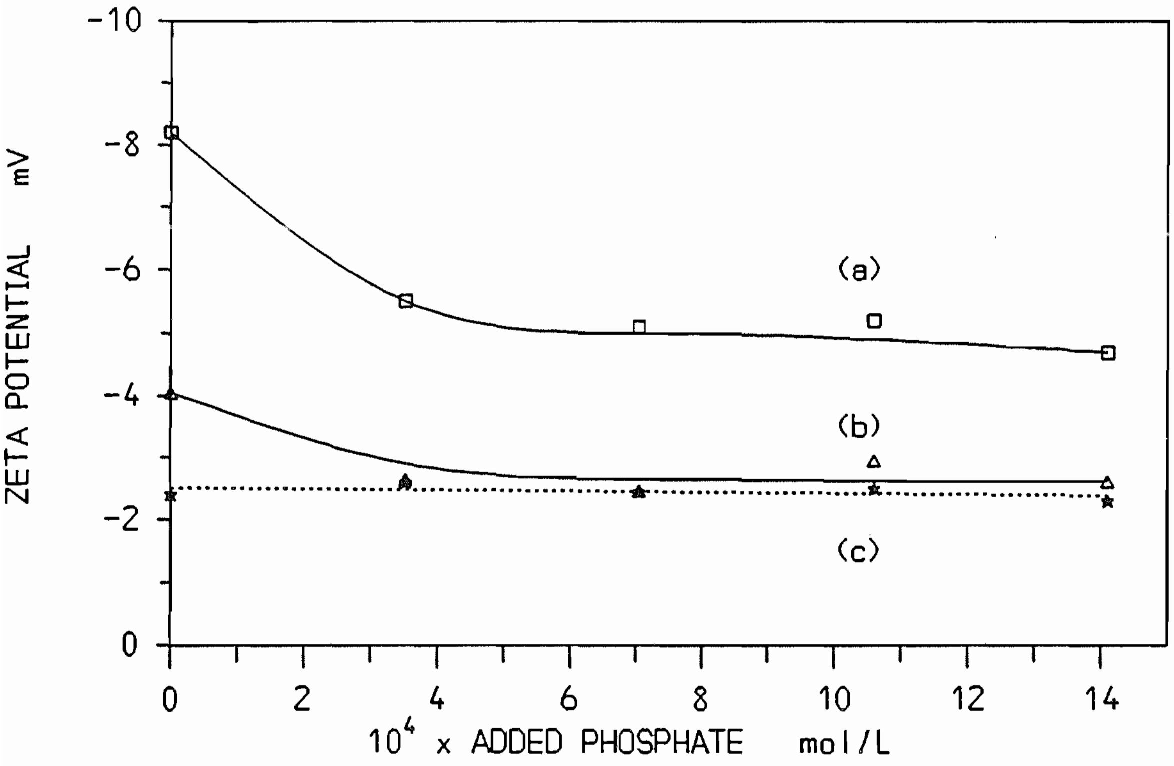

Figure 3.2 Effect of Added Phosphate on Zeta Potentials of juices with an initial PO_4^{3-} content of:

(a) 2.3×10^{-3} M

(b) 3.1×10^{-3} M

(c) 3.9×10^{-3} M

potential. However it is also important to note that, with the highest zeta potential, quite large amounts of additional phosphate were required to reduce the zeta potential to the normal level for the region. At the highest initial phosphate concentration, which occurred in the juice from the Burdekin region, the addition of more phosphate has no noticeable effect on the zeta potential.

It would be easy to postulate from these results that the zeta potential is controlled by the phosphate concentration in the juice. While this is undoubtedly so in many cases, an exhaustive study of phosphate levels and zeta potentials would be required to confirm a quantitative relationship. Unfortunately, experiences in factory operations have demonstrated clearly that there are other factors, many of which remain undefined, which can also influence it in an unpredictable manner.

The most important feature of the results in Figure 3.2 is not the magnitude of the change in zeta potential but the simple fact that the value can be reduced. The controlled addition of phosphate to the juice stream thus enables factories where the zeta potential is relatively high to reduce it to the levels of other factories in other regions. This feature is of vital importance in optimising the flocculation reaction both in laboratory experiments and in factory operations and is discussed at length later in this chapter.

The importance of calcium can be seen from Figure 3.3 which compares the zeta potentials obtained with the normal liming procedure using calcium saccharate with those obtained when NaOH was used to adjust the pH. The concentrations of Ca^{2+} remaining in the clarified juice are also shown. With calcium saccharate, the zeta potential remained almost constant although the residual Ca^{2+} increased throughout. With NaOH, there was a sharp increase in zeta potential above pH 8 but a decline in Ca^{2+} towards zero near pH 9.

Heidi[138] has demonstrated that, when calcium phosphate is precipitated from hot sucrose solution by increasing the pH, the precipitate is a microcrystalline hydroxyapatite which can be

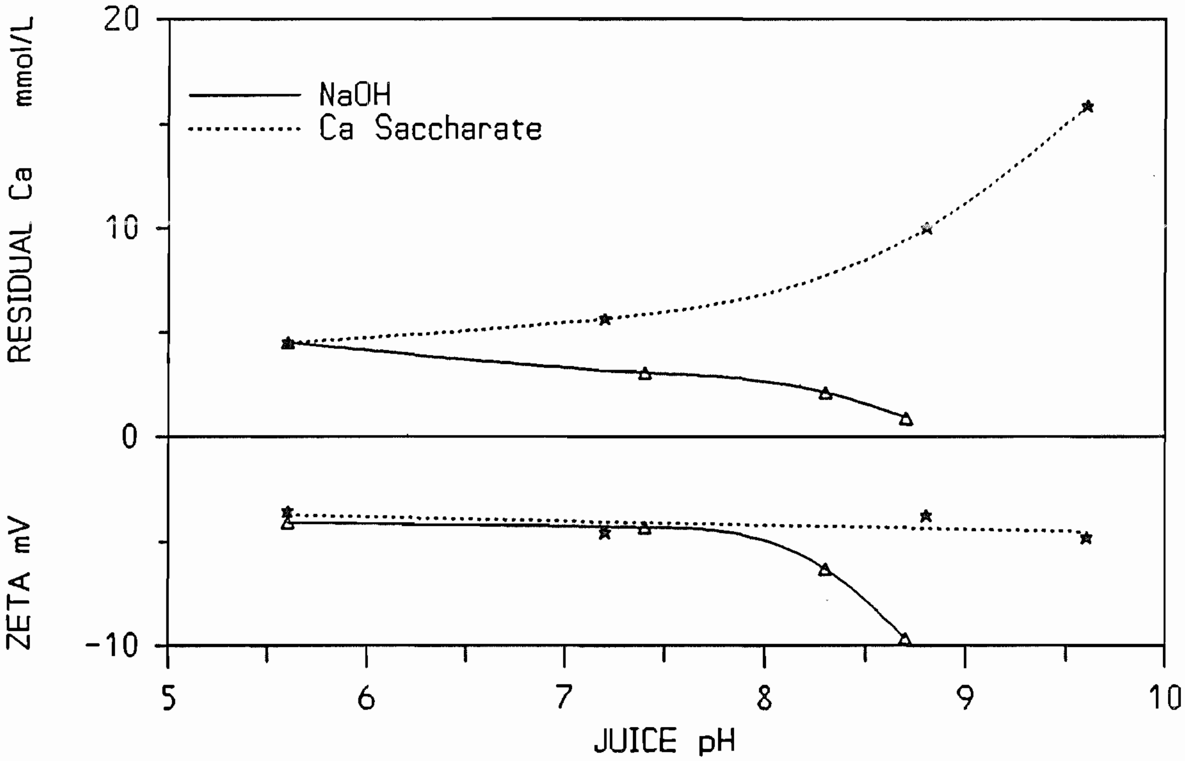

Figure 3.3 Effect of Lime and NaOH on Calcium Phosphate Precipitates.

represented as $Ca_5(OH)(PO_4)_3$. However this formula does not take into account the wide variations which commonly occur in both the stoichiometry and hydration of hydroxyapatites. Clearly, Ca^{2+}, OH^- and PO_4^{3-} are all potential-determining ions for the precipitate. Foster[142] found that, when the pH was adjusted with NaOH, the ratio of Ca:P in the precipitate remained constant at 3:2 until precipitation of the phosphate was complete at pH 7.5. The addition of further NaOH would produce the observed increase in zeta potential through the adsorption of OH^-. When saccharate is used, both the cation and the anion are potential-determining with the result that the nett effect on zeta potential is only slight.

The method of lime addition has been found to influence the rate of the precipitation reaction, the zeta potential of the particles and the flocculation reaction. When added simply as milk of lime (an aqueous slurry of $Ca(OH)_2$) the reaction with phosphate is slow and many minutes are required before the pH becomes constant. When added in the soluble form as calcium saccharate, the reaction is very fast and the zeta potential lower. Bridging flocculation then produces larger aggregates and leaves a much clearer supernatant. Drawing a parallel with other chemical reactions, the rapid reaction which occurs in the latter case would be expected to produce more particles of smaller mean size and greater surface area. Since the adsorbed acidic polysaccharides which are responsible for the negative surface charge will then be distributed over a larger area, the surface charge density and, consequently, the zeta potential are lower. From a practical viewpoint, the removal of impurities by adsorption should therefore be facilitated.

In normal factory operation in Australian mills, full advantage is taken of the effects described above to enhance the quality of clarified juice. Calcium saccharate is prepared by mixing milk of lime with an appropriate amount of syrup (60-70% sucrose by weight). As the proportion of syrup increases, the proportion of lime dissolved increases while both the particle zeta potential and the turbidity of the clarified juice decrease (Figure 3.4).

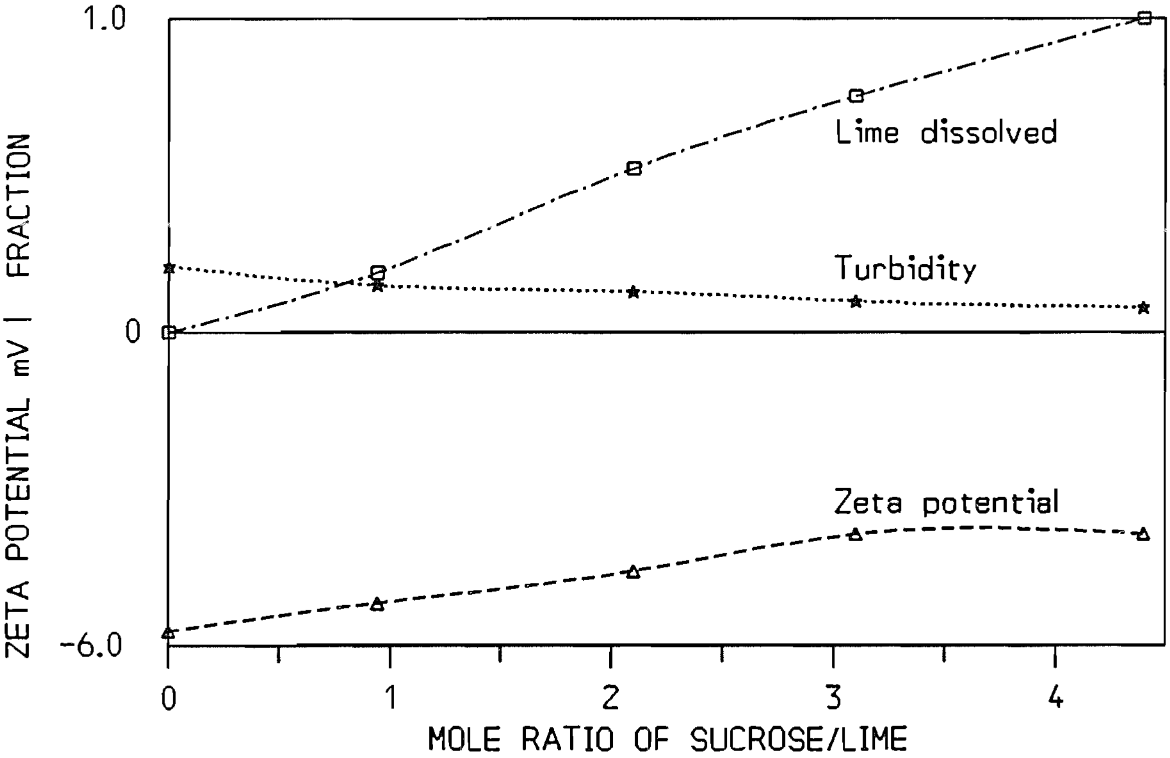

Figure 3.4 **Effect of Saccharate Composition on Clarification.**

It is evident from the extensive literature on hydroxyapatites that wide variations in stoichiometry, particle size and electrokinetic properties occur in their precipitation from aqueous solutions. In a mixed environment such as cane juice, it is an even more complex reaction which has already been investigated by Heidi[138], Bennett[139,140] and Foster[142]. No further investigations have been undertaken during this work beyond that described above. However, it will be shown later in this chapter that any factor which influences the electrokinetic properties of the particles also affects the bridging flocculation reaction.

3.2 PARTICLE CONCENTRATION EFFECTS

It is apparent from the results in the following sections and from practical experiences in actual factory operations that there are many variables which can effect the flocculation reaction and lead to variations in performance between factories. One of the principal factors involved clearly must be the mud solids or particle concentration in the incoming juice.

The influence of solids concentration on cane mud flocculation was examined in three series of experiments in which the particle concentration in the juice was varied by adding or withdrawing clear juice prior to the addition of flocculant. In each series, the ratio of polymer to solids was maintained at a constant value and the range of concentrations selected to cover all but the most extreme situations encountered in factory operations. In each case the settling rate decreased as the particle concentration increased (see Figure 3.5).

Equations (1.9) and (1.10), which were derived by Gregory[30] by treating polymer adsorption as a case of heteroflocculation, predict that the rate of flocculation should increase as the particle concentration increases. This effect is used to advantage in municipal water treatment and other applications where the particle concentrations are very low. The rate of flocculation can be increased by recirculating settled solids to the feed to increase the particle concentration. In cane mud flocculation the rate constants and particle

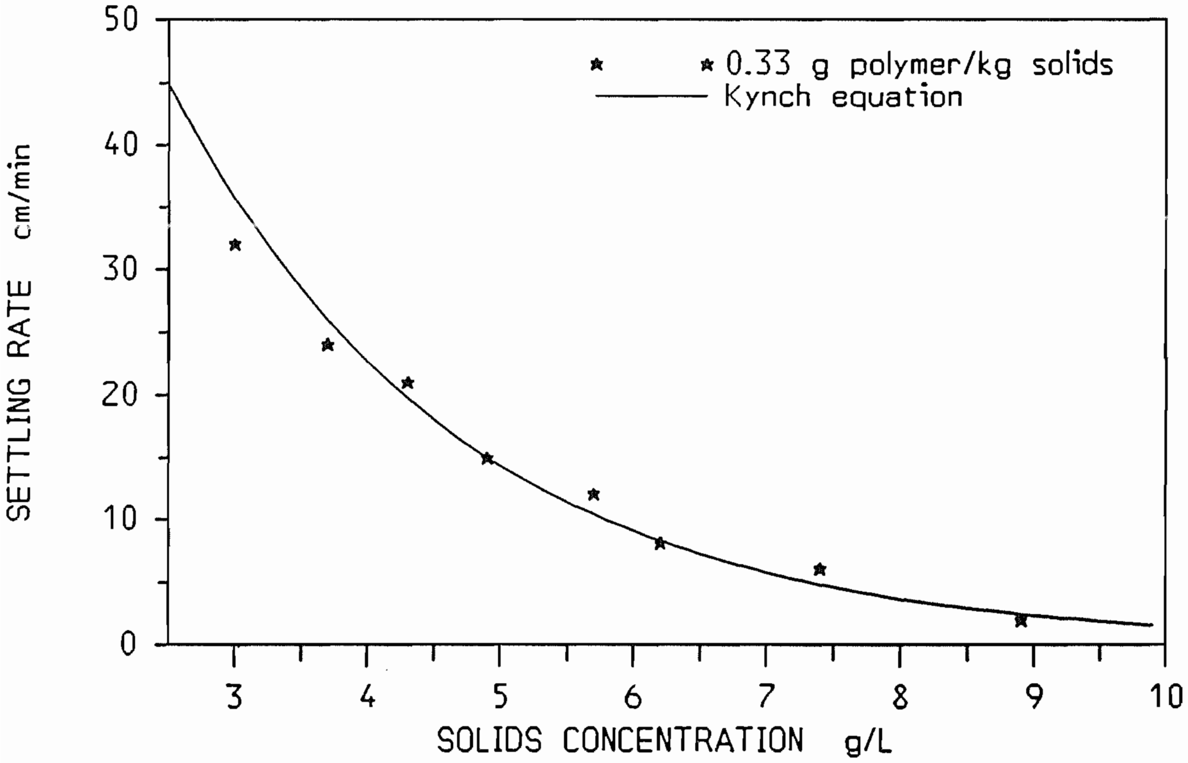

Figure 3.5 Effect of Solids Concentration on Settling Rate.

concentrations are such that the characteristic adsorption time (t_a) and the flocculation time (t_f) are very small. Although accurate determinations could not be made from the batch settling tests, it appeared that both t_a and t_f were of the order of only a second or less. Differences in these two parameters due to changes in particle concentration could not be detected but, in view of the results in Figure 3.5, this was not important.

The particle concentrations in typical Australian cane juices are such that the aggregates formed during flocculation cannot settle independently but interact strongly with other particles. Settling is therefore characterised by a distinct interface between the solids and the clear supernatant. This state is usually described as 'hindered settling'. Kynch[143] has developed equations to relate the sedimentation rate of the interface to the solids concentration in this regime. In Figure 3.5 the points represent experimental data while the line has been calculated using the Kynch equation applied to the highest concentration. The ability of the Kynch equation to accurately predict the effect of changes in concentration within the hindered settling regime is evident.

Small changes in particle concentration can have a marked influence on the settling rate. Whilst this observation is of little consequence in determining the mechanism of the reaction, it is important in the interpretation and comparison of results obtained at different factories. It is also has great practical significance in actual factory operations and must be considered closely when attempting to optimise factory operations or when designing process equipment.

Throughout this work, there were many variations in the absolute values of settling rates which were obviously due to differences in solids concentrations. Rather than attempting to normalise the results to a constant solids concentration using the Kynch equation, absolute values have been compared only within sets of experiments carried out on single samples of juice. All other comparisons have been by reference to an arbitrarily selected reference polymer, usually the one giving the best performance at the time.

3.3 POLYMER PROPERTIES AND FLOCCULATION

3.3.1 ANIONIC CHARACTER

The effect of copolymer composition referred to briefly in Chapter 1 was examined in great detail in batch settling tests at each of the factories referred to in Figure 3.1, in conjunction with measurements of the electrophoretic properties of the cane mud particles. In each series of experiments, both the settling rate of the flocculated muds and the turbidities of the clarified juices were measured as functions of the anionic character of the copolymers covering the normal range of factory operating conditions. The variations of zeta potentials were also measured by simulating factory pH control operations on a laboratory scale to provide samples suitable for the particle electrophoresis apparatus.

As was the case with zeta potentials discussed in 3.1, the results from each major mill area were found to follow a consistent and definite pattern (Figure 3.6). In each case there was a clearly identifiable optimum polymer composition which corresponded to a maximum in the settling rate and a mimimum in the turbidity of clarified juice. The differences in the absolute values of both settling rates and turbidities reflect variations in particle concentrations and process operating conditions prevailing at each factory at the time of the experiments.

When these results are compared with the electrokinetic data in Figure 3.1, it can be seen that the anionic character of the optimum polymer increased as the zeta potential increased. This effect has not been reported previously, although Michaels[20] observed that there was an optimum polymer composition for the flocculation of silt and clay suspensions with partially hydrolysed polyacrylamides. He suggested that the optimum degree of hydrolysis represented a compromise between the requirement for amide groups for polymer adsorption and the effect of the ionized groups in extending the conformation of the polymer in solution to enable it to bridge greater interparticle distances. It will be shown later that this situation does not apply to cane muds.

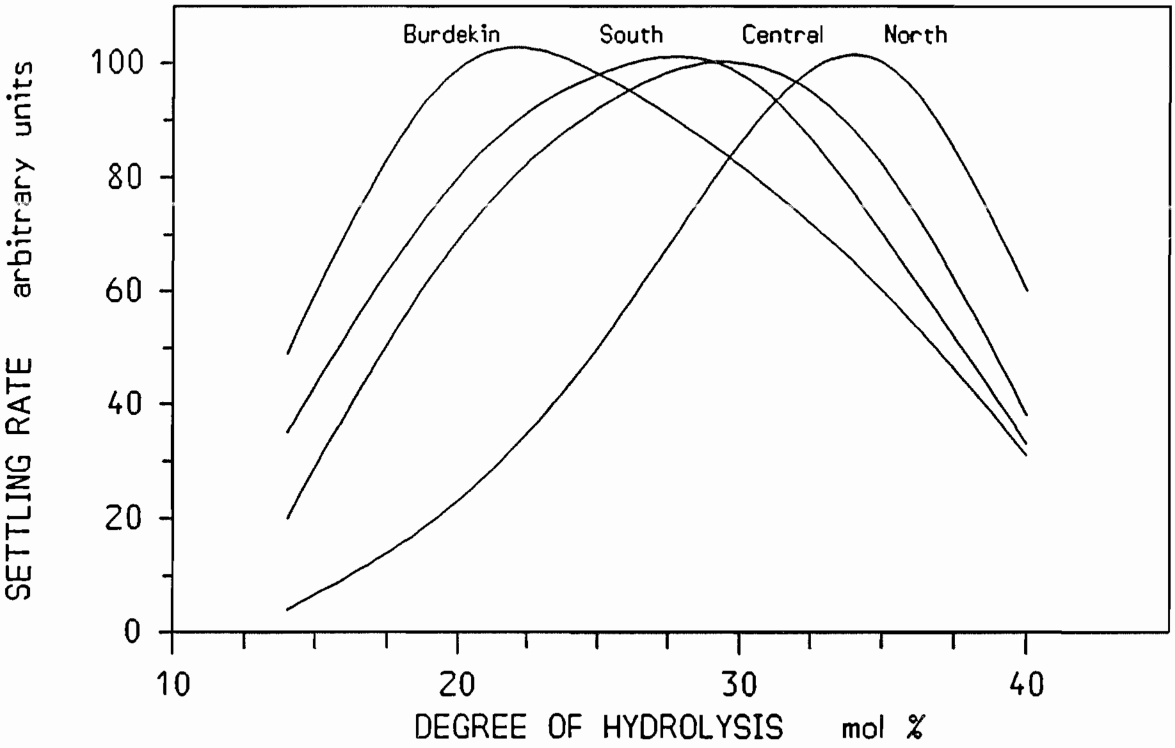

Figure 3.6 Comparative Performance of Flocculants in the Major Regions of the Industry.

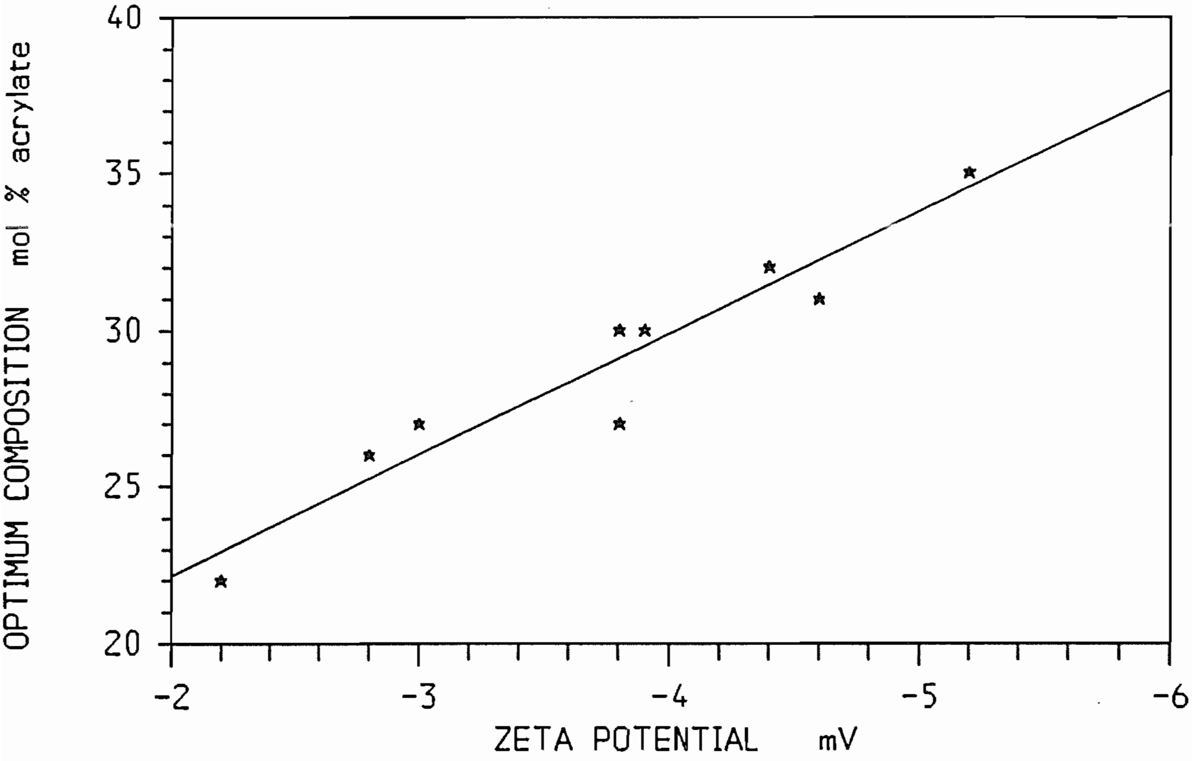

Figure 3.7 Variation of Optimum Polymer Composition with Zeta Potential.

The dependence of the optimum anionic character on the zeta potential of the particles was observed on a local as well as a regional basis. A general trend observed throughout this work was that, as the cane harvesting season progressed, both the particle zeta potential and the optimum anionic character decreased slightly. This trend could be deliberately disrupted, but in a predictable manner, by changes in operating procedures such as the use of saccharate for pH control and the addition of phosphate to juice. These aspects have been discussed above. Unpredictable disruptions also occurred in response to seasonal climatic variations and other unknown factors. However, the dependence of the optimum anionic character on zeta potential remained, as demonstrated by Figure 3.7 which shows the results of the the experiments described above together with those from a number of others in several regions under an assortment of operating conditions.

The increase in the optimum acrylate content with increasing particle charge has not been previously reported. From a simple electrostatic approach, the effect is anomalous since the nett electrostatic repulsion between a particle and an approaching polymer segment will increase as the charge on either increases. In the present case, however, the particle charge is very low so the resultant forces of repulsion must be very weak. Furthermore, if electrostatic forces played a significant role in polymer/particle interactions, there should be a decrease in the amount of polymer adsorbed as the ionic content of the polymer increases. Results presented later in this chapter show quite definitely that this does not occur.

It could be argued that the observation is in accord with Michaels' theory that the incorporation of ionic groups in the polymer serves only to extend the conformation of the molecules in solution. As the particle charge increases, the mean particle separation will also increase and a more extended polymer would be better able to bridge the larger gap. However, the range of zeta potentials encountered was so low that the particles always underwent rapid coagulation (as defined by Smoluchowski). This effect was clearly visible throughout this work and is evident also in actual factory operation. Consequently, there can be no nett energy barrier to aggregation so variations in particle separation are not a consideration. Furthermore, no consideration has been given to the influence of charged monomers on the flexibility of the polymer. As the frequency of ionic groups increases, the electrostatic interactions between neighbouring groups which force the molecule into an extended conformation can also inhibit the free rotation of segments. The contributions of each of these effects to adsorption and bridging have not been explored previously.

An alternative explanation can be postulated based on the model employed by Clayfield and Lumb[31] in their computer simulations of the adsorption of a copolymer comprising polar and non-polar monomers. In this model, adsorption was assumed to occur only at the polar monomer. As the proportion of the polar monomer increased, the fraction of molecules adsorbed increased rapidly from zero to unity. At the same time, the dimensions of the adsorbed molecule decreased dramatically from the unperturbed solution conformation as the number of adsorbed groups increased and the molecule collapsed onto the surface. The model predicts a narrow range of compositions where most of the molecules remain adsorbed but do not collapse rapidly onto the surface. It is postulated here that the optimum copolymer composition illustrated in Figure 3.6 corresponds to this condition.

In the model of Clayfield and Lumb, the adsorption behaviour was a function of the total energy of adsorption which was defined as the product of the fraction of polar groups and the energy of adsorption of a single group. Any change in the latter parameter will require a corresponding change in the frequency of polar groups to maintain the critical total energy of adsorption as postulated above. This hypothesis will be discussed in more detail in the following sections.

3.3.2 MOLECULAR WEIGHT

It has been found without exception that an increase in molecular weight resulted in improvements in both settling rate and turbidity. In the period during which this work was undertaken, and as a consequence of the results obtained, the manufacturers of commercial polyacrylamide flocculants supplied to the Australian sugar industry have increased the molecular weights of their products from < 10×10^6 to more than 25×10^6 daltons. There has been no indication that any limiting value has been approached yet.

The precise effect of molecular weight on settling rate is also influenced by the solids content of the juice as discussed in 3.2, and by the acrylic acid content of the polymer. For a series of polymers of constant composition, the settling rate increased linearly with the molecular weight, as Figure 3.8 shows. At the same time, the turbidity decreased although the results are not included in Figure 3.8. The influence of polymer composition described in the preceding section is also evident in Figure 3.8. It was evident from visual observations during the experiments that the increases in settling rates resulted from increases in the size of the aggregates formed by bridging flocculation.

Since the size of the aggregates and their settling rates depend on the solution dimensions of the polymer molecule, it might be expected that there should be a simple relationship between molecular weight and settling rate. Although the aggregates are large open structures, their behaviour can be approximated using the concept of an equivalent hydrodynamic sphere of radius R_e. Stokes' Law can then be used to relate R_e to the settling velocity:

$$v = 2(\rho - \rho_o)gR_e^2/9\eta \qquad (3.1)$$

where v = settling rate of a particle
ρ = density of particle
ρ_o = density of liquid
g = gravitational constant
R_e = radius of equivalent hydrodynamic sphere
η = viscosity of liquid

Stokes' Law indicates that the settling rate of the aggregates is proportional to R_e^2. Since Figure 3.8 shows that v is also a linear function of molecular weight, it follows that R_e must then be directly proportional to the mean radius of gyration $(\bar{R}_g^2)^{1/2}$ of the flocculating polymer. This observation is in accord with the concept postulated in the previous section that

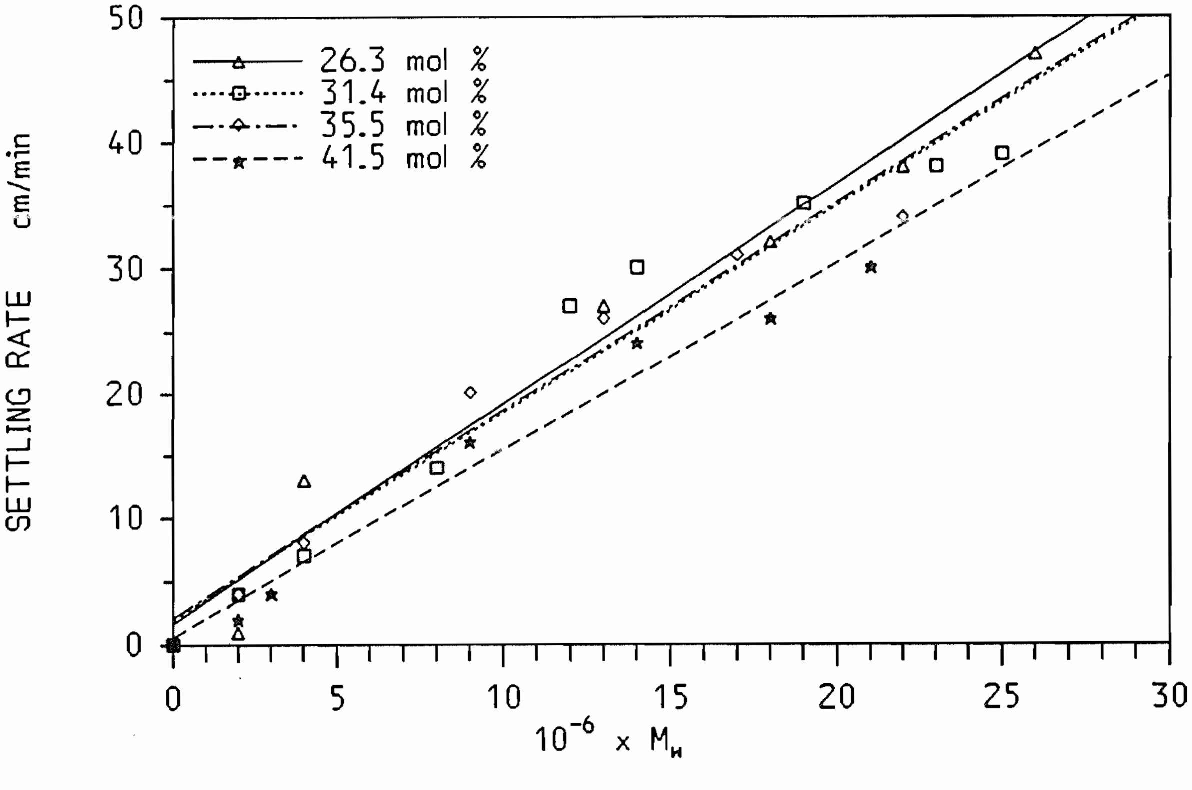

Figure 3.8 Effect of Molecular Weight on Settling Rate.

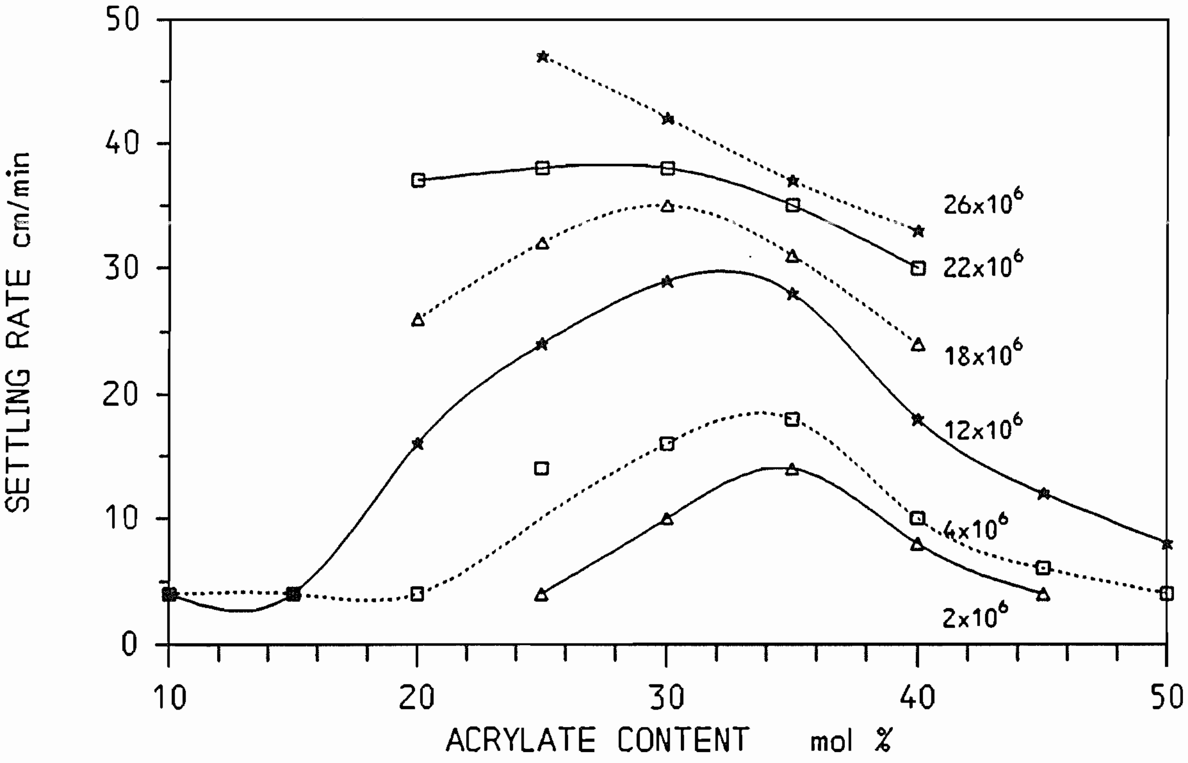

Figure 3.9 Effect of Molecular Weight upon Settling Rate for a Series of Copolymers.

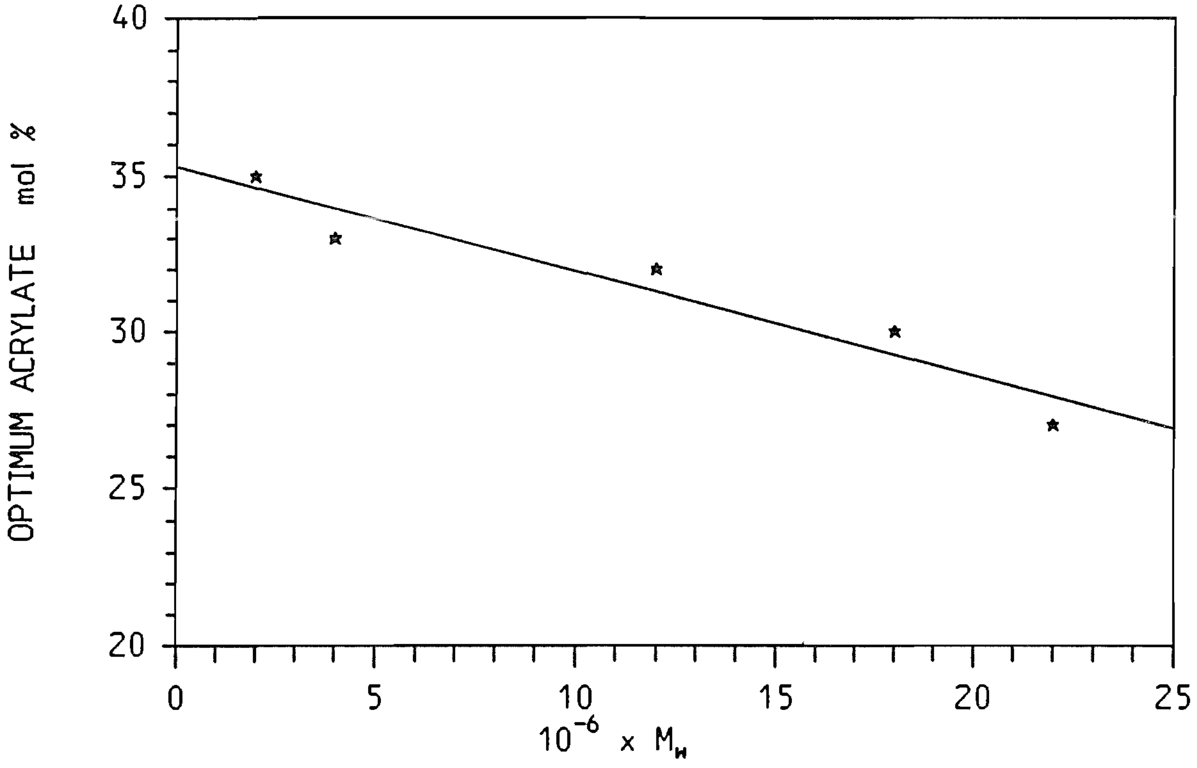

Figure 3.10 Variation of Optimum Acrylate Content with Polymer Molecular Weight.

bridging flocculation is most effective when the adsorbed polymer retains its solution conformation on the particle surface. If expansion of the polymer molecule due to intramolecular electrostatic interactions was a controlling parameter, it would be expected that R_e would be directly proportional to the extended length of the molecule and therefore also to its molecular weight. The settling rate would then be proportional to M^2. Partial expansion of the polymer would similarly result in a dependence on M to a power of between one and two.

It was also observed that the optimum copolymer composition was dependent upon the molecular weight (Figure 3.9). As the molecular weight increased, the optimum acrylate content decreased approximately linearly (Figure 3.10). The explanation for this observation depends on whether adsorption occurs through the amide or the acrylate group. As discussed in Chapter 1, adsorption of copolymers has not been studied as extensively in either theoretical or experimental studies as homopolymer adsorption. However, a general observation of all adsorption studies has been that both the thickness of the adsorbed layer and the amount of polymer adsorbed increase with increasing molecular weight.

As discussed in Chapter 1, it has been considered in most instances that the adsorption of anionic polyacrylamides occurs at the amide group, usually by hydrogen bonding. In the few cases where an optimum acrylate content has been observed, it has been argued that the function of the ionic groups has been to provide the electrostatic forces required to cause the molecule to assume an extended conformation in solution. If this is so, and if the amount of polymer absorbed increases with molecular weight as described above, then fewer amide groups should be required to maintain the optimum level of adsorption for flocculation. As the amide content decreases, the acrylate content must increase, the polymer will assume a more extended conformation and flocculation should be enhanced. Extending this argument further leads to the prediction that the optimum acrylate content should increase as the molecular weight increases.

It is clear from Figure 3.9 that flocculation improves as the molecular weight increases. However, the effect of molecular weight on the optimum acrylate content is contradictory to that predicted in the preceding paragraph. The logical interpretation of this result is that adsorption occurs via the acrylate group. If the principal role of the ionic groups is in adsorption, it further suggests that electrostatic repulsion and extention of the polymer chain are not important factors.

The adsorption of polyacrylamide flocculants will be examined in greater detail in the next section. However, there are two important practical consequences of the results in Figures 3.8, 3.9 and 3.10. Firstly, as the molecular weight increases, both the settling rate and the residual turbidity improve so that the operating capacity of factory equipment can be increased and the quality of the final raw sugar improved. Both of these factors produce important economic benefits, not only for individual factories but also for the industry as a whole.

The second aspect relates directly to the optimization of the factory clarification stage. To produce the best quality juice at the lowest cost, it is quite clearly essential to select the flocculant with the highest possible molecular weight and with the optimum acrylate content for the juice being processed. Any variation in either of these parameters will result in a decrease in the level of performance achieved and attempts to compensate by increasing the polymer dose may not be successful.

The results in Figure 3.11 show the quantities of low molecular weight polymers (12×10^6) required to match the settling rates achieved with 2.5 mg/L of the equivalent higher molecular weight (21×10^6) polymers at a factory where the optimum acrylate content was approximately 30 mol %. With an acrylate content below the optimum, it was impossible to achieve acceptable juice turbidity. This fact alone would be sufficient to halt factory production immediately. Furthermore, it was also impossible to compensate for the reduction in settling rate by increasing the polymer addition rate without exceeding the legal maximum dose of 5 mg/L.

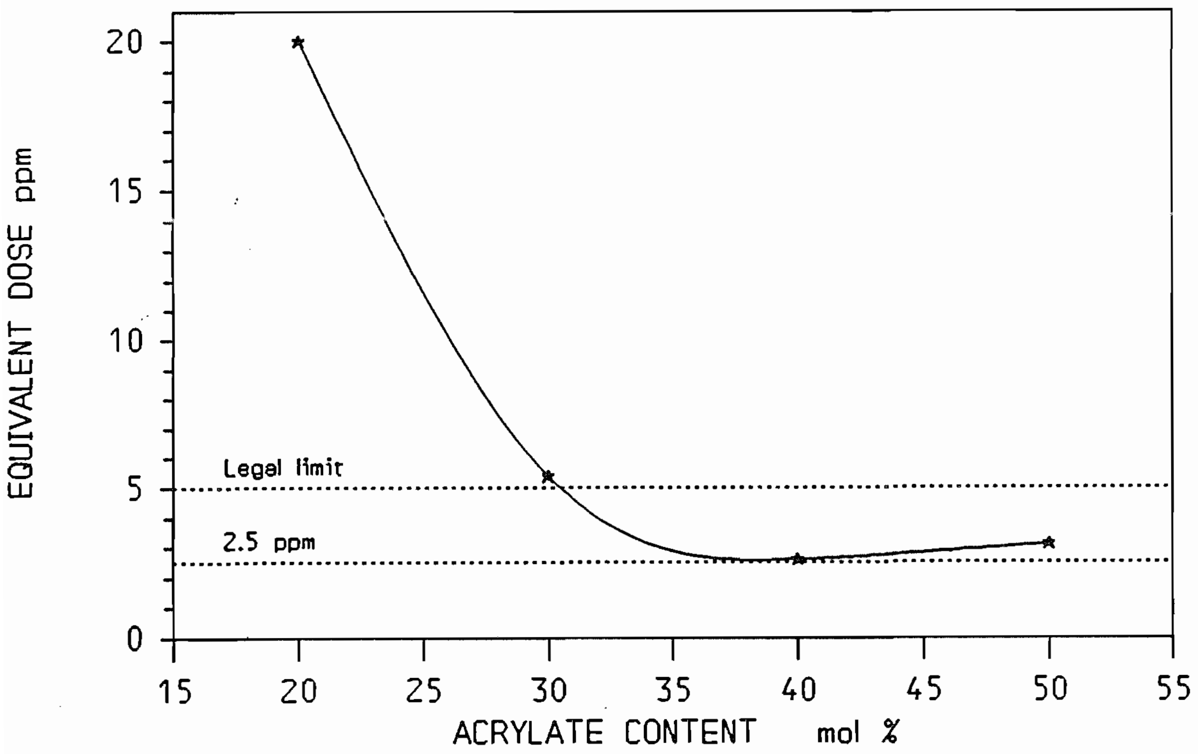

Figure 3.11 Increase in Dose of low molecular weight polymer (12×10^6) required to match the settling rate of 2.5 mg/L of the equivalent high molecular weight polymer (21×10^6).

At acrylate contents above the optimum, a much smaller increase was required to compensate for the lower molecular weight. It was possible to maintain high juice clarity and to increase the settling rate to match that of the higher molecular weight polymer without exceeding the legal limit. However, it is important to note that Figure 3.11 shows only the dose required to compensate for the lower molecular weight, and not the dose needed to match the performance of the optimum high molecular weight polymer. Figure 3.9 shows that the settling rates obtained with polymers with high acrylate contents are considerably lower than at the optimum acrylate content. Thus, while Figure 3.11 indicates that a relatively small increase in dose may compensate for a reduction in molecular weight alone, it is generally not possible to match the performance of the optimum polymer without exceeding the legal dose limit.

It is evident from the preceding paragraphs that there are compelling reasons for factories to attempt to optimize the operation of their clarification equipment and that this can be achieved only through the careful selection of the best polymer for the prevailing conditions.

3.3.3 OTHER SOLUTION PROPERTIES

The effects of copolymer composition and molecular weight described above were observed consistently throughout this work and have been clearly demonstrated by their very successful application to the normal operations of all Australian raw sugar mills. However there were variations in the established patterns of performance with polymers prepared by different methods. These effects have been attributed to differences in the solution properties of the polymers.

Polymer composition and molecular weight are the obvious parameters to determine in the first instance as they are the ones over which the manufacturers have direct control. However it is equally apparent that the behaviour of the polymer molecules in the aqueous environment in which they are to be used will also profoundly influence their performance as flocculants. A simple guide to this aspect is available in the Huggins' constant which can be obtained from the graphical analysis of viscosity data in the determination of molecular weights as described in detail in the previous chapter.

The interpretation of the Huggins' constant (k) in terms of polymer solution properties and its relation to other solution parameters are discussed in depth in the next chapter. The discussion here is limited to experimental observations and a broad interpretation of the effect of k on the flocculation reaction. In general, polymers prepared by different reactions but with the same composition and the same intrinsic viscosity had different values of k. When compared in batch settling tests, polymers prepared by solution copolymerization of acrylamide and acrylic acid were superior to those prepared by disperse phase copolymerization but generally inferior to hydrolysed homopolymers. An example of this effect is given in Table 3.1.

There are two further observations which are also relevant here. Polymers with values of k which were higher than the norm for a particular molecular weight usually came from commercial products having a visibly significant proportion of insoluble material or from polymers manufactured by emulsion polymerization. Those where k was less than expected for the molecular weight were, in general, commercial products which had been manufactured by polymerization and subsequent hydrolysis of acrylamide rather than copolymerization of acrylamide with acrylic acid or its sodium salt.

It has been widely accepted that the Huggins' constant is related in some way to the solution conformation of the polymer molecule although the exact relationship is still open to conjecture. One point of agreement is that $k = 2$ for an uncharged rigid sphere and that $k = 0.35$ (approximately) for a flexible polymer in a good solvent. In the latter case, values of $k>0.35$ occur in poor solvents. Presumably, therefore, $k<0.35$ indicates a 'better' solvent. The interpretation of the Huggins' constant as an indicator of solution properties is discussed further in the next chapter. However there are several important observations which can be made here.

POLYMER		AP273	A130	8025
METHOD OF MANUFACTURE		Hydrolysis	Copolymer	Disperse phase
IONIC CONTENT (mol %)		40	40	39
$10^6 \times$ Mw		11.2	10.8	9.8
HUGGINS' CONSTANT		0.22	0.27	0.32
SETTLING RATE -	Mill A	18	16	8
(cm/min)	Mill B	16	21	10
	Mill C	16	11	8
	Mill D	27	21	13
	Mill E	15	9	6
	Mill F	4	6	5

Table 3.1 Effect of Huggins' Constant on Flocculation.

The most common process used for the commercial production of anionic polyacrylamides is by solution copolymerization. The initial reaction mixture is an aqueous solution of acrylamide and acrylic acid containing approximately 30% by weight of total monomer. The pH of the solution is adjusted by the addition of NaOH before the reaction is initiated. The reaction is exothermic and, on an industrial scale, requires considerable care to control the temperature of the mixture during the reaction if the polymer is to reach the very high molecular weight and high solubility demanded by the end users.

Deviations from the optimum conditions during polymerization can result in branching and/or crosslinking through several possible reaction mechanisms. In concentrated solutions at high temperatures (80°C) or with long reaction times, intramolecular and intermolecular imidization are known to occur[145]:

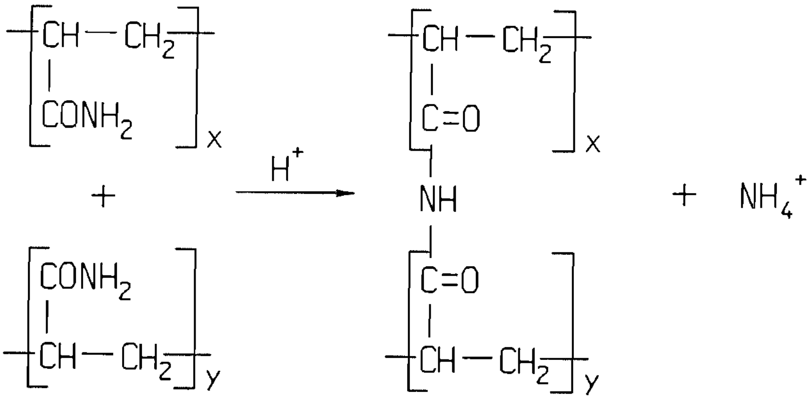

Imidization of either type makes the polymer more hydrophobic and may render it insoluble if sufficient crosslinking occurs[145]. The reaction can be accelerated in acidic solutions but can be reversed at pH 10-12, although alkaline hydrolysis may then occur. The possibility of this mechanism being responsible for increases in k was examined and the results are presented in the next chapter.

Insolubility can result from the reaction of the polymer in alkaline solutions with aldehydes[145] which may be present as impurities remaining from the manufacture of the original monomers. Determination of the extent of these reactions has not been attempted.

The legal constraints on the use of polyacrylamide flocculants in sugar factories include a requirement for the level of residual monomer to be reduced to less than 0.05% by mass. In the commercial process using solution polymerization, the final reaction product is a gel which contains around 30% by weight of polymer. The gel is usually chopped into small particles of 2-5 mm size and the water removed by progressive methanol washing followed by drying in fluidized bed driers. The removal of residual monomer is accomplished during the methanol washing. Variations in k were only rarely observed with polymers prepared by this process and were almost always associated with unusual proportions of insoluble polymer. Maintaining solutions at pH 10.5 for prolonged periods did not reduce k or increase the solubility. It was concluded that the differences were due to variations in operating conditions within the factory which lead to irreversible crosslinking by a mechanism other than through imide formation. Exposure of samples to sunlight, even at the levels entering the laboratory through windows, for extended periods had similar irreversible effects, increasing k and reducing solubility.

There is no methanol washing procedure in the commercial disperse phase polymerization process. Reduction of residual monomer levels to below the specified limit is achieved by raising the temperature of the reaction mixture during the final stages to ensure that the reaction goes to completion. Conditions therefore exist in the normal course of production for the formation of crosslinks or other products leading to insolubility and it is perhaps not surprising that these polymers have higher values of k.

It is evident that mechanisms exist and conditions may prevail, even if only by accident, which can lead to decreases in solubility and to increases in k. However, Table 3.1 demonstrates that lower values of k also occur. It is notable that this has been observed only in polymers prepared by hydrolysis of the acrylamide homopolymer. It is possible that better control of unwanted reactions of the monomer can be achieved in this process. Differences in reaction conditions may also result in differences in the sequence distribution of the monomers within polymers prepared by the various processes.

Both the acrylamide and acrylic acid monomers and their homopolymers are readily soluble in water. However, any variations in the distribution of the ionic monomer within the polymer must influence the intramolecular electrostatic interactions which can have a major bearing on its solution properties. It has been argued that the high concentration of supporting electrolyte employed in the viscosity determinations effectively limits the range of such forces to the extent that they no longer influence the conformation of the molecule. Nonetheless, the possibility cannot be entirely discounted that some interaction, however slight, remains between neighbouring ionic groups, particularly if they are attached to adjacent carbons of the polymer skeleton.

In a genuinely random copolymer of such high molecular weight, it is inevitable that there must be numerous blocks of each monomer. Each such block of ionic monomer will be a region of high local electrostatic interaction. However, a regular copolymer containing less than 50 mol % of acrylic acid will have at least one non-ionic acrylamide monomer between each ionic group. Electrostatic interactions will thus be more evenly distributed over the length of the polymer molecule.

Several possible mechanisms which could be wholly or partly responsible for the effects observed and illustrated by Table 3.1 have been postulated. They are discussed at length in Chapter 4 where results are presented to demonstrate the contribution of each mechanism to the effects described above.

3.4 POLYMER ADSORPTION

In order to understand the relationship between the electrokinetic properties of the cane muds and the composition of the flocculating polymers, the adsorption of a range of copolymers was examined in batch settling tests at several factories. Figure 3.12 shows the results obtained at one factory where the optimum polymer composition was found to be 31.4 mol % acrylate. Although there were some variations between factories, particularly around the optimum composition, the general trend was similar in all cases. There are two particularly significant features of these results. Firstly, there was no significant adsorption of the non-ionic polyacrylamide, indicating clearly that adsorption occurs through the ionic acrylate group as suggested above. The importance of the ionic groups is therefore much greater than has been previously recognised. Although, as Michaels[20] suggested, they may play a role in extending the polymer molecule in solution through electrostatic interactions, in this instance they influence the flocculation reaction primarily through their control of the adsorption step.

The other important feature of Figure 3.12 is that polymers containing more than the optimum proportion of acrylate monomer were almost completely adsorbed. Figure 3.12 also indicates that, at the optimum composition, approximately 80% of the added polymer was adsorbed. In practice it was found that there was considerable variation in the extent of adsorption in this region and that the results were strongly influenced by the degree of agitation applied during the tests. Brief vigorous agitation increased the amount of polymer adsorbed but also resulted in a decline in the settling rate and an increase in the supernatant turbidity (Table 3.2).

Stirring Time (s)	Amount Adsorbed (mg/L)	Settling Rate (cm/min)	Optical density at 800 nm
0	1.37	18.0	0.11
5	2.13	17.6	0.12
10	2.66	8.7	0.17
20	2.87	5.7	0.26

Table 3.2 Effect of Vigorous Agitation on the Adsorption of the Optimum Polymer.

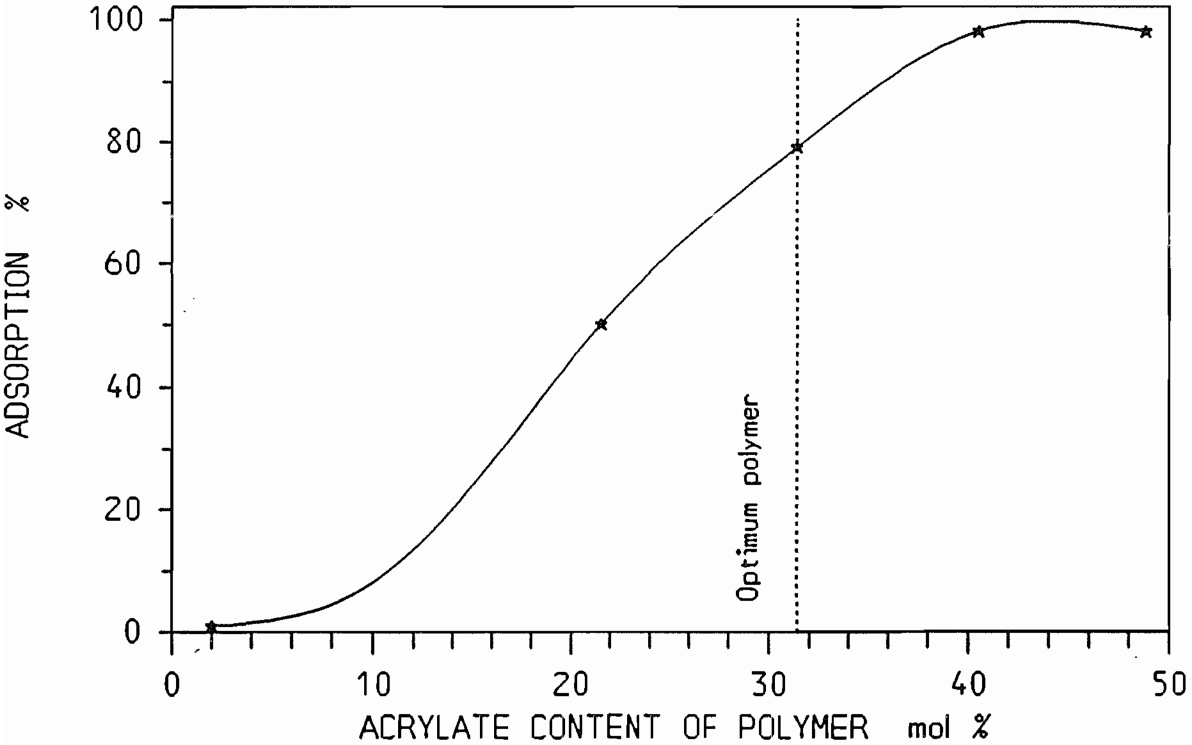

Figure 3.12 Effect of Copolymer Composition on Adsorption where the Optimum Acrylate Content was 31.4 mol %.

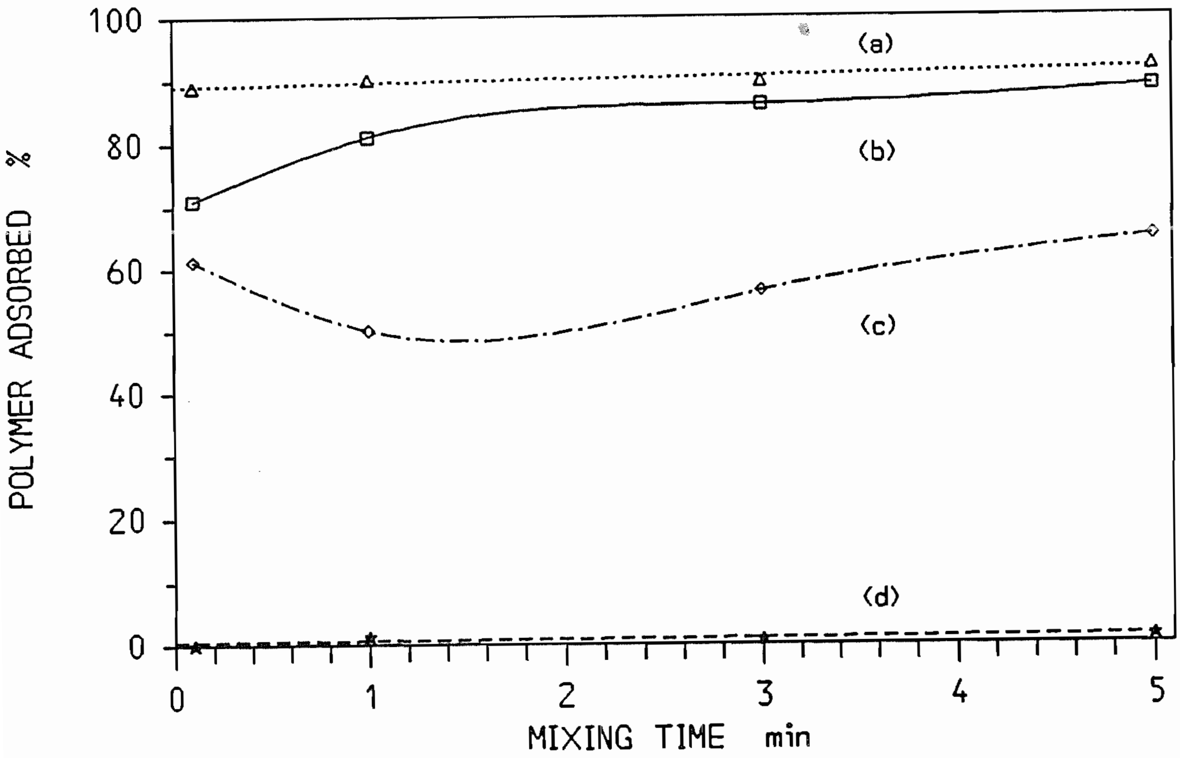

Figure 3.13 Effect of Mild Agitation on Polymer Adsorption where the Optimum Acrylate Content was 31.4 mol %.

Acrylate Content of Polymers:

(a) 48.5 mol %
(b) 31.4 mol %
(c) 21.5 mol %
(d) <2 mol %

Prolonged gentle agitation (just sufficient to prevent settling) had a similar effect on adsorption but resulted in much less severe deteriorations in settling rate and turbidity. The effects of prolonged gentle agitation on adsorption are illustrated by the results in Figure 3.13. These data were obtained in conjunction with those of Figure 3.12 at a factory where the optimum acrylate content was 31.4 mol %.

At the lowest acrylate content (<2 mol %), there was no adsorption and no flocculation. As the ionic content of the polymers increased, so too did the extent of adsorption. At 48.5 mol % acrylate, which was well above the optimum, adsorption was almost complete and remained constant with continued agitation. At the same time, aggregates were small, the settling rate was low and decreased only slightly while the turbidity was also low but increased slightly. From visual observations, it was apparent that the aggregates remained essentially intact during the period of agitation. Adsorption of this polymer must have occurred rapidly and irreversibly, and been strong enough to resist the shear forces encountered.

Below the optimum, at 21.5 mol % acrylate, adsorption occurred to a much lesser extent. Figure 3.13 shows a slight decrease in adsorption initially, followed by a slow increase. While some large aggregates were visible, the turbidity was high due to the large number of very small aggregates which were also present. Furthermore, there was visible evidence of aggregates breaking and reforming during agitation. The settling rate and turbidity were both poor and remained approximately constant. Thus, while adsorption occurred rapidly, it was irreversible and generally not strong enough to resist even mild shear forces.

At the optimum acrylate content, adsorption was again rapid but showed a slight increase during the initial agitation. With this polymer there was some evidence of breakage and reforming of aggregates, though to a lesser extent that at 21.5 mol %. Both the settling rate and the turbidity deteriorated slightly but remained high throughout. Under these conditions, then, adsorption was sufficiently strong to resist the applied shear forces and irreversible but sufficiently dynamic to enable reformation of broken aggregates.

The adsorption behaviour observed here can be interpreted using the model proposed by Clayfield and Lumb[31] and discussed in Chapter 1. If the energy of adsorption (q) of the individual acrylate groups remains constant and independent of polymer composition, the total energy of adsorption of a molecule can be given by the product f.q, where f represents the fraction of ionic monomer in the polymer. At low acrylate contents, f.q will be small so that the adsorbed molecules retain their solution dimensions but adsorption will be weak and molecules will desorb readily. The results indicate that adsorption occurs rapidly, at least within the timescale of these tests, and that the system also rapidly reaches a state of dynamic equilibrium between adsorbed and free molecules. It was apparent from visual observations during the tests that the high supernatant turbidity was largely due to the inefficiency of particle scavenging during growth of the aggregates. It was also obvious that, whilst there were some very large aggregates, there was also a considerable amount of debris from aggregates which were broken by the shear forces encountered during settling. Both of these observations are consistent with the concept of weak adsorption.

At high acrylate contents, adsorption again occurred rapidly, although in this case it was also complete. However, the initial state does not represent a stable equilibrium as there was clearly some rearrangement of the adsorbed molecules on the surface which could be prolonged for some time. This is demonstrated by the slight decrease in settling rate observed with prolonged agitation.

At intermediate levels close to the optimum acrylate content, the value of f.q was sufficient for adsorption to occur irreversibly, since the amount adsorbed increased with time. However, the latter observation also indicates that the system did not reach a stable equilibrium state under the conditions of the normal batch test procedure in which the mixing time was approximately 10 seconds. The simulation by Clayfield and Lumb showed that, at this state, the rate of adsorption of the individual acrylate groups of a single polymer molecule was equal to the rate of desorption. There were always sufficient groups attached to the particle to ensure that the molecule remained adsorbed although the polymer remained flexible and mobile.

There are a number of theoretical isotherms, several of which were described in Chapter 1, for the adsorption of polymers from solution. None have been particularly successful when applied to experimental data except in a few simple cases and it has been found that a simple equation such as the Langmuir isotherm for monolayer adsorption often fits the data just as well. The Langmuir equation is based on the assumption that a dynamic equilibrium exists between adsorbed and desorbed molecules or, in the case of polymeric adsorbates, adsorbed and desorbed segments.

In the present case, it has been postulated that such an equilibrium exists only for polymers containing low proportions of acrylate monomer. The adsorption data for these should therefore fit the Langmuir isotherm. Figure 3.14 shows results obtained for the adsorption of Superfloc A110, a polymer containing 21 mol % acrylate, at two different factories, one where the optimum acrylate content was 34 mol % and one where it was 26 mol %. In each case, polymer addition rates varied from 1.0 to 6.0 mg/litre. The data are plotted according to the Langmuir equation:

$$N/(N_o - N) = 1/(b.N_m) + N/N_m \qquad (3.2)$$

in which $b = b'.\exp(Q/RT)$ (3.3)

where N = amount of polymer in solution

$N_o - N$ = amount of polymer adsorbed

N_m = amount of polymer needed to form a monolayer

Q = enthalpy of adsorption per mol.

R = gas constant

T = temperature

b' = constant

The Langmuir equation does not fit the data particularly well and the range of the data is limited in the case where the optimum ionic content was 26 mol %. At the factory where the optimum acrylate content was higher, the value of N_m was approximately 9 mg. Similar values were obtained at other factories where the optimum acrylate contents were similar.

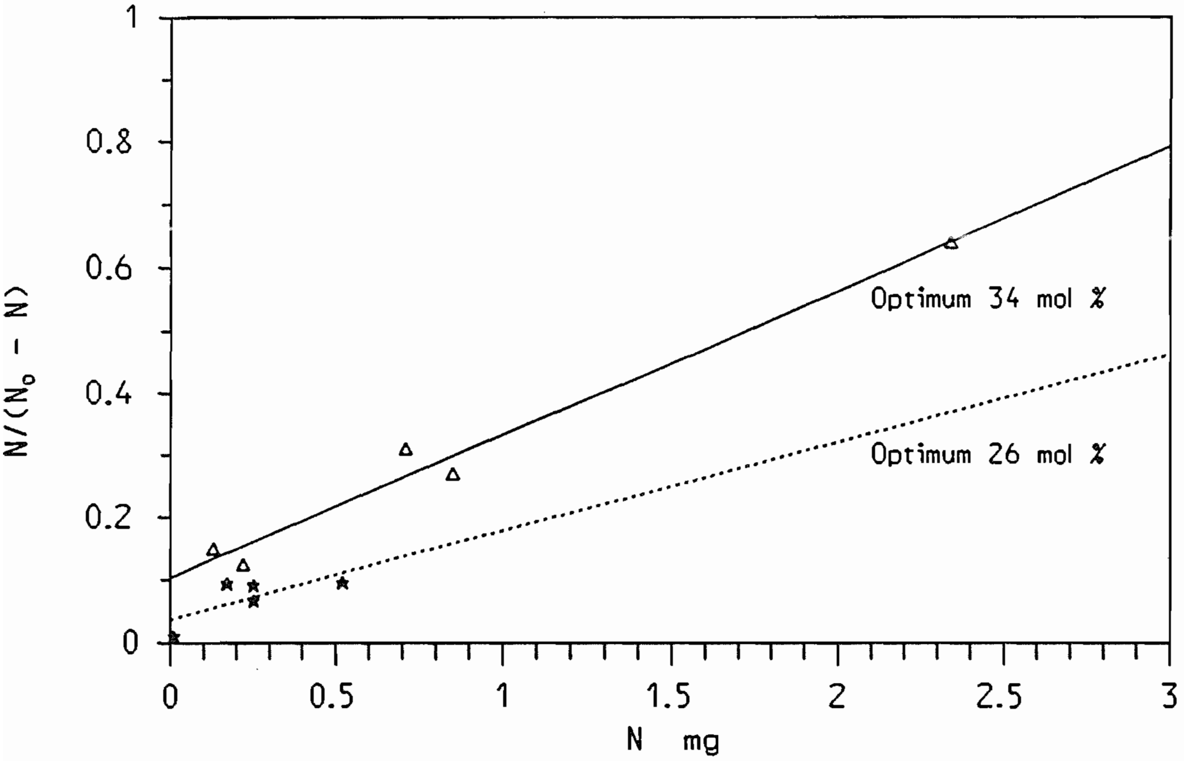

Figure 3.14 Adsorption Isotherms for A110 at Two Factories.

According to the classical interpretation of the Langmuir isotherm, this represents the amount of adsorbate needed to form a monolayer, or perhaps more correctly, the number of adsorption sites available. However, it is doubtful whether the classical interpretation can be applied to copolymer adsorption where the concept of monolayer coverage is quite different. The adsorbed polymer will comprise trains of adsorbed segments and loops and tails of desorbed segments. Although the segments in the loops and tails are not adsorbed themselves, they preclude other segments from the surface and, in effect, will still cover the surface. If there are specific sites at which adsorption occurs then their distribution over the available surface should also affect N_m. It may therefore be more reasonable to interpret N_m as being some function of both the number and the density of adsorption sites.

The other parameter (b) which is obtained from the Langmuir plot is a function of both the capacity (N_m) and the enthalpy of adsorption (Q). Again, it is not really possible to draw any firm conclusions regarding the enthalpies of adsorption from Figure 3.14.

The isotherms for a series of polymers have been examined at a number of factories. Figure 3.15 shows the data obtained at the factory from Figure 3.14 with the 34 mol % optimum acrylate requirement. These data have not been plotted in the traditional Langmuir linear form. Instead, the amount adsorbed has been displayed as a function of the total amount of polymer added. In this way, the adsorption effects can be more readily related to the legally permitted dose of polymer. It is evident that, as the acrylate content increased, the amount of polymer required to completely cover the surface decreased. The data were plotted according to the Langmuir equation (3.1) to obtain the values of N_m and b.

In Figure 3.16, $1/N_m$ has been plotted as a function of the acrylate content of the polymer. This parameter increases in a non-linear manner with increasing acrylate content, which is broadly consistent with the observation that adsorption occurs through the ionic groups as discussed above.

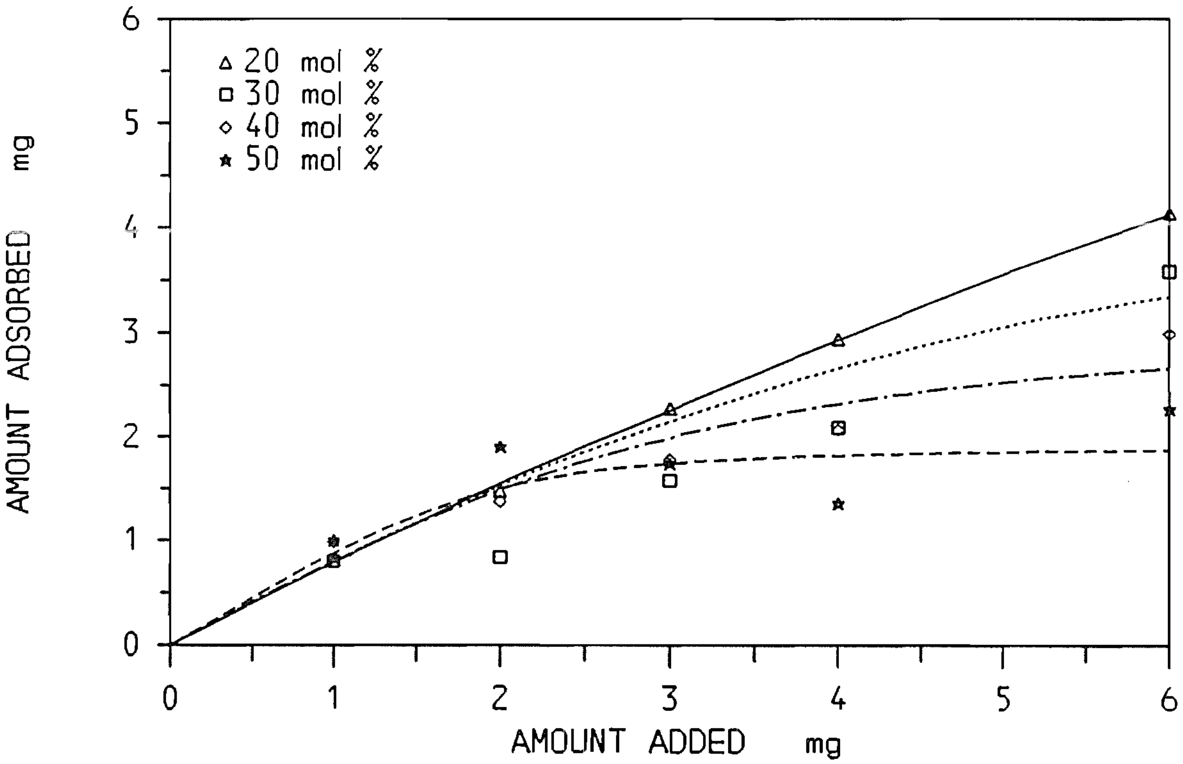

Figure 3.15 Adsorption Isotherms for a Series of Polymers.

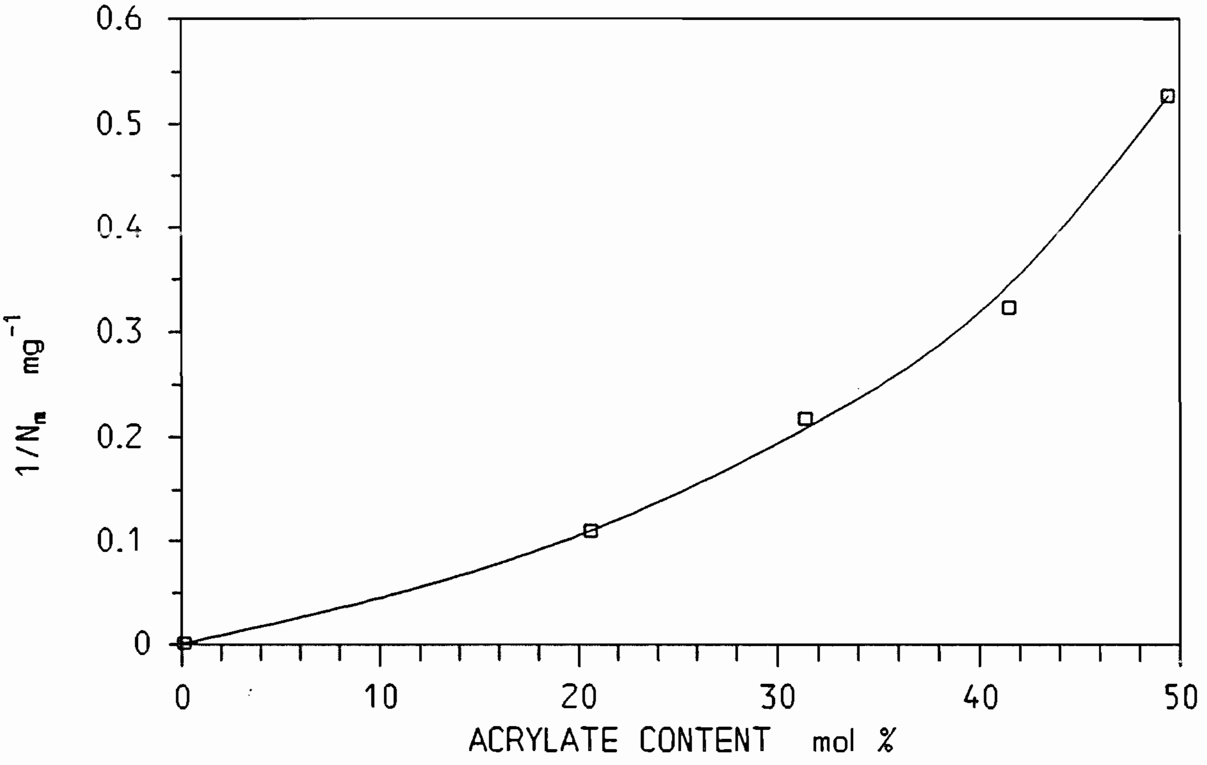

Figure 3.16 Variation of $1/N_m$ with Polymer Composition.

From equation (3.3), the enthalpy of adsorption of the polymer (Q) has a linear dependence on ln(b). When the latter is plotted against acrylate content (Figure 3.17), the results indicate that Q increased in direct proportion to the acrylate content. Since Q represents the enthalpy of adsorption per mole, it can also be defined as:

$$Q = n'.q \tag{3.4}$$

where q = enthalpy of adsorption per monomer and
n' = number of adsorbed monomer units per mole

The results could indicate that the number of points of adsorption remained constant, in which case q, the enthalpy of adsorption per acrylate group, must increase. If so, the lengths of loops and tails will remain constant. Bridging will be unaffected and settling rates should remain constant. In fact, it was quite obvious that bridging became less effective and settling rates declined as the acrylate content increased beyond its optimum value.

Alternatively, the results could indicate that the number of points of adsorption per molecule increased while q remained constant. Bridging would then be less effective since the lengths of loops and tails would decrease and smaller aggregates with lower settling rates should result. It is not possible to confirm this hypothesis directly in the absence of data on the numbers of loops and tails or the number of points of attachment per molecule. However, the explanation is in accord with the experimental observations of this chapter.

If the enthalpy of adsorption of a single acrylate unit is independent of polymer composition for a given cane juice or mud, an explanation then evolves for the dependence of the optimum polymer composition upon particle zeta potential.

The concept of an optimum value for the product (f.q) postulated earlier in this chapter leads to two possibilities. Firstly, the optimum value of f.q may increase as the zeta potential increases so that even if q is independent of both

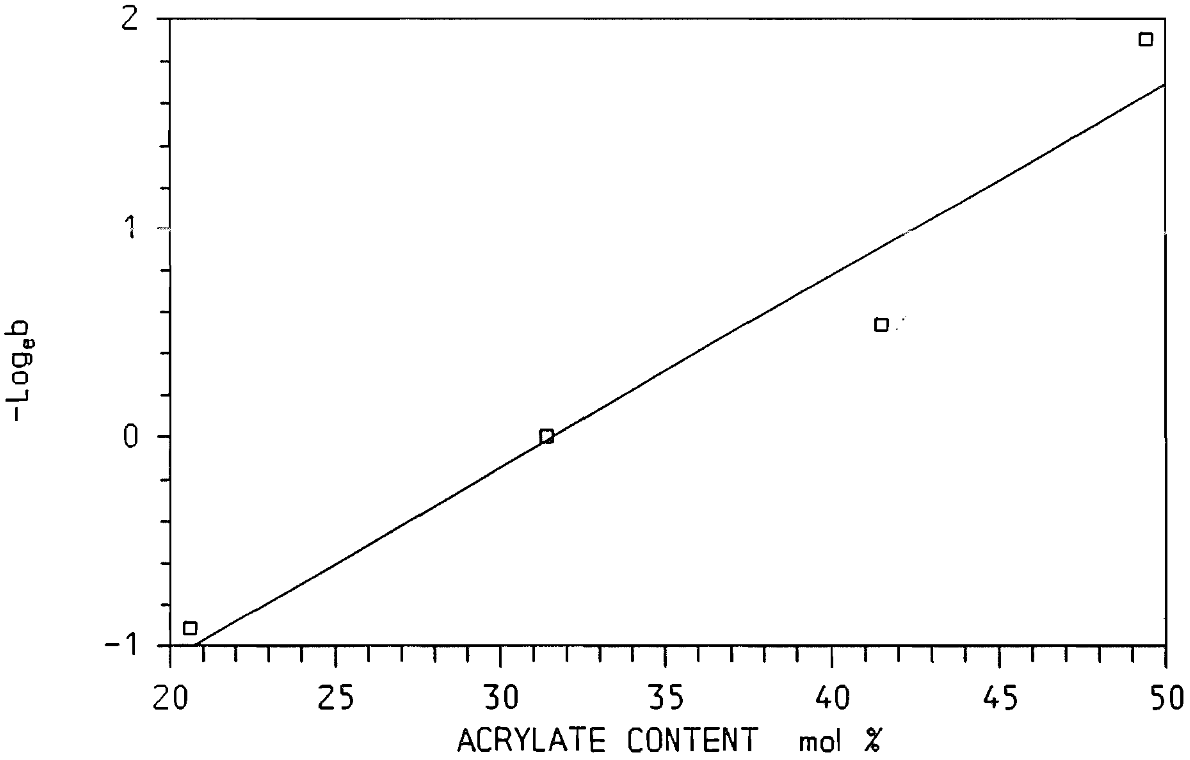

Figure 3.17 **Variation of Enthalpy of Adsorption with Polymer Composition.**

polymer composition and particle or juice characteristics, f must increase as the zeta potential increases. Alternatively, if the optimum f.q is fixed, q must decrease as the zeta potential increases. In either case, it could be postulated that the increase in electrostatic repulsion which occurs as the zeta potential increases may be responsible.

Direct confirmation of either mechanism requires experimental determination for the values of f or q under the same conditions as for the adsorption data. Practical limitations precluded any attempt to conduct such experiments. However, there is some indirect support for the second hypothesis.

In discussing polymer adsorption in Chapter 1, reference was made to the mechanism of adsorption of polymers containing carboxylate groups at surfaces which also contain carboxylates. There is evidence to show that the adsorption can occur through the formation of a 'cation bridge' in which a divalent ion such as calcium forms a bond between a carboxylate on the surface and another on the polymer. Since calcium is by far the predominant ion in cane juices, the same mechanism may well apply here. It should be possible to vary q by replacing the Ca^{2+} in cane juice with other multivalent ions which form similar bonds but with different energies. Unfortunately, this is impossible without altering other factors in a manner which is both unknown and unpredictable. However, it was observed that, when the lime used to raise the juice pH was replaced with an equivalent amount of magnesium oxide, there was no visible evidence of any bridging flocculation with any of the usual anionic polymers.

3.5 SUMMARY

The results described in this chapter have been obtained under actual factory operating conditions or under conditions which closely simulate the factory environment. Although it has not been possible always to define completely all of the parameters which influence bridging flocculation under these conditions, those whose influence has a significant effect on the operation and optimization of process equipment have been identified. The principles which have been discussed are now applied in the operation of clarification equipment in all raw sugar mills throughout Australia and have resulted in significant improvements in product quality and reductions in both capital and operating costs.

Flocculation of cane muds by anionic polyacrylamides occurs by adsorption of the polymer followed by growth of the aggregates. Unlike many other cases where anionic polyelectrolytes react with particles of like charge, adsorption of the polymer occurs through the ionized acrylate functional group. With non-ionic polyacrylamide, there is no adsorption and no flocculation. As the ionic content of the polymers increases, so does the extent of adsorption.

There is a distinct optimum value for the ionic content of the polymer at which the maximum settling rate and the minimum turbidity are obtained. When the acrylate content of the polymers is above this optimum, adsorption is almost complete. It also occurs rapidly and irreversibly, and is strong enough to resist the shear forces encountered during normal agitation and sedimentation. However, the growth of aggregates is restricted by the lack of mobility of the adsorbed polymer. As a result, the residual turbidity is very low but the aggregates are small and the settling rate low.

Below the optimum, adsorption occurs to a much lesser extent. While adsorption still occurs rapidly, it is reversible and generally not strong enough to resist even mild shear forces. While some large aggregates may form, the turbidity remains high due to inability of the polymer to efficiently scavenge all of the particles present. The settling rate and turbidity are therefore both poor.

The optimum acrylate content is a critical condition which represents a compromise between competing effects. Adsorption must be sufficiently strong and irreversible to enable the polymer to effectively collect all of the particles and to enable the aggregates to resist the shear forces encountered during normal agitation and sedimentation. However, the adsorbed polymer must retain its solution dimensions as far as possible and remain flexible and dynamic to promote growth of the aggregates. This balance of competing effects produces the largest aggregates with the highest settling rate and the lowest turbidity.

Although there are some aspects which cannot be proved unequivocally from these observations, there is substantial evidence to support the model in general. In the following chapters, specific aspects are addressed and further evidence presented to support the postulates made here. In particular, polymer properties which have been identified as having an impact on flocculation have been studied in controlled laboratory experiments. Aspects of the adsorption/desorption equilibria and the kinetics of adsorption have been examined using model particle systems and a final model for the mechanism of the bridging flocculation reaction has been proposed.

CHAPTER 4

THE PROPERTIES OF HIGH MOLECULAR WEIGHT FLOCCULANTS

The results in the preceding chapter have demonstrated that the solution properties of the polymers have a profound influence on the flocculation reaction. Some of the properties identified in that work have not been recognised previously as being important in bridging flocculation and thus have received little attention.

In the main, the limited information available in the literature has been obtained with molecules whose molecular weights were often below that required for effective bridging flocculation and well below those used in normal commercial operations. They certainly have been far below the range employed throughout this work, which has concentrated on polymers of real significance to the sugar industry. Experiments with low molecular weight polymers often yield interesting and useful results and certainly present fewer practical difficulties. However, there are always doubts about the validity of extrapolating such results to molecular weights two or more orders of magnitude higher. Often, too, the polymers have been prepared under laboratory conditions which are vastly different from those employed in the commercial manufacturing process. Potentially important parameters such as molecular weight distributions, chemical heterogeneity, branching and crosslinking, and monomer sequence distributions may well be significantly different from those of the commercial products.

Without detailed information about the properties of the polymers actually used in industrial operations, speculation about the effects of the various polymer properties on the flocculation reaction cannot be substantiated. The principal aim of the work described in this chapter has been to examine the solution properties of a range of commercially important polymers, particularly those used in normal sugar factory operations and in the experiments discussed in Chapter 3.

4.1 HETEROGENEITY

Almost all particle systems are heterogeneous, to some extent at least, and display distributions in surface properties. Bennett[84] has stated that cane mud particles are, electrophoretically at least, reasonably homogeneous. However, close examination of the results obtained here show an approximately Gaussian distribution of zeta potentials (Figure 4.1). During the calibration of the electrophoresis apparatus using red blood cells it was estimated that the contribution to this distribution from experimental errors was ± 0.1 mV. Whilst the range of potentials in Figure 4.1 is substantially less than the range encountered throughout the sugar industry it is significant with respect to its possible influence on the optimum copolymer composition (see Figure 3.7).

All synthetic polymers also exhibit some degree of heterogeneity. With simple homopolymers, this may be apparent only as a distribution of molecular weights. In the case of copolymers there are at least two further possibilities. Chemical heterogeneity resulting in differences in the relative amounts of the different monomers in individual polymer molecules is almost inevitable. At the next level there may also be differences in the size and distribution of the sequences of each monomer. In view of the effects of molecular weight and copolymer composition on flocculation described in the preceding chapter, heterogeneity in each of these parameters would be expected to influence the flocculation reaction. While the effects may be subtle, they may be important nonetheless when attempting to optimize a process operation.

4.1.1 MOLECULAR WEIGHT DISTRIBUTIONS

The fractionation of copolymers has been reviewed by Riess and Callot[146]. They concluded that the classical techniques of homopolymer fractionation could be applied to copolymers although fractionations according to different types of heterogeneities may overlap. There are numerous references in the literature to

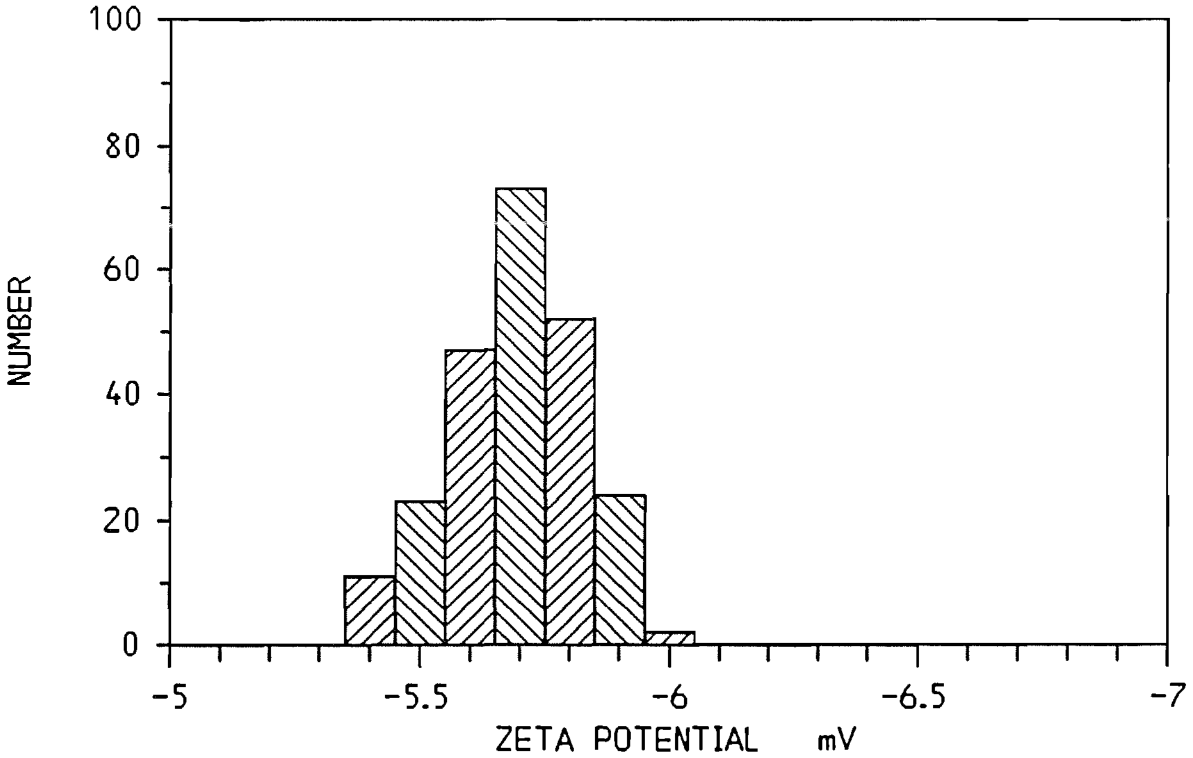

Figure 4.1 Zeta potential distribution in a typical cane mud.

the fractionation of non-ionic copolymers, particularly by gel chromatographic techniques (GPC). GPC has been applied also to the fractionation of polyelectrolyte homopolymers including polyacrylic acid and its salts. When sufficient supporting electrolyte is used to suppress the electrostatic interactions between the ionised groups, polyelectrolytes have been fractionated on the basis of molecular weight heterogeneity alone.

A novel approach to the fractionation of polyacrylic acid has been reported by Bain et al[147]. The preferential adsorption of low molecular weight polymers was used to fractionate polyacrylic acid by adsorption onto crystals of barium sulphate. However, apart from some work by Klein and Westerkamp[148], all of the reported fractionations of acrylamide and acrylic acid polymers have employed polymers with molecular weights of less than 10^6 daltons. There have been no reported fractionations of acrylamide/acrylic acid copolymers with molecular weights in the range of normal commercial application.

Several of the commercial copolymers referred to in the preceding chapters were fractionated by conventional fractional precipitation techniques. Two of the polymers selected were of medium molecular weights (approximately 12×10^6 daltons) while the third was a high molecular weight product (18×10^6 daltons). Fractionation was carried out in the normal manner using methanol as the nonsolvent. Each fraction was thoroughly washed with methanol and dried under vacuum at 40°C. The molecular weight of each fraction was determined by viscometry and the ionic content by elemental analysis as described in Chapter 2.

The molecular weight distributions obtained for three different polymers are displayed in Figure 4.2 and show several interesting features. Despite the fact that, during the course of polymerization in the industrial process the reaction mixture rapidly changes from a solution to a rigid gel, the distributions are surprisingly regular. There appears to be a skew on the low molecular weight side of the LT27 polymer but the lower molecular weight products are quite regular. Whether this difference has any influence on the flocculation reaction is unknown.

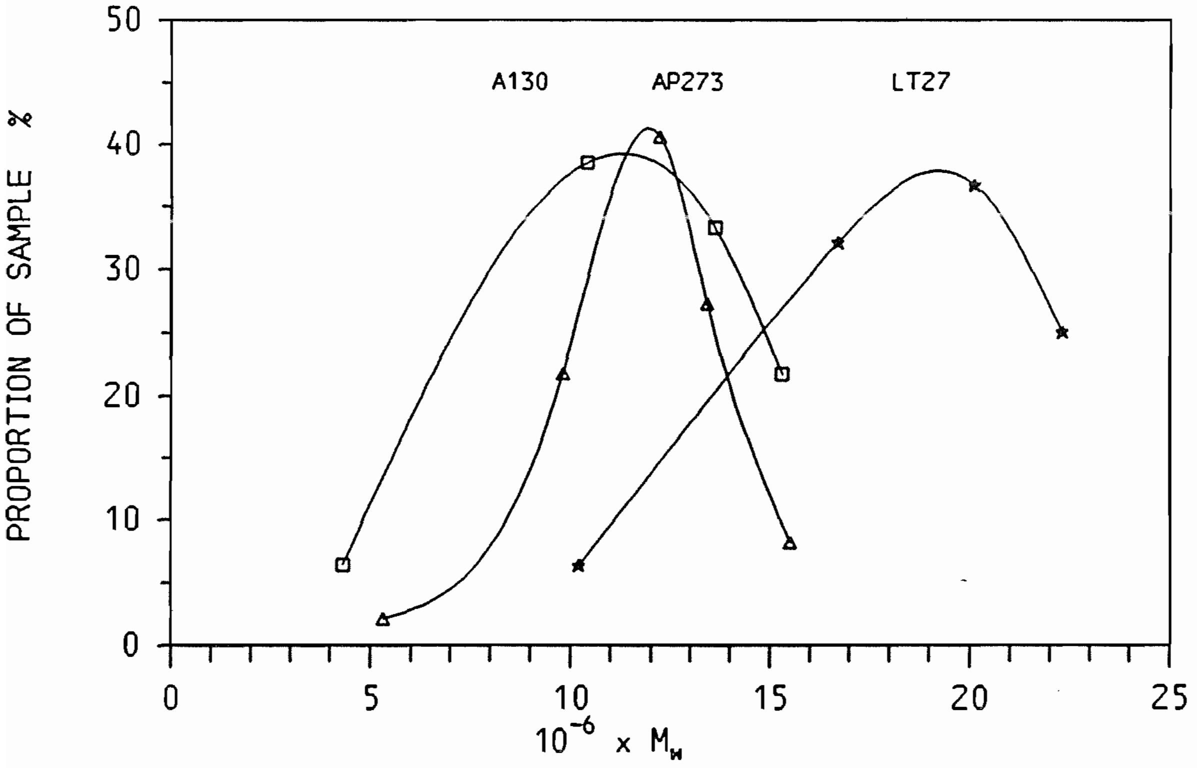

Figure 4.2 Molecular weight distributions of some commercial polymers.

The comparison between the other two products, A130 and AP273, is perhaps more interesting. Although their molecular weights as determined by viscometry were similar (11.8×10^6 and 12.2×10^6 daltons respectively) their distributions are quite different. A130 has a broader distribution similar to LT27. It is interesting to note that A130 and LT27 are manufactured by similar processes in which acrylamide and sodium acrylate are copolymerized while AP273 is produced by polymerization and hydrolysis of acrylamide.

There is little to be gained from speculation on the reasons for the effects observed or on the possible effects of the different reaction conditions which may have been employed as these are closely guarded commercial secrets. However, it is interesting to compare these results with the observations made in the preceding chapter on the relative performances of these two apparently similar polymers in batch settling tests.

The results in Table 3.1 showed that A130 generally produced lower settling rates and that it had a slightly higher Huggins' constant (k). It was postulated that the differences in k may be due to the presence of a small number of crosslinks in some samples or to differences in the distributions of monomer sequences. The results in Figure 4.2 introduce the additional possibility that k may also be a function of the molecular weight distribution.

The significance of the Huggins' constant is discussed in detail later in this chapter but some discussion is warranted here. As demonstrated previously (see Figure 3.8) the settling rate increases linearly with molecular weight for a given copolymer composition. The broader molecular weight distribution of A130 means it has a higher proportion of higher molecular weight polymer. The differences between A130 and AP273 which are apparent in Table 3.1 thus may be simply due to the difference in molecular weight distributions. However the relative differences in settling rates are substantially larger than would be expected from Figure 3.8 for such subtle molecular weight effects.

In previous chapters, it was observed that molecular weight fractionation of copolymers, particularly polyelectrolytes, is usually accompanied by at least some fractionation of chemical heterogeneity as well. Therefore, the results in this section must also be discussed in conjunction with those which follow.

4.1.2 CHEMICAL HETEROGENEITY

Very few others have identified the importance of copolymer composition in bridging flocculation although it appears that many industrial users attempt, perhaps unknowingly, to utilise the effect through ad hoc testing and selection procedures. It has been clearly demonstrated here that, at least in raw sugar processing, copolymer composition is a critical parameter in the flocculation reaction. Because of the pronounced effects which have been observed, it would be somewhat surprising if chemical heterogeneity did not also affect the reaction.

In the fractional precipitation experiments described above, each of the fractions recovered was also analysed to determine its copolymer composition. The results are displayed in Figure 4.3. The curve for A130 shows an unusual tail at the low acrylate end although this may be nothing more than an experimental error. Apart from that, the data are very similar to those for AP273. LT27 has a lower mean, as expected, and a broader distribution but shows no major differences which might be expected to influence flocculation behaviour.

When the two sets of data are combined (see Figure 4.4), the results show evidence of a relationship between molecular weight and copolymer composition. All three products show similar trends, with the highest molecular weight fractions having the lowest proportions of acrylate monomer. This trend has been confirmed for LT27 in experiments by the manufacturer, Allied Colloids Pty. Ltd., where polymerization reactions were terminated at different stages from 25 % to 100 % completion. Analysis of the resulting samples demonstrated that polymers

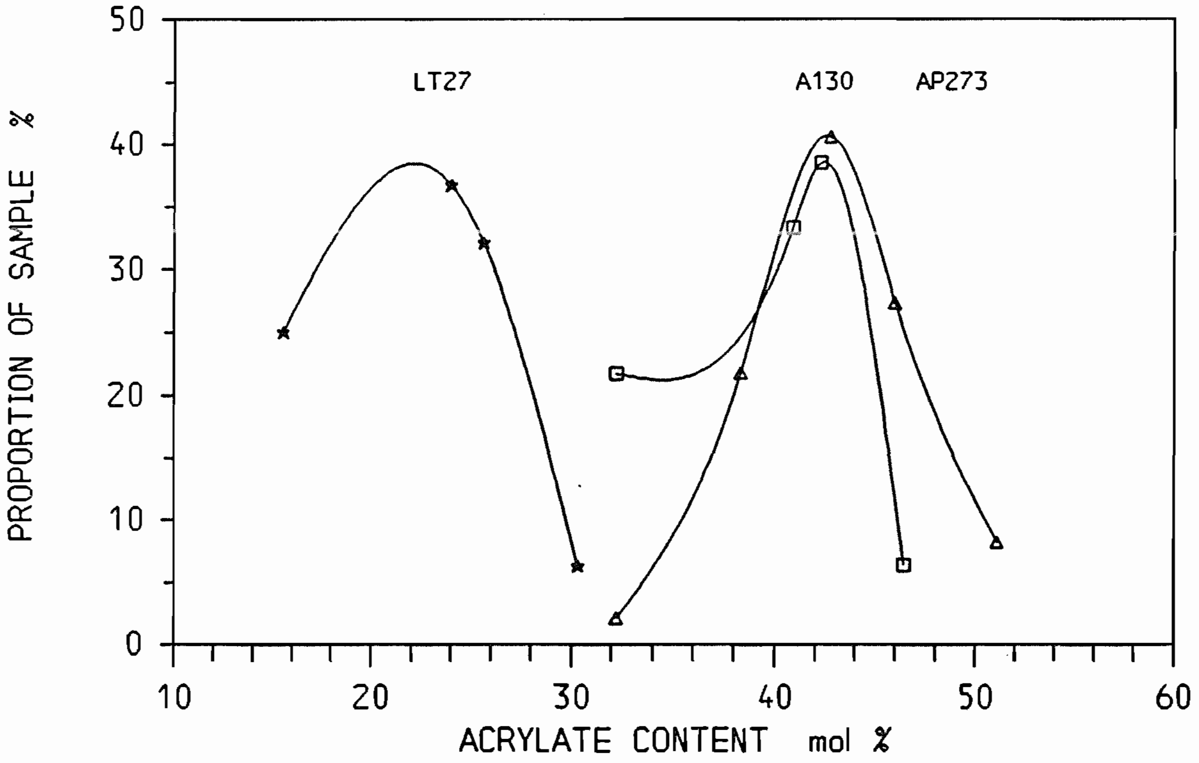

Figure 4.3 Chemical heterogeneity of some commercial polymers.

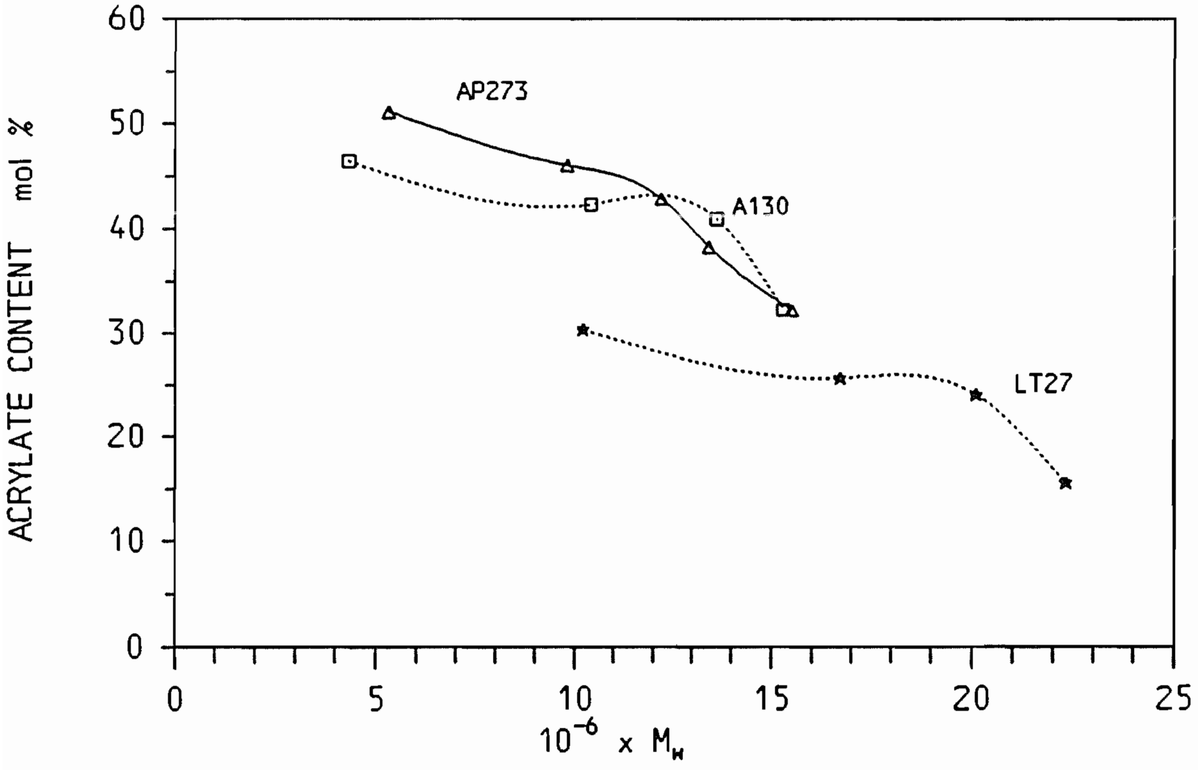

Figure 4.4 Comparison between molecular weight and copolymer composition.

recovered in the early stages of the reaction had the lowest acrylate content and the highest molecular weight.

Molecular weight distributions in free radical polymerizations follow no simple patterns and no attempt has been made to predict them for acrylamide polymerizations. However, some useful general observations can be made which assist in the interpretation of Figure 4.4. To achieve the very high molecula weights observed here, it is apparent that the rates of chain transfer and termination must be extremely small, to the extent that chain termination probably occurs predominantly through coupling of polymeric radicals.

As the reaction proceeds, the viscosity increases rapidly and the reaction mixture becomes a semi-rigid gel after a short period. The mobility of actively growing polymers would be increasingly restricted and the rate constant for termination by coupling would decline. At constant monomer concentration and in the absence of other terminating reactions, an increase in molecular weight would be expected. However, in a reaction which proceeds effectively to complete conversion, the monomer concentration cannot be considered constant. The molecular weight would be expected to decrease as monomer concentration declines. Other factors which may also influence the degree of polymerization include changes in rate constants with the increasing viscosity and changes in the concentration of polymer radicals during the reaction. In the absence of data on conditions during the reaction, estimation of molecular weights during the course of polymerization is impossible.

The variation in copolymer composition during the course of the reaction can be predicted using the reactivity ratios of the monomers in aqueous solution (see Table 4.1) and the equation:

$$F_1 = \frac{r_1.f_1^2 + f_1.f_2}{r_1.f_1^2 + 2.f_1.f_2 + r_2.f_2^2} \qquad (4.1)$$

where F_1 = mole fraction of monomer 1 in polymer mixture
f_1 = mole fraction of monomer 1 in monomer mixture
f_2 = mole fraction of monomer 2 in monomer mixture
= $1 - f_1$
r_1, r_2 = reactivity ratios of monomers

Table 4.1 Reactivity Ratios for Acrylamide Polymerization[155]

Monomer 1	Monomer 2	r1	r2
Acrylic acid	Acrylamide	1.43	0.60
Sodium acrylate	Acrylamide	0.35	0.35

The variation of copolymer composition with monomer composition calculated from equation (4.1) for the polymerization of acrylamide with acrylic acid and with sodium acrylate are shown in Figure 4.5.

It is apparent that the pH of the reaction mixture will have an important bearing on the result. From the dissociation constant of acrylic acid ($pK_a = 5.25$), simple calculation shows that dissociation will be more than 99 % complete at pH > 6.25. At any pH above this value, the copolymer composition should follow the curve for sodium acrylate shown in Figure 4.5. Except in the limiting cases of pure acrylamide or pure sodium acrylate, the acrylate content of the polymer fraction will always be lower than in the monomer mixture. At low pH where the degree of dissociation is small, polymerization should follow the curve for acrylic acid and the converse should apply.

It is evident that slight changes in pH during the polymerization can have a dramatic effect on the composition of the polymer. In the absence of detailed information on the actual conditions employed in commercial reactions, prediction of the distribution of compositions in commercial polymers is not possible. However, the information provided by Allied Colloids Pty. Ltd. on their product LT27 indicates that the course of the reaction roughly follows the curve for sodium acrylate.

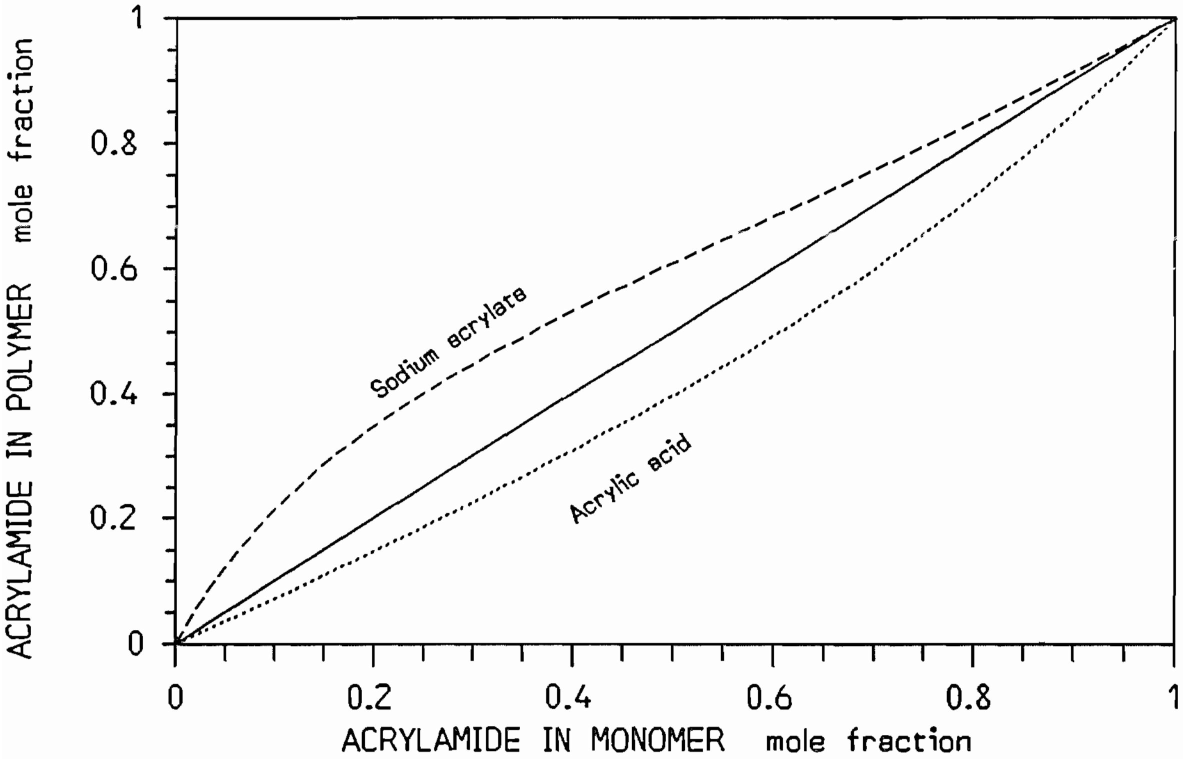

Figure 4.5 Predicted polymer compositions for the copolymerization of acrylamide with acrylic acid.

The general conclusion which arises from the preceding discussion is that polymer produced during the initial stages of the reaction has the highest molecular weight and the lowest acrylate content. Further, the observation from Figure 4.4 that AP273 and A130 had similar chemical heterogeneities, despite the differences in their Huggins' constants and settling rates shown previously in Table 3.1, indicates that chemical heterogeneity is not the explanation for their different performances in flocculation reactions. However, it is not suggested that chemical heterogeneity has no influence on the flocculation reaction in general - this aspect remains to be resolved.

4.2 SOLUTION PROPERTIES

The influence of the polymer molecule on the flocculation reaction is manifested in two ways. In addition to the kinetics and thermodynamics of polymer adsorption which were discussed in the previous chapter, the solution properties of the polymer also play an important role. Study of these properties under the conditions of actual factory use is impractical. However, examination of certain solution properties under controlled laboratory conditions provides a valuable insight into the mechanism of the reaction and the reasons for the differences observed in the performances of the polymers studied.

Polymer solution properties have a direct bearing on the industrial application of modern commercial flocculants. There are numerous examples of industrial applications where some benefit has been obtained even under very crude factory conditions. However, if full advantage is to be taken of the improvements in polymerization technology and the efforts of manufacturers in this regard are not to be wasted, industrial equipment must be designed to match the properties of the polymers. This is possible only if these properties are well understood.

4.2.1 KINETICS OF DISSOLUTION

The kinetics of polymer dissolution have important consequences both in laboratory experiments and in industrial applications. In the former, they determine the minimum time required for and the practical approach to experiments. In the latter, they strongly influence the design of processing equipment and thus also the economics of the particular application.

The rate of dissolution of large charged polymers is determined principally by the rate at which solvent, usually water, can penetrate the solid particle and by the rate at which the molecular conformation can rearrange. Both of these will be influenced by the usual variables of agitation, temperature and ionic environment, although more so than simple compounds.

Visual assessment of polymer dissolution is frequently misleading. When a small quantity of polymer powder is added to distilled water with gentle mixing, the solution generally appears homogeneous to the eye within a relatively short period (10 to 30 minutes). However there is ample experimental evidence that several hours are required for the system to reach equilibrium. No more clearly has this been demonstrated than in factory experiments where the amount of polymer remaining in solution, after flocculation and settling, was measured as a function of the elapsed mixing time (see Figure 4.6). After only ten minutes dissolution time, the polymer was sufficiently dissolved to enable considerable flocculation to occur. However dissolution was far from complete as almost 30 % of the added polymer was not adsorbed during the flocculation reaction. Adsorption did not reach its maximum value until approximately three hours mixing time had elapsed. Such a result may be of little significance in many industries but it is of considerable importance in raw sugar manufacture. Not only is there a financial loss due to the unnecessary use of extra polymer but the presence of the polymer in clarified juice has a severely depressing effect on raw sugar quality.

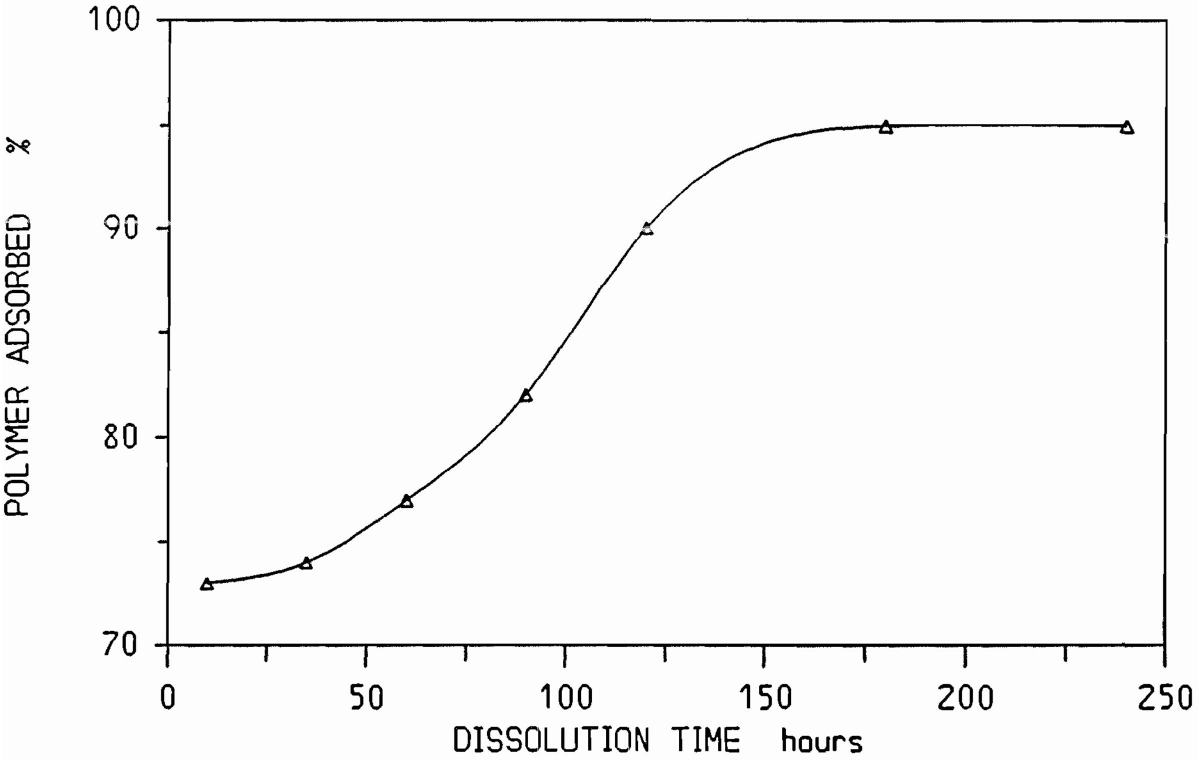

Figure 4.6 Effect of dissolution time on polymer adsorption.

The effect of ionic environment on the dissolution rate has been demonstrated in laboratory experiments in which refractive index gradients (dn/dc) were determined for a series of solutions prepared in a manner similar to that described in Chapter 2 for the determination of intrinsic viscosities. Reference samples were prepared in the normal manner by dissolving the polymer in distilled water for four and eight hours, then adding 2.00 M $NaNO_3$ to give a final ionic strength of 1.00 M. Several solutions of the same polymer were also prepared by dissolving the powder directly in 1.00 M $NaNO_3$ with mixing times which varied from four hours to 40 hours. The results (Table 4.2) showed that (dn/dc) for the samples prepared directly in 1.00 M $NaNO_3$ was initially high but decreased with mixing time, although it had not reached the value of the reference samples even after 40 hours.

It was observed also that dn/dc for the same polymer in distilled water was similar to that for the reference samples in $NaNO_3$ and that the value was independent of mixing time after four hours.

The explanation of these observations is simple. The electrostatic forces of repulsion between neighbouring ionic groups in a polyelectrolyte provide a strong driving force to change the conformation of the polymer molecule. In distilled water, where the ionic strength is lowest, the electrostatic forces have their greatest effect and the time in which the molecule reaches its equilibrium conformation will be shortest. Having reached equilibrium in distilled water, the molecule then rapidly reaches a new equilibrium conformation when the ionic strength is increased by the addition of $NaNO_3$.

In contrast to the preceding case, when the powder is added directly to 1.00 M $NaNO_3$, the high ionic strength of the solvent reduces the effective range of the electrostatic forces. The driving force for rearrangement is greatly reduced. This is clearly reflected in the time required to approach the equilibrium value of dn/dc. Similar effects have been demonstrated by measuring solution viscosities as a function of time.

The relatively slow approach to equilibrium should not be surprising for molecules of such high molecular weight and creates no serious practical difficulties. However, the techniques employed in this work and, subsequently, in factory operations throughout the Australian sugar industry have been carefully designed to take account of the phenomenon.

Table 4.2 Kinetics of Polymer Dissolution

SAMPLE	MIXING TIME (hours)	dn/dc
A130 in 1.00 M $NaNO_3$	4	0.4886
	16	0.4455
	40	0.2146
A130 reference	4	0.1721
	16	0.1732
A130 in water	4	0.1883
	16	0.1863

4.2.2 SOLUTION DIMENSIONS

The solution dimensions of a range of typical commercial polymers were investigated by the usual techniques of viscometry and light scattering. Additional information was obtained from other experiments which were related in various ways to these techniques. The procedures employed are described in the relevant sections.

The properties of polyelectrolytes in aqueous solution differ from those of their uncharged counterparts primarily through the effects of the ionized groups. Undoubtedly the most striking characteristic of high molecular weight polyelectrolytes is the rheology of their solutions. Not only is the viscosity of aqueous solutions very high, even at very low concentrations, but the viscosity often increases as the solution is diluted. This behaviour occurs because the electrostatic repulsion between neighbouring ionic groups of the polymer forces the molecules to assume an extended conformation. The phenomenon has been well documented by numerous others and need not be discussed in detail here.

The effects of the ionic groups can be reduced by increasing the ionic strength of the solvent. If sufficient simple electrolyte is added, the polymer behaves almost as an uncharged polymer and the equations used for uncharged polymers can be applied to the experimental data. The determination of molecular weights from intrinsic viscosities, which has been discussed in detail previously, is an example.

Solutions of negligible ionic strength or of very high ionic strength represent limiting cases and the conditions of actual use lie somewhere in between. The changes in solution dimensions and in polymer/solvent interactions have been examined previously by the author[149] with polymers of up to 12 x 10^6 daltons. Using a combination of light scattering and viscometry techniques, it was shown that, in 1.00 M $NaNO_3$, the molecules behaved as flexible random coils even when the pH was raised to ensure complete dissociation. At lower ionic strengths, the solution dimensions increased as the ionic content of the polymer increased.

Some of these experiments have been repeated here with polymers of higher molecular weight. The combination of the very high molecular weights and the obvious polydispersity of the samples resulted in Zimm plots which were characterized by a distinct curvature in the angular variation of Kc/R, particularly at angles > 90°. Although the angular variation was almost linear at low angles, extrapolation to zero angle was achieved by fitting a third order polynomial to the data. The variation with concentration was linear. A typical Zimm plot for one of the polymers discussed below is illustrated in Figure 4.7.

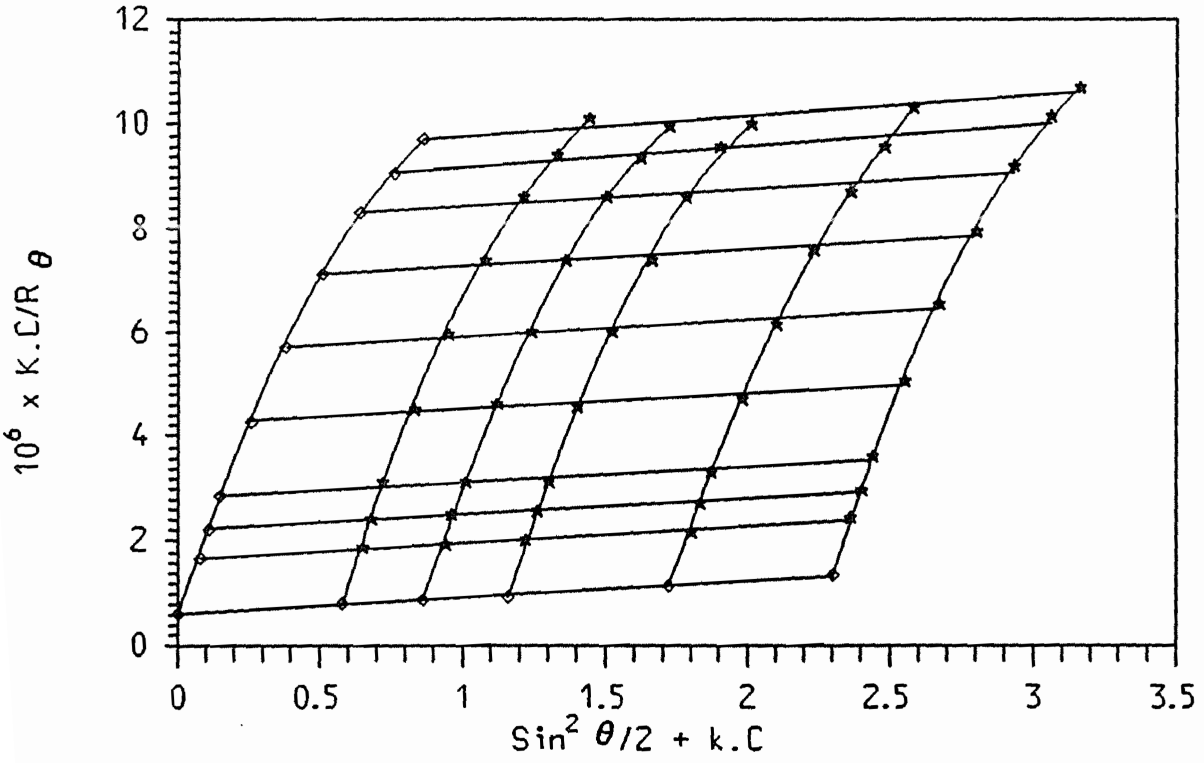

Figure 4.7 Zimm plot for A2130 in 1.00 M $NaNO_3$

The radii of gyration were determined for a series of commercial polymers of approximately 20 x 10^6 daltons in 1.00 M $NaNO_3$ at pH 8.5 and 30°C . Figure 4.8 shows that, while R_g is very large, both it and the second virial coefficient are nonetheless independent of the acrylate content of the polymers, within experimental error.

The values of R_g are so large that they are similar to the wavelength of light employed in the light scattering measurements. Consequently the number average rather than weight average values of molecular weight and Rg are obtained by light scattering (see Chapter 2). Since the coefficients employed in the Mark-Houwink equation (1.21) relate intrinsic viscosity to the weight average molecular weight, an estimate of the molecular weight distribution is available from the ratio M_w/M_n. The values of M_w/M_n for the polymers referred to in Figure 4.8 range from 4.7 to 7.3, indicating a very broad distribution. However, these results must be treated very cautiously as the molecular weights are more than an order of magnitude greater than the range for which equation 1.21 was determined. Extrapolation of the equation to such an extent may not be justified.

The significance of the large radius of gyration becomes evident when attempting to filter solutions. The nominal pore size of many membrane filters is smaller than R_g and should therefore retain the polymer. Even membranes of nominally larger pore size will have some pores smaller than R_g. Filtration therefore offers a simple means of confirming the molecular dimensions determined by other methods.

Figure 4.9 shows the retention of a sample of one of the above polymers, A2130 (40.6 mol % acrylate) for which $R_g = 466$ nm. A nominal pore size at least 10 times larger than R_g was required to ensure that none of the polymer was selectively retained by the membrane. Apart from confirming the values of R_g, these simple experiments demonstrate that filtration cannot be used to clean solutions for light scattering. A membrane large enough to allow the polymer to pass freely will also pass dust particles of similar size which will introduce substantial errors to the measurements. Visual observations made using the

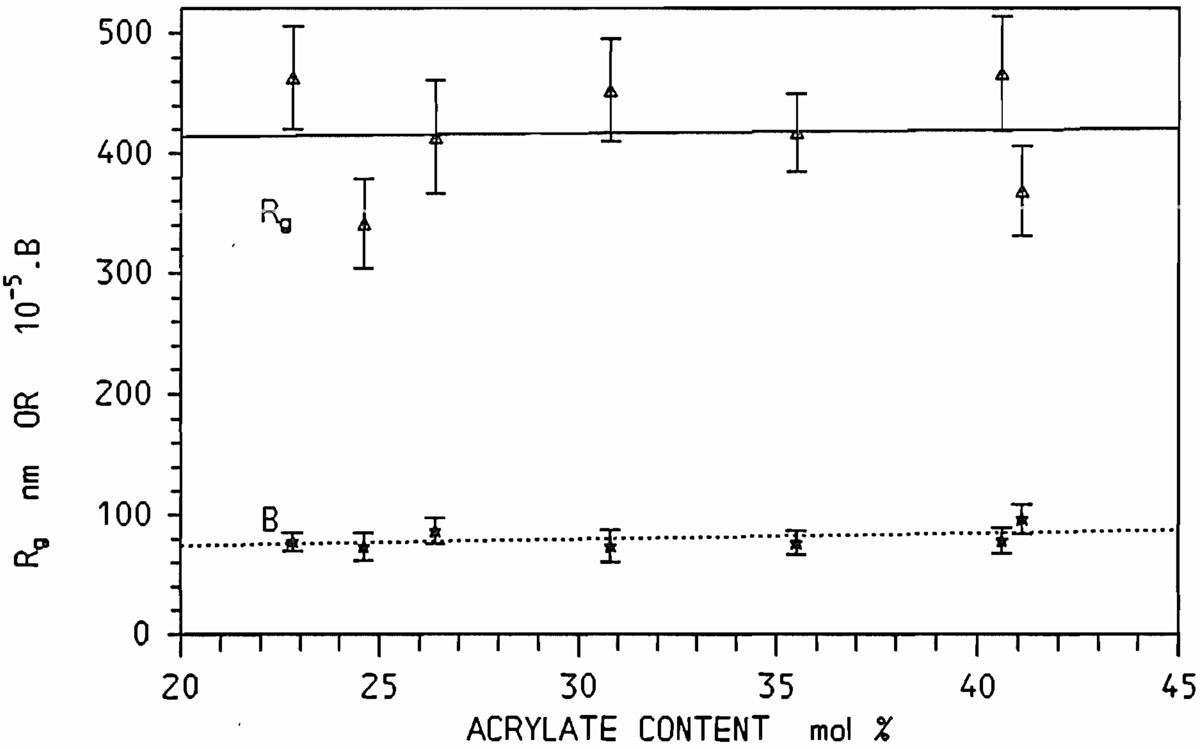

Figure 4.8 Effect of acrylate content on solution dimensions.

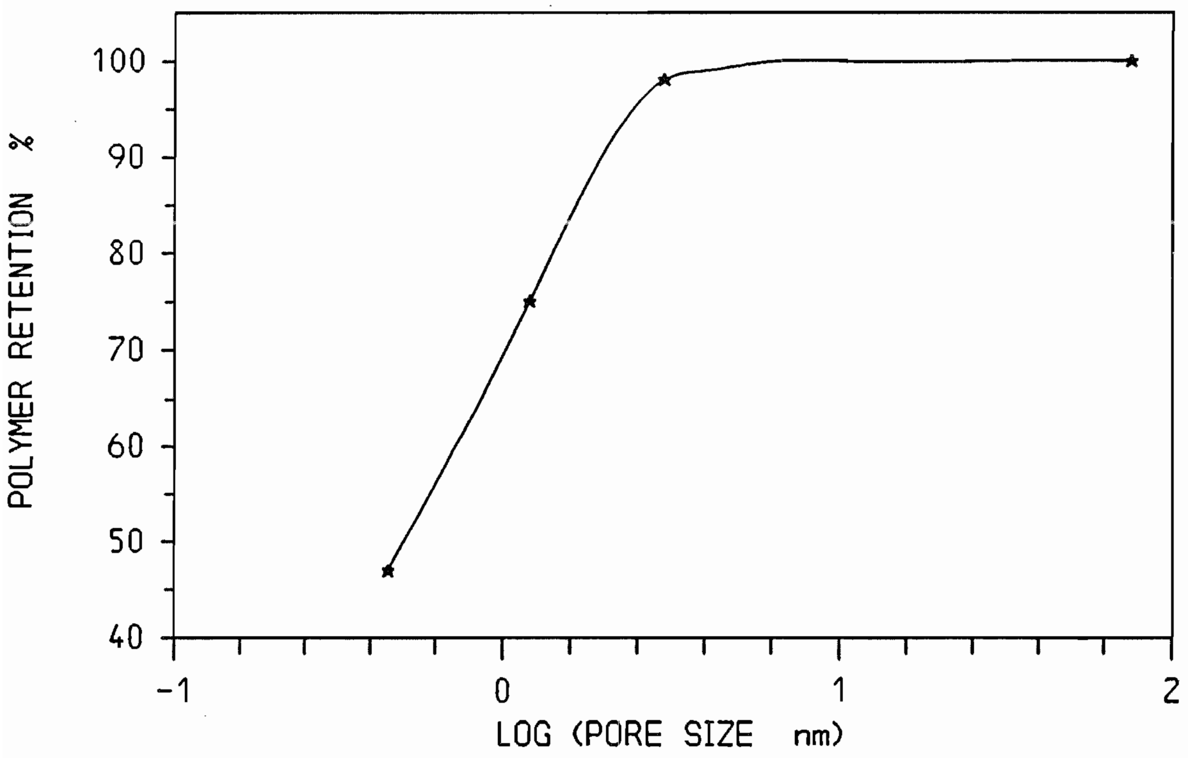

Figure 4.9 Effect of filtration on a solution of A2130 (41 mol % acrylate; 21 x 10^6)

special viewing facility of the Sofica photometer confirmed this problem on numerous occasions.

Since cane juice typically has an ionic strength of approximately 0.3 m with the predominant cations being potassium and calcium, values of R_g were also determined in a similar environment. Table 4.3 shows the results obtained with a series of commercial polymers of similar molecular weights (average 21 x 10^6) at pH 8.0. R_g was constant at least up to 42 mol % acrylate both in 0.30 m $NaNO_3$ and in 0.30 m $NaNO_3$ containing 5.00 x 10^{-3} m of $CaNO_3$.

Table 4.3 Solution Dimensions of Polymers in 0.30 M $NaNO_3$

Polymer	Acrylate mol %	R_g (nm)	
		0.30 m $NaNO_3$	0.30 m $NaNO_3$ + $5x10^{-3}$ m Ca^+
A2110	22.8	379 ± 42	337 ± 48
A2115	26.4	480 ± 47	-
A2120	30.8	457 ± 37	409 ± 55
A2125	35.5	345 ± 43	411 ± 36
A2130	40.6	450 ± 52	433 ± 62
Average		422 ± 40	398 ± 50

A similar effect was observed in the previous work with lower molecular weight polymers[149]. However, an interesting new result was found when two polymers with different Huggins' constants, but similar molecular weights and acrylate contents, were examined. Unfortunately the only suitable polymers available had lower molecular weights than those in Table 4.3 but it is reasonable to assume that similar results would be obtained at the higher molecular weights. AP273 was a product reportedly prepared by polymerization and hydrolysis of acrylamide while A130 was prepared by copolymerization with sodium acrylate.

In 0.3 M $NaNO_3$, the values of R_g (See Table 4.4) were the same for the two polymers and were unaffected by the addition of 5×10^{-3} Ca^{2+}, which is typical of the level encountered in cane juice. In contrast, the second virial coefficient for AP273, which had the lower Huggins' constant, was very much larger than for A130 in 0.3 M $NaNO_3$. The addition of 5×10^{-3} M Ca^{2+} did not affect B for the latter but was sufficient to reduce the value for AP273 to the level of its copolymer counterpart. The implication of these results for bridging flocculation is that the two polymers should have identical physical properties in cane juice because of the ionic environment. However, this is not supported by the experimental results of batch settling tests where AP273 was shown to give superior results. Unfortunately, the limited shelf life of the polymers meant that the samples referred to in this chapter could not be identical to those in Table 3.1. However, they showed very similar differences in Huggins' constant and in flocculation behaviour so comparisons between the two tables are still valid.

Table 4.4 Solution Properties of AP273 and A130 in 0.3 M $NaNO_3$

	A130	AP273
Acrylate (mol %)	40.6	41.1
$Mw \times 10^{-6}$	12.8	13.5
k	0.32	0.18
R_g (nm) (without Ca^{2+})	330 ± 25	330 ± 40
(with Ca^{2+})	317 ± 55	295 ± 35
$B \times 10^3$ (without Ca^{2+})	0.98 ± 0.03	1.33 ± 0.07
(with Ca^{2+})	0.87 ± 0.03	0.82 ± 0.07

The second virial coefficient, B, for polyelectrolytes is a function of the volume occupied by the molecule, the solvent/segment interactions and the electrostatic interactions. However, it has been shown that, in their interactions with other polyions, polyelectrolyte molecules behave as if they were essentially uncharged[150]. Values of B have been calculated for the polymers in Table 4.4 using the equation for uncharged polymers[150]:

$$B = \frac{16.\pi.\gamma^3.N.R_g{}^3}{3M^2} \qquad (4.2)$$

where γ = interaction parameter
N = Avogadro's number

The interaction parameter was calculated using the equations of Flory and Krigbaum described in reference 150 for a flexible polymer in a good solvent. The value of B obtained was 1.67×10^{-3} mol.cm^3.g^{-1}, which is similar to the values in the table above. The values of R_g in the table must be considered constant, within the limits of the experimental error, although the variations are sufficient to explain the differences in B for A130. However, the change in R_g for AP273 is much too small to account for the large change observed in B. From equation (4.2), the latter change must therefore reflect a difference in the interaction parameter. Furthermore, since the volume of the molecule, as estimated by R_g, remains constant, the major contribution must come from the thermodynamic component for the solvent/segment interactions. Whether it is the entropic or the enthalpic component which exerts the controlling influence cannot be determined.

Whilst the precise reasons for the present results cannot be determined, it is interesting to consider the possible effects of the distribution of monomer sequences. As discussed previously, in a random copolymer of this composition and molecular weight, there must be numerous blocks of the acrylate monomer. In a regular copolymer, on the other hand, acrylate monomers would be separated by at least one acrylamide unit. Thus COO^- groups in the latter will be separated by greater distances than in the blocks of the random copolymer. The interaction between the COO^- groups and other ions, particularly divalent ions, would be expected to be different.

4.2.3 HUGGINS' CONSTANT

Reference has been made frequently to the apparent relationship between the flocculating ability of apparently similar polymers and their Huggins' constants (k) determined by viscometry. In the discussion in Chapter 1, it was stated that k is approximately constant for a series of polymer homologues in a good solvent and that it is often about 0.35 for a flexible polymer in a good solvent[150]. While k for many of the polymers studied here was often around 0.35, it was not constant (see Figure 4.10).

While the molecular significance of k has not been elucidated, theoretical studies indicate that it comprises a hydrodynamic factor and a thermodynamic factor and can be described by an equation:

$$k = k' - 3.B.M.f(\alpha)/[\eta] \qquad (4.3)$$

where k = Huggins' constant
k'= hydrodynamic factor
B = second virial coefficient
$[\eta]$ = intrinsic viscosity
$f(\alpha)$ = molecular expansion factor

The value of k' is typically 0.5 - 0.7. However k will be a complex function of molecular weight since B, $[\eta]$ and the expansion factor are all functions of M. Some indication of the possible relationship can be obtained by substituting for these parameters. The second virial coefficient is related to the molecular weight by a relatively simple function:

$$B = \frac{N\ u}{2\ M^2} \qquad (4.4)$$

where N = Avogardo's number
u = excluded volume

The excluded volume term is itself a more complex function of molecular weight and the expansion factor α:

$$u = f[M^2,(\alpha^2 - 1)] \qquad (4.5)$$

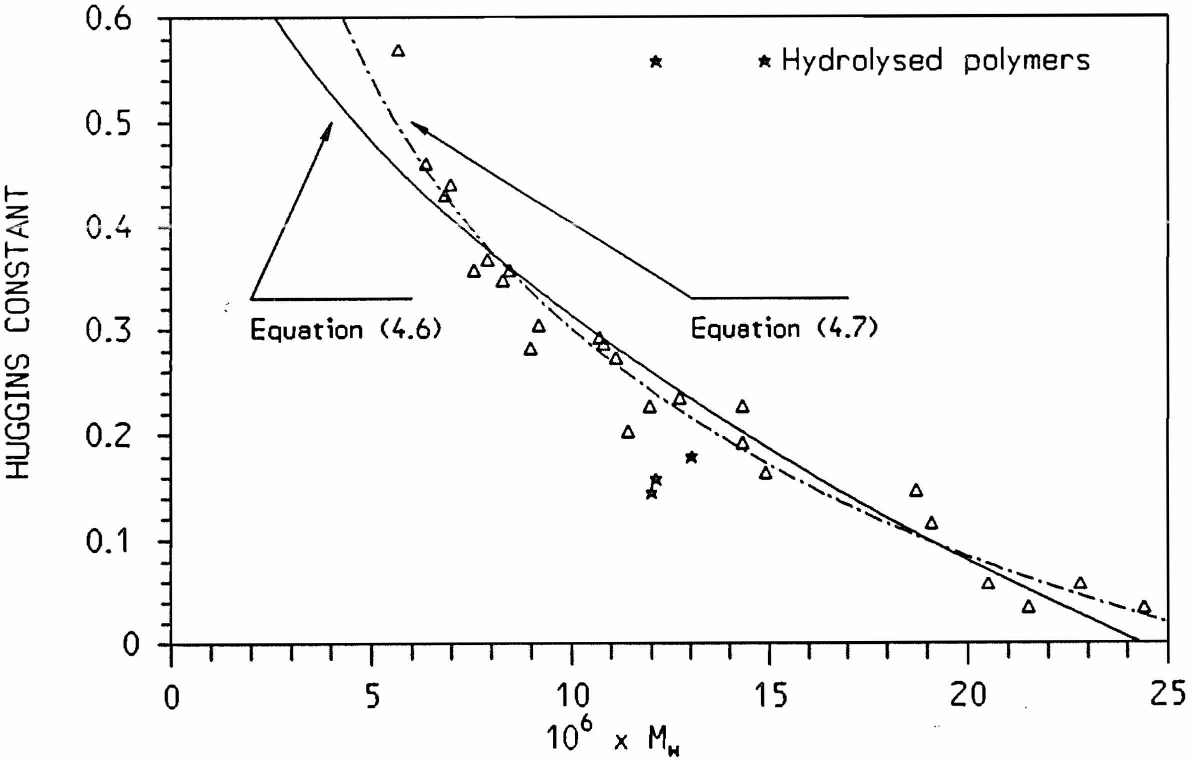

Figure 4.10 Variation of Huggins' constant with molecular weight.

If α is very large, it becomes proportional to $M^{0.1}$, which then represents the upper limit in its dependence on M. When equation 4.3 is combined with (4.4) and (4.5), together with the Mark-Houwink equation (1.21), the dependence of k on M becomes, in the limit of large α:

$$k = k' - A.M^{0.46} \qquad (4.6)$$

where A = constant

Regression analysis of the experimental data of Figure 4.10 yielded a value of 0.93 for the hydrodynamic factor k'. The solid line in Figure 4.10 was calculated by substituting this value in equation (4.6). Considering the simplicity of the approach taken above, the agreement with the experimental data is good and enables a more comprehensive examination of the variations in k observed for polymers of similar molecular weight.

Referring again to equation 4.3, if it is assumed that the hydrodynamic parameter k' remains constant, then variations in k at a given molecular weight must result from changes in either B or $f(\alpha)$. Previous work[149] in 1.00 M $NaNO_3$ has shown that there was no correlation between k and B. The implication then is that the expansion factor α must change. From (4.3), a decrease in α due to such factors as branching or intramolecular interactions would result in an increase in k. Both of these effects would also be detrimental to flocculation. Conversely, then, a reduction in k would enhance flocculation.

Viscosity determinations have been made in a solvent of very high ionic strength, deliberately chosen to suppress intermolecular and intramolecular interactions. Under such conditions, subtle differences in polymer/solvent interactions probably will not be evident. At lower ionic strengths, similar to that encountered in actual use, these interactions may become apparent. The possibility of a relationship between k and the second virial coefficient cannot be ignored.

There is evidence of this in Table 4.4, where values of B have been obtained in 0.30 M $NaNO_3$. AP 273 has the higher virial coefficient and, as expected from (4.3), also has the lower Huggins' constant. As discussed above, B is a function of the solvent/segment interactions, electrostatic interactions and the volume of the molecule. However, the fact that R_g is essentially the same for the two polymers indicates that the latter is not a contributing parameter. Presumably then, the larger value of B thus represents a better solvency condition. In the absence of specific interactions, this would be less favourable for polymer adsorption. Using the model described at the conclusion of Chapter 3, weaker adsorption should result in an improvement in flocculating ability for a polymer whose acrylate content is greater than the optimum. Conversely, below the optimum acrylate content, weaker adsorption should result in poorer flocculation. Since the optimum acrylate content is almost always below that of AP273, the performance of this polymer should be better than other polymers of similar composition. The results in Table 3.1 of the preceding chapter indicated that this effect was observed in many tests although there a few occasions where the opposite trend was recorded.

An alternative interpretation of the Huggins' constant has been presented recently by Gundert and Wolf[151]. The theory was based on the concept that k was composed of unequal contributions from inter - and intra-molecular contacts between polymer segments. On this basis, an equation was developed for the dependence of k on molecular weight:

$$k = \frac{k_e + k_i}{2} + \frac{k_e - k_i}{2} \cdot \frac{K_o}{K} \cdot M^{-(\alpha-0.5)} \qquad (4.7)$$

where k_e = k for intermolecular interactions
k_i = K for intramolecular interactions
K, α = Mark Houwink parameters
K_o = K at theta condition

This equation predicts that k is a function of $M^{-0.16}$. As for (4.6), a regression analysis was used to fit the data in

Figure 4.10 to this equation. The resulting line, also shown in Figure 4.10, fits the data better than equation (4.6). Since a value is not available for the Mark Houwink parameter K under theta conditions in 1.00 M $NaNO_3$, the individual values of k_e and k_i cannot be determined. However, the regression analysis did show that $(k_e + k_i) < 0$, indicating that at least one of the parameters is also < 0. Gundert and Wolf reported negative values of the intramolecular term k_i for values of the Mark-Houwink parameter $\alpha < 0.75$ and interpreted this as an indication of relatively poor solvency.

With the data available here, the relative contributions of the two terms to the Huggins' constant cannot be determined. However, this approach appears to offer an interesting alternativem to (4.3) and eventually may yield a valuable insight into polymer/solution interactions.

In the preceding chapter, it was observed that unusually high values of k corresponded to polymers with some evidence of branching or crosslinking. That observation has been reinforced by the discussion above.

4.3 MONOMER SEQUENCE DISTRIBUTIONS

In the preceding sections, various solution properties have been examined and their possible influences on the flocculating ability of the polymers discussed. In those instances where k was larger than expected, there was evidence to show that increased branching or crosslinking was probably responsible. In other cases, no simple explanation was available but it was suggested that changes in the distribution of monomer sequences may be a contributing factor.

There are numerous techniques which can be used to determine average structural information such as the ratio of comonomers in polymers. However, ^{13}C nmr offers a unique opportunity to determine detailed information, not otherwise available, on both the complete distribution of monomer sequences and the number average sequence lengths. However, interpretation of spectra can be a difficult analytical problem since responses associated with stereochemical configurations are often imposed on other responses from the carbon skeleton or attached functional groups.

In principle, it should be possible to obtain sequence distributions for acrylamide/sodium acrylate copolymers from the methylene, methine or carbonyl regions of the spectrum. As discussed in Chapter 2, it was found that the methylene and methine carbon chemical shifts were more difficult to interpret due to a sensitivity to configurational differences superimposed upon the comonomer sensitivity. However, the carbonyl resonances appeared to be sensitive only to comonomer triad sequences. Analysis of the copolymers was confined, therefore, to the carbonyl region of the spectrum.

4.3.1 ASSIGNMENT OF CHEMICAL SHIFTS

Despite the long accumulation times employed with commercial copolymers (typically 16 hours), the resolution of spectra obtained were inadequate for direct assignment of chemical shifts. Consequently, it was necessary to make assignments by reference to a series of lower molecular weight polymers, prepared as described in Chapter 2. The lower molecular weight meant that higher concentrations were possible so that good spectra (see Figure 2.10) were obtained in relatively short times.

The kinetics of alkaline hydrolysis for acrylamide homopolymer were discussed in Chapter 2 (see Section 2.2.6). Under the mild conditions employed here, it was predicted that the hydrolysed polymer should have a regular distribution of acrylamide and sodium acrylate monomers and that the hydrolysis should reach a limiting value of about 45 mol %. In fact, the highest hydrolysis achieved was 42 mol % although no attempt was made to determine the limit by direct experimentation. Further confirmation of the existence of a limiting hydrolysis, albeit different because of different conditions, was obtained from observations on solutions of commercial polymers which had been stored at pH 9 for periods of up to one year. Six polymers which initially varied from 25 mol % to 42 mol % acrylate were found to have identical spectra in the carbonyl, methylene and methine regions. The final acrylate content of each polymer was 63 mol %.

None of the laboratory prepared polymers, even up to 42 mol % acrylate, showed any evidence of a peak corresponding to the BBB triad (see Figure 2.9). Assigment of this triad was made using a separate sample of sodium polyacrylate. In a random copolymer of this composition, both the BBB and the ABB triads would be expected to be present in sufficient proportions to give clearly defined peaks. In fact, even the ABB triad was barely discernible in the 42 % hydrolysed polymer, further confirming the regularity of the sequence distribution.

These results are in agreement with the predictions made from the reported kinetics of alkaline hydrolysis. However, further investigation of the kinetics and calculation of the distribution frequencies for the various triads were not warranted. The assignments of carbonyl peaks could be made quite readily for these samples as indicated previously in Figure 2.9. The chemical shifts determined from those spectra for the six possible triads are listed in Table 4.5. Values reported recently by Halverson et al[152] and Panzer et al[153] are included also and are in good agreement with the results obtained here.

Table 4.5 Assignment of Chemical Shifts for Carbonyl Carbons

TRIAD *	CHEMICAL SHIFTS ppm		
	This work	Halverson et al	Panzer et al
AAA	180.2	180.3	180.2
AAB	180.8	181.1	181.1
BAB	181.3	181.5	181.6
ABA	183.4	183.6	183.6
ABB	183.9	184.0	184.3
BBB	185.6	185.1	185.2

* A = Acrylamide
B = Sodium acrylate

4.3.2 CARBONYL SPECTRA OF COMMERCIAL POLYMERS

The carbonyl spectra of three commercial polymers are shown in Figure 4.11. Of these, A2115 (25.8 mol % acrylate) and A2130 (38.0 mol % acrylate) are from the Superfloc series and were manufactured by direct copolymerization while XF4282 (41.0 mol % acrylate) was manufactured by polymerization and subsequent hydrolysis. XF4282 represents the upper limit of acrylate contents which are of practical significance to the sugar industry. Integration of the peaks required some approximation but the estimates of acrylate contents obtained from the relative areas of the A- and B- centred triads (26, 35 and 42 mol % respectively) agreed with the previously determined values. The spectrum of a fourth commercial copolymer, also from the Superfloc series and with an acrylate content of 48 mol % has not been included in Figure 4.11 but has been used to obtain additional data which are used later.

In the series of Super floc copolymers, the peak corresponding to the AAA triad decreased relative to the AAB triad with increasing acrylate content. There is a possibility that a small BAB peak existed at the highest acrylate content but this was uncertain due to the level of noise. In the B-centred triads, the ABA triad decreased relative to the ABB triad as expected. However, there was no evidence at all of a BBB triad.

The sequence distribution in a completely random copolymer can be predicted using the Bernoullian statistical model[154]. The comparison between this model and the triad mole fractions of the Super floc series, determined from Figure 4.11 and other spectra, is shown in Figure 4.12 for B-centred triads, where the lines are the calculated compositions and the points are experimental data. At low acrylate contents, the experimental data conform to the random distribution but, as the acrylate content increases, the deviation from the predicted curves becomes pronounced, particularly with the BAB and BBB triads. Similar results were obtained for the A-centred triads. This suggests that the monomer at the end of the growing chain has some bearing on the next monomer which is added.

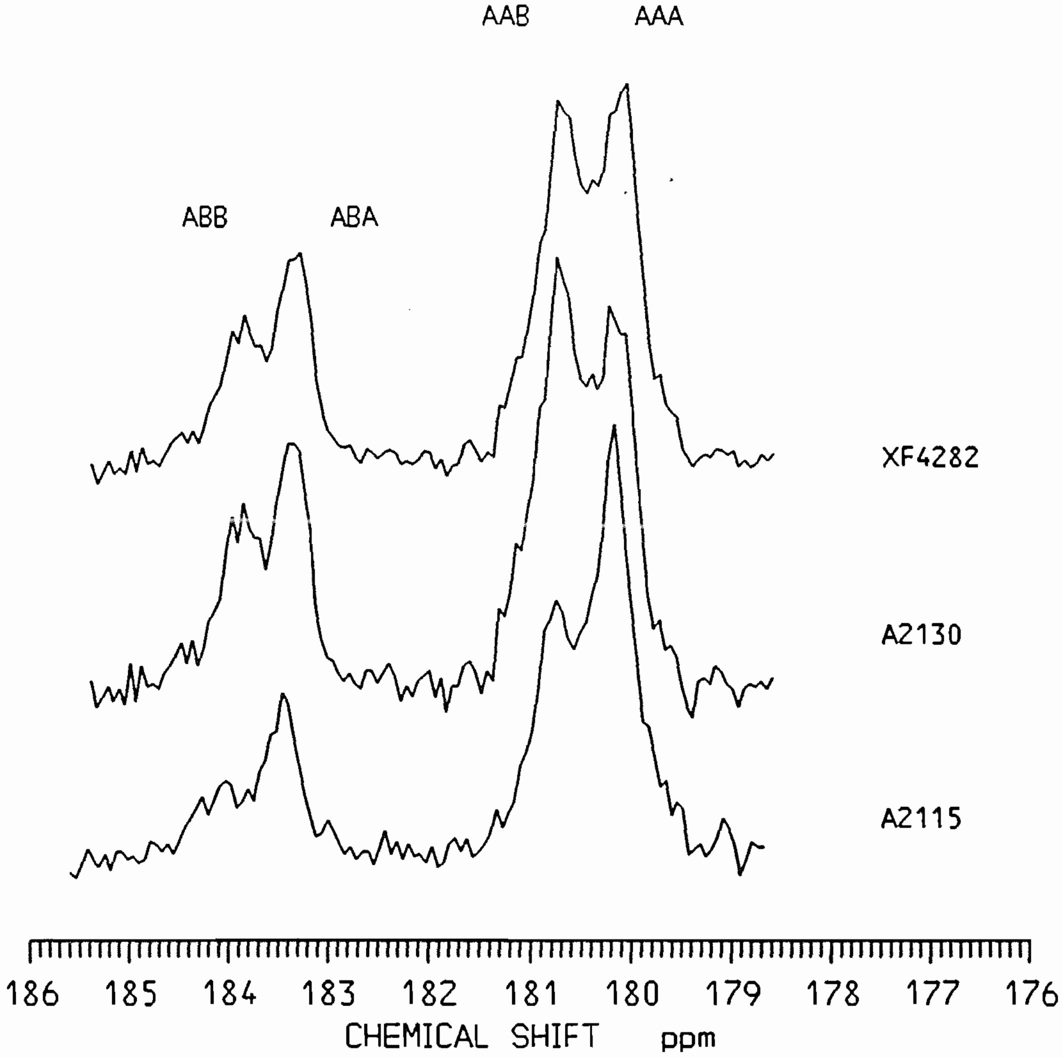

Figure 4.11 Carbonyl spectra for A2115 (25.8 mol %), A2130 (38.0 mol %) and XF4282 (41.0 mol %).

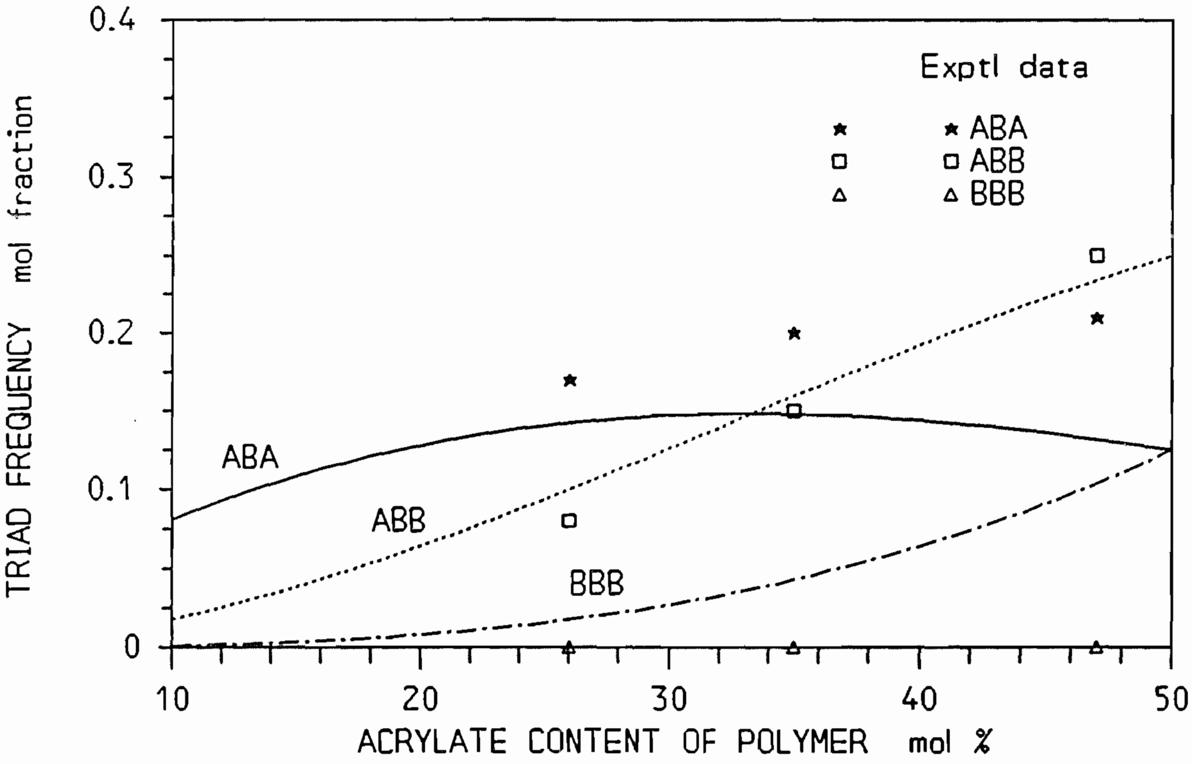

Figure 4.12 **Bernoullian analysis of B-centred triads for the series of copolymers.**

Polymerizations in which the probability of adding a particular monomer is influenced by previous events can be described by Markovian statistical models[154]. In a first-order Markov system, the probability of adding either monomer depends on the immediately preceding addition. The equations to derive the mole fractions of the six triads are given in reference 154 and will not be reproduced here. Essentially, the probabilities of adding either monomer to the chain related to the mole fraction of each monomer in the reaction mixture and are not independent variables. Therefore, it is necessary to specify only the composition of the reaction mixture and the relative increase in the probability of adding one monomer to define the system. One advantage of the Markov system is that it reduces to the Bernoullian model when the probabilities are equal to the mole fractions of monomers.

By analogy with the nearest-neighbour effects observed during alkaline hydrolysis, it is likely that electrostatic interactions will similarly inhibit the addition of consecutive acrylate units to a growing chain. A trial and error comparison of the experimental data in Figure 4.11 with Markov statistics was employed to determine a probability for the addition of acrylate monomer. Good agreement was obtained when the probability of adding an acrylate to a chain which already ends in an acrylate was reduced to 70 % of its mole fraction (see Figure 4.13). The number average sequence length of acrylate monomer estimated from the Markov analysis varied from 1.16 at 20 mol % to 1.54 at 50 mol %.

These results demonstrate that this particular range of polymers, which are from the same manufacturer and are manufactured by copolymerization, do not represent random copolymers but have a strong tendency towards a regular distribution which must approach an alternating sequence at the higher acrylate contents.

Table 4.6 shows the results of a similar analysis carried out on a commercial product prepared by polymerization and subsequent hydrolysis of acrylamide and which contained 41 mol % acrylate. In this case, the probability was reduced from 70 % to 50 % of the acrylate mole fraction. The corresponding Bernoullian distribution is included in the table also. Although the mole fraction of AAB triads calculated from Markovian statistics is considerably less than the experimental result, the agreement is generally good for the other triads. It is certainly superior to the random distribution calculated from the Bernoullian equations.

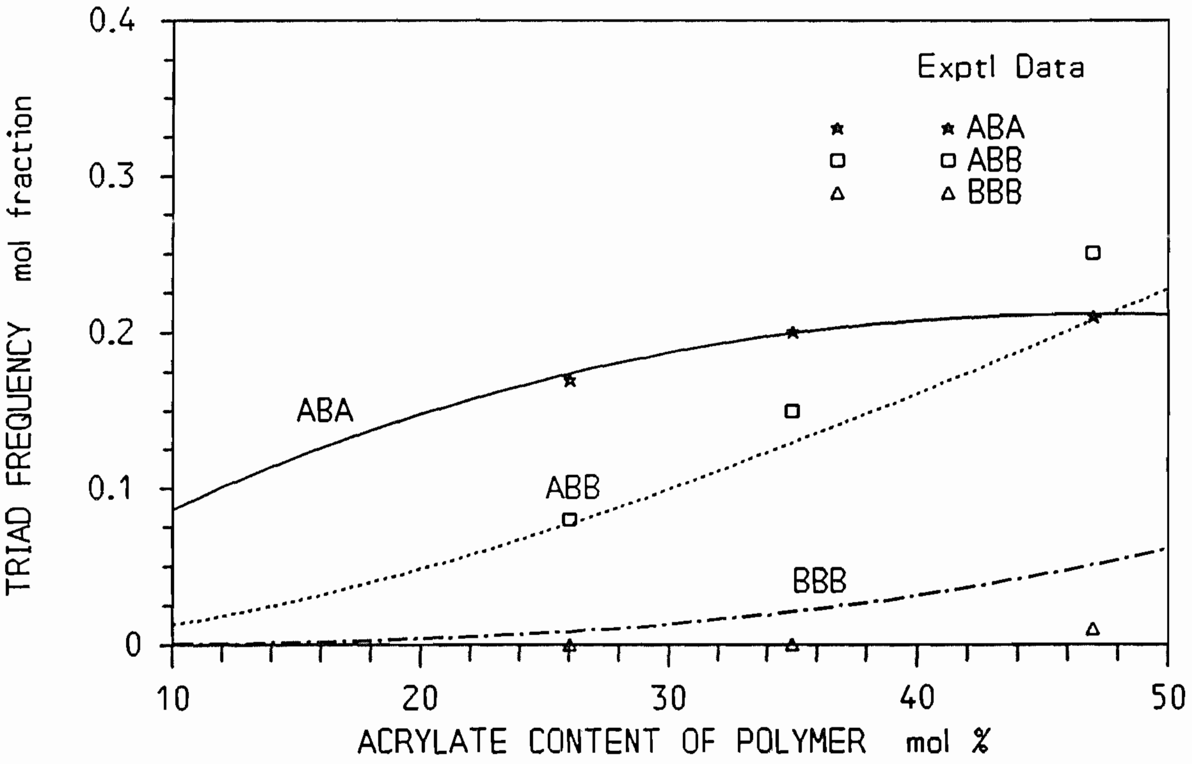

Figure 4.13 Markovian analysis of b-centred triads for the series of copolymers.

Table 4.6 Markov Analysis of XF4282 Polymer (41 mol % acrylate)

	MOLE FRACTIONS OF TRIADS					
	AAA	AAB	BAB	ABA	ABB	BBB
Bernoullian Statistics	0.21	0.29	0.10	0.14	0.20	0.07
Markov Statistics	0.12	0.29	0.18	0.26	0.13	0.02
Experimental Values	0.10	0.36	0.10	0.27	0.14	0

These results indicate that there is a greater tendency towards a regular distribution in the hydrolysed polymers than in the copolymers. Comparison with the results in Table 3.1, which showed that the hydrolysed polymers also gave better flocculation, leads to two important conclusions. Firstly, a regular distribution of acrylate groups along the polymer chain is the preferred distribution for successful flocculants. Secondly, the regular distribution also results in "better" solvent/segment interactions as indicated by the lower Huggins' constant.

4.3.3 METHYLENE AND METHINE SPECTRA OF COMMERCIAL POLYMERS

The carbonyl region was employed for determining sequence distributions because of the absence of additional splitting due to other effects. The results above have demonstrated the importance of the monomer sequence distribution in bridging flocculation. However, the absence of splitting due to other configurational effects in this region cannot be regarded as evidence that they do not contribute to the reaction in some way.

It was postulated above that electrostatic forces were sufficient to inhibit substantially the addition of consecutive ionic monomer units to the end of a growing polymer chain. It follows, then, that the same forces should also exert some influence on the configuration of the molecule. The NMR data show that the effect can extend at least to triad level. It is reasonable to expect, therefore, that the addition of the second ionic monomer in a BAB triad would occur with a preference for syndiotactic rather than isotactic addition. With this philosophy, the likely configuration of the various polymers can be predicted.

In the absence of electrostatic effects, acrylamide homopolymer would be expected to be atactic, unless other steric effects are important. Copolymers produced by alkaline hydrolysis of polyacrylamide should thus be atactic also. Copolymerization of acrylamide and sodium acrylate at alkaline pH should introduce some tacticity. When the proportion of acrylate is low, the probability of BAB triads is low. Unless the influence extends beyond triad level, there polymer should remain largely atactic. As the proportion of ionic monomer and, consequently, the BAB probability increase, so also should the number of syndiotactic sequences.

It was evident, even with the samples of low molecular weight acrylamide homopolymer, that there is some splitting in the methylene and methine regions due to configurational effects, probably tacticity. Isotactic and syndiotactic reference polymers were not readily available and preparation of suitable samples would have been a major project in itself. Consequently, no attempt was made to resolve the configurational sequences either in the low molecular weight samples used for peak assignments, or in the commercial polymers.

Methylene and methine spectra were recorded for only a few of the commercial polymers. Figure 4.14 is an example which shows the additional splitting that occurs. In many cases, the signal to noise ratio was considerably worse than in Figure 4.14 and was often so poor that it became difficult to distinguish genuine peaks from noise. Comparison of spectra to detect differences in these regions due to configurational effects was hampered by this problem with the result that no meaningful conclusions could be drawn.

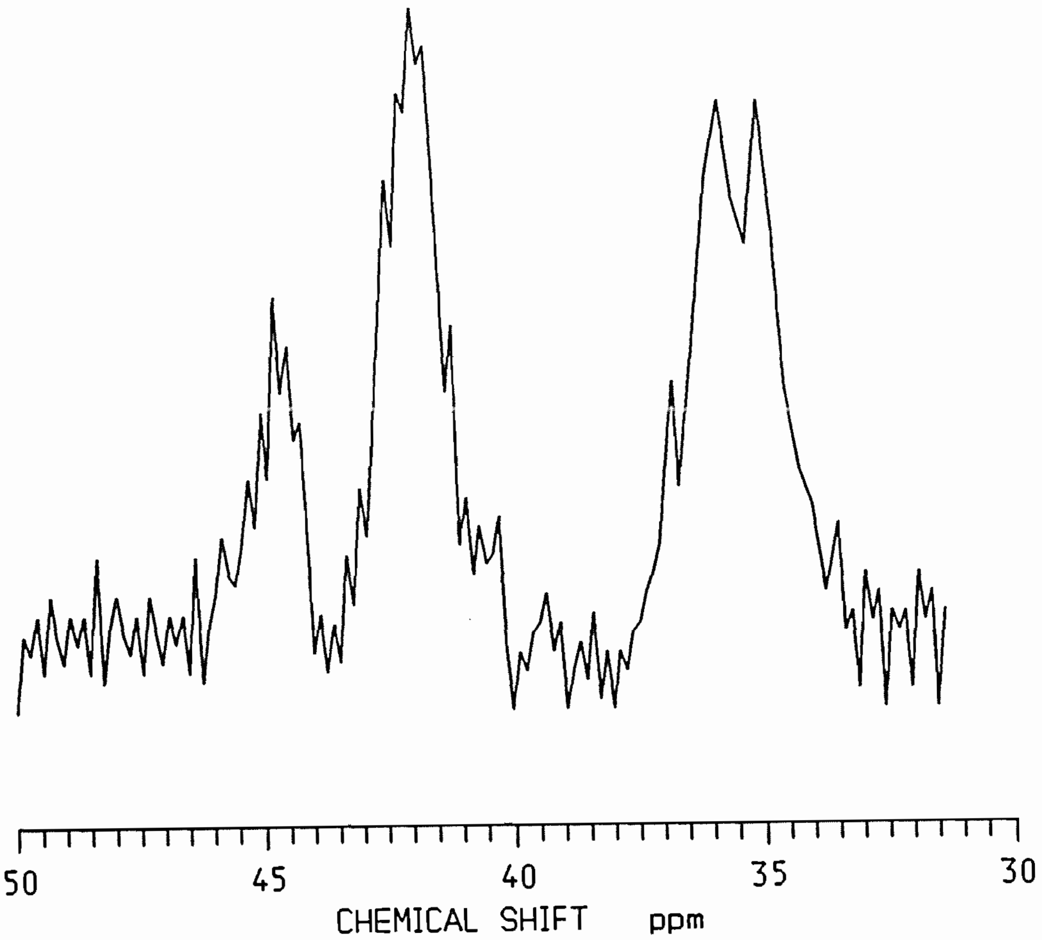

Figure 4.14 Methylene and methine spectra of the commercial polymer XF4282

4.3.4 IMIDE FORMATION

It was postulated previously that the higher Huggins' constant in many commercial copolymers resulted from the formation of intra- or inter-molecular crosslinks through imide groups. There was no evidence of a peak in the vicinity of 178.5 ppm corresponding to the expected chemical shift of the imide group. This observation is not surprising when it is recognised that peaks corresponding to mole fractions of less than 0.10 were difficult to resolve from signal noise. A polymer with 10 % of crosslinks would almost certainly be completely insoluble and would thus be easily recognised as different without recourse to NMR.

4.4 SUMMARY

In Chapter 3, it was demonstrated that flocculation of cane muds by anionic polyacrylamides occurs by adsorption of the polymer followed by growth of the aggregates. Unlike many other cases where anionic polyelectrolytes react with particles of like charge, adsorption of the polymer occurs through the ionized acrylate functional group. With non-ionic polyacrylamide, there is no adsorption and no flocculation. There is a distinct optimum value for the ionic content of the polymer at which the maximum settling rate and the minimum turbidity are obtained. This optimum is a critical condition which represents a compromise between competing effects. Adsorption must be sufficiently strong and irreversible to enable the polymer to effectively collect all of the particles and to enable the aggregates to resist the shear forces encountered during normal agitation and sedimentation. However, the absorbed polymer must retain its solution dimensions as far as possible and remain flexible and dynamic to promote growth of the aggregates.

It is apparent from the results in this chapter that there are many properties of flocculant polymers which can influence bridging flocculation. Molecular weight and copolymer composition are obviously the principal parameters, although the importance of the latter has been overlooked frequently. Other parameters which have been examined here are solvent/polymer interactions, heterogeneity (both chemical and molecular weight), monomer sequence distribution and general solution properties.

The results in this chapter support the reaction mechanism which was postulated in the preceding chapter on the basis of observations and experiments with actual sugar mill process streams. It has been confirmed that the principal role of the ionized acrylate comonomer is as the functional group in polymer adsorption. Under the conditions encountered in normal factory operation, the ionic groups do not increase the dimensions of the polymer molecule in solution as suggested in other applications. It has been shown also that bridging flocculation is favoured by a regular distribution of ionic groups along the polymer chain. The Huggins' constant, which is obtained readily during the determination of molecular weights by viscometry, is a useful indicator of polymer/solvent interactions. Some of the variations in this parameter can be explained by differences in monomer sequence distributions. Other variations appear to result from the formation of a small proportion of imide cross-links.

CHAPTER 5

MODEL PARTICLE SYSTEMS

Model particle systems are used frequently in studies of colloid stability. Their principal advantage is that it is possible to prepare model systems in which most of the important parameters can be controlled so that the number of variables which influence their stability, aggregation and flocculation can be minimized. There are numerous references describing methods of preparation and characterization of monodisperse particles of inorganic and synthetic polymer compounds. Variations in particle size and size distributions, stabilization by steric effects and variations in surface charge have all been described.

Generally, as colloidal systems become more complex chemically, it becomes increasing difficult to define all of the parameters which control their stability. It would be difficult to find a better example of this point than the cane muds which are the subject of this thesis. As discussed in Chapter 2, detailed electrokinetic studies by other workers (see Chapter 1) have shown that the particle surfaces exhibit the characteristics of adsorbed plant proteins and polysaccharides. However, the diversity of chemical species and reactions involved makes it virtually impossible to change any parameter without influencing several others. For example, to confirm the role of the calcium ion in the adsorption of the polyelectrolyte, it is necessary either to change its concentration or to replace it with other divalent ions. In either event, the precipitation of phosphate ions will be affected and the electrokinetic behaviour of the particles will change.

These problems must be confronted if the mechanism proposed for the bridging flocculation reaction in cane juice systems is to be confirmed unequivocally by direct experiment. Model particle systems offer a possible means of examining individual facets of the reaction independent of most or all of the other complicating variables. Several different systems were employed in this work to examine the polymer adsorption step and, in particular, the effect of copolymer composition on adsorption since this was seen as a critical feature of the hypothesis proposed for the bridging flocculation of cane muds.

To provide data which could be related directly to the results of the experiments with cane muds, it was considered that a suitable model system would have to satisfy a number of important criteria. Firstly, it would need to have minimal polydispersity with respect to both particle size distribution and surface charge so that effects due to variations in these parameters were minimised. Secondly, the surface charge should be the result of the dissociation of carboxylic acid groups incorporated into, rather than adsorbed onto, the particle surface. This would ensure that polymer adsorption did not occur simply by displacement of adsorbed molecules. Thirdly, the kinetics of adsorption and flocculation should be of the same order as for cane muds so that the system should reach a similar metastable equilibrium state during the reaction.

5.1 POLYSTYRENE LATEX PARTICLES

Of all the synthetic polymer particle systems which have been used in studying the properties of colloidal systems, those based on polystyrene polymers and copolymers are by far the most common. Particles with varying surface charge densities have been prepared by the adsorption of ionic surface active agents onto particles of homopolymer and by copolymerization of styrene with a variety of ionic comonomers. With both techniques, it is reportedly possible to produce particles with anionic, cationic and amphoteric surfaces. Similarly, a variety of ionizing functional groups can be employed to produce surfaces with similar charge densities but different chemical properties.

As pointed out above, the use of adsorbed surface active agents to produce surface charges was not appropriate in this work. Although amphoteric particles with both amide and carboxylic acid functional groups, as expected for a surface coated with sugar cane protein, could be produced, adsorption of the polyelectrolyte could then occur either by displacement of the surfactant or by reaction with it. Incorporation of fixed surface charges by copolymerization with an ionic monomer produces particles whose charged groups are an integral part of the polymer and cannot be displaced. The interaction between these groups and the adsorbing polyelectrolyte can be studied without the risk of displacement. This was considered to be a more appropriate approach for the system under investigation.

5.1.1 POLYSTYRENE/ITACONIC ACID POLYMERS

The preparation of latexes in which the surface charge was due to fixed carboxylic acid groups was achieved by the copolymerization of styrene with itaconic acid. A modification of the procedure reported by Hen and described in Chapter 2 was used successfully to produce particles of low polydispersity and similar average sizes. A total of 35 samples were prepared using different proportions of the two monomers to provide particles with a range of surface charge densities.

All of the samples prepared were titrated using a rapid conductometric procedure to obtain a rough estimate of the charge density. From these results, five samples, covering the widest available range of charge densities, were selected for further work. Each was then purified by prolonged dialysis and characterized thoroughly by a combination of conductometric titrations, potentiometric titrations and electrokinetic measurements. Particle size determinations were not undertaken prior to the flocculation tests discussed below. In view of the results of those tests, it was later unnecessary to undertake the size analyses.

Ion exchange, centrifugation, dialysis and various combinations of these have been used by other workers to purify synthetic latex systems. In this work, centrifugation was not attempted while ion exchange, though effective, was found to be less convenient than dialysis. The combination of potentiometric and conductometric titrations provided a simple means of following the progress of the dialysis. Purification was deemed to be complete when there was no further change in either of the titration curves for two consecutive days.

Typical conductometric titration curves before and after dialysis are shown in Figure 5.1 for the latex designated as #1. These curves were obtained by adding excess dilute NaOH solution to the latex and titrating with HCl. The water soluble component present in the original sample was removed completely by the dialysis and was assumed to be a low molecular weight polymer of itaconic acid. Figure 5.2 is the pH titration curve for the same sample of undialysed latex and was obtained simultaneously with the data in Figure 5.1. The end points were much more difficult to detect and it was felt that this procedure provided no useful data for this work.

From the conductometric titrations of the five samples selected for further work, the particle charge densities were calculated. The details are listed in Table 5.1. Their electrokinetic potentials were measured as a function of pH in 0.3 M KCl (see Figure 5.3). It is clear from both Table 5.1 and Figure 5.3 that the surface charge on the purified latex particles was approximately proportional to the amount of itaconic acid in the original reaction mixture.

Table 5.1 Properties of Polystyrene Latex Samples

Sample No.	Mole fraction of itaconic acid in monomer mixture	Solids (wt %)	Charge (equiv/g)
1	1.75×10^{-2}	16.64	0.161
2	6.62×10^{-3}	16.53	0.095
3	4.42×10^{-3}	16.65	0.070
4	2.22×10^{-3}	16.21	0.046
5	1.11×10^{-3}	15.20	0.027

The flocculation of the latexes was investigated using a series of commercial polymers with molecular weights in the range 12-14 x 10^6 and with acrylate contents between 24 mol % and 41 mol %. In preliminary tests at pH 8.0, it was found that no flocculation occurred when the supporting electrolyte contained monovalent ions only. Simple visual observations during the

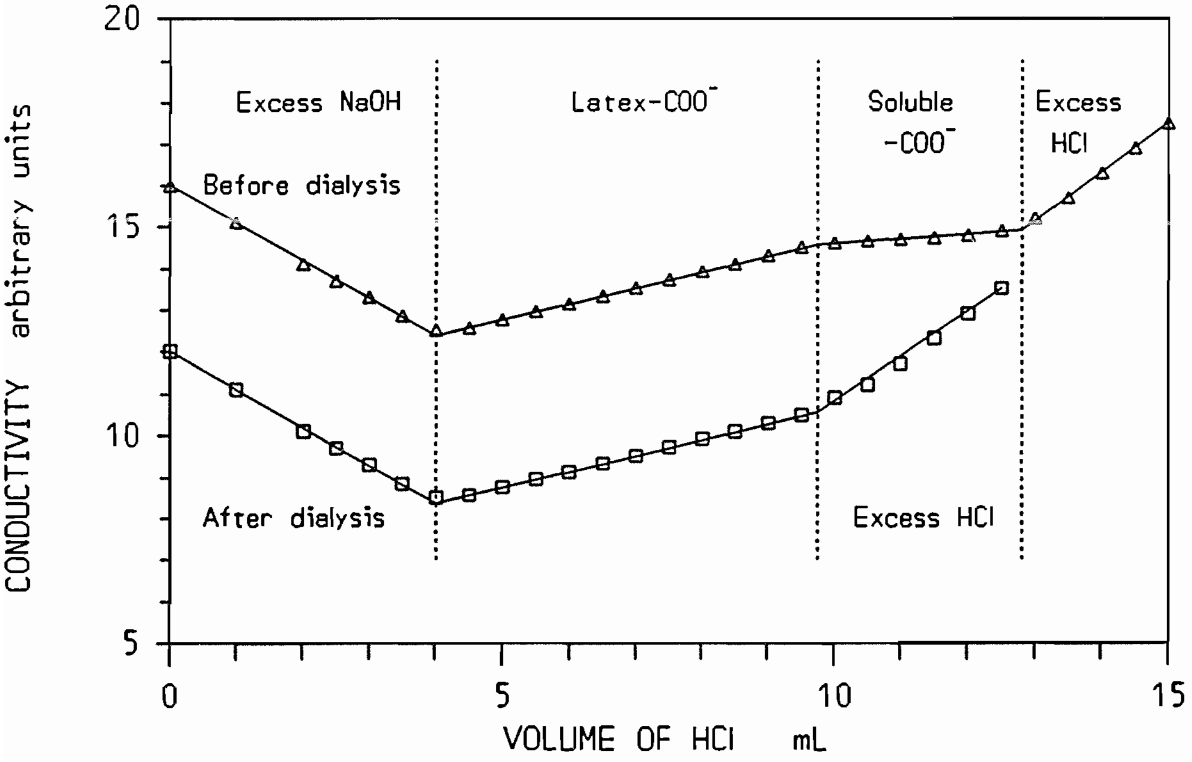

Figure 5.1 Conductometric Titration Curve for Latex #1.

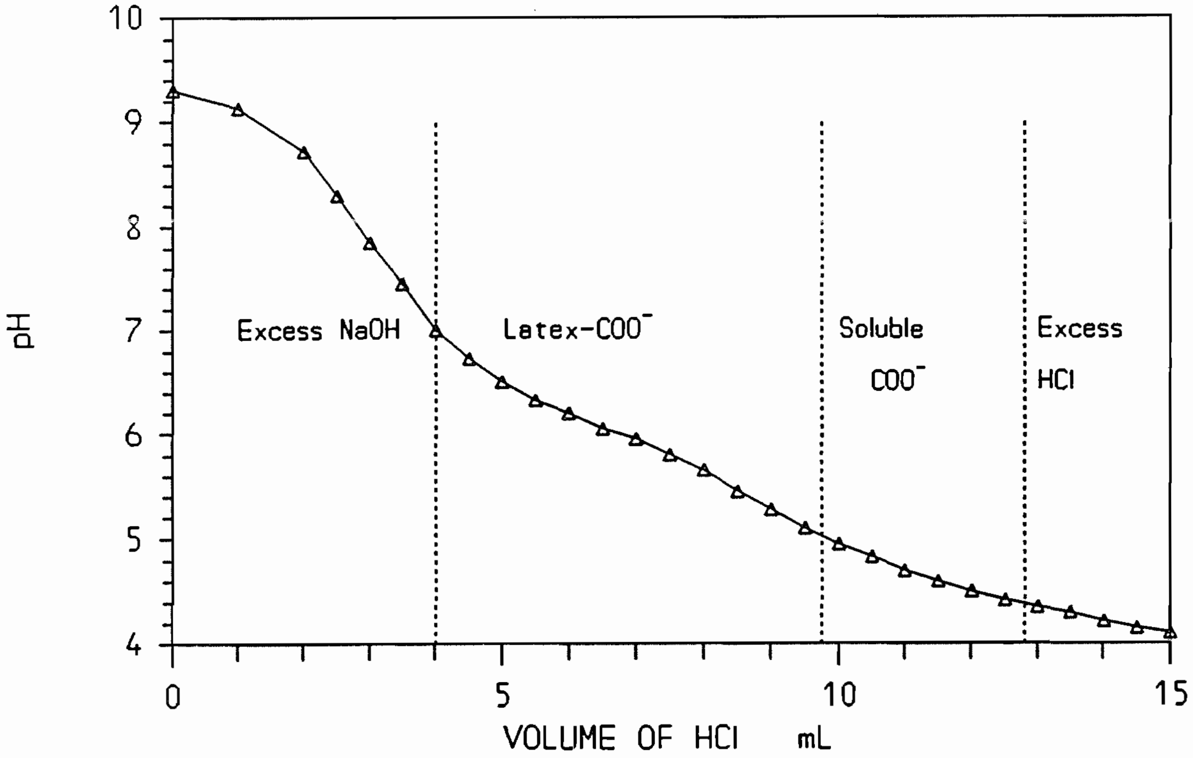

Figure 5.2 pH Titration Curve for Latex #1.

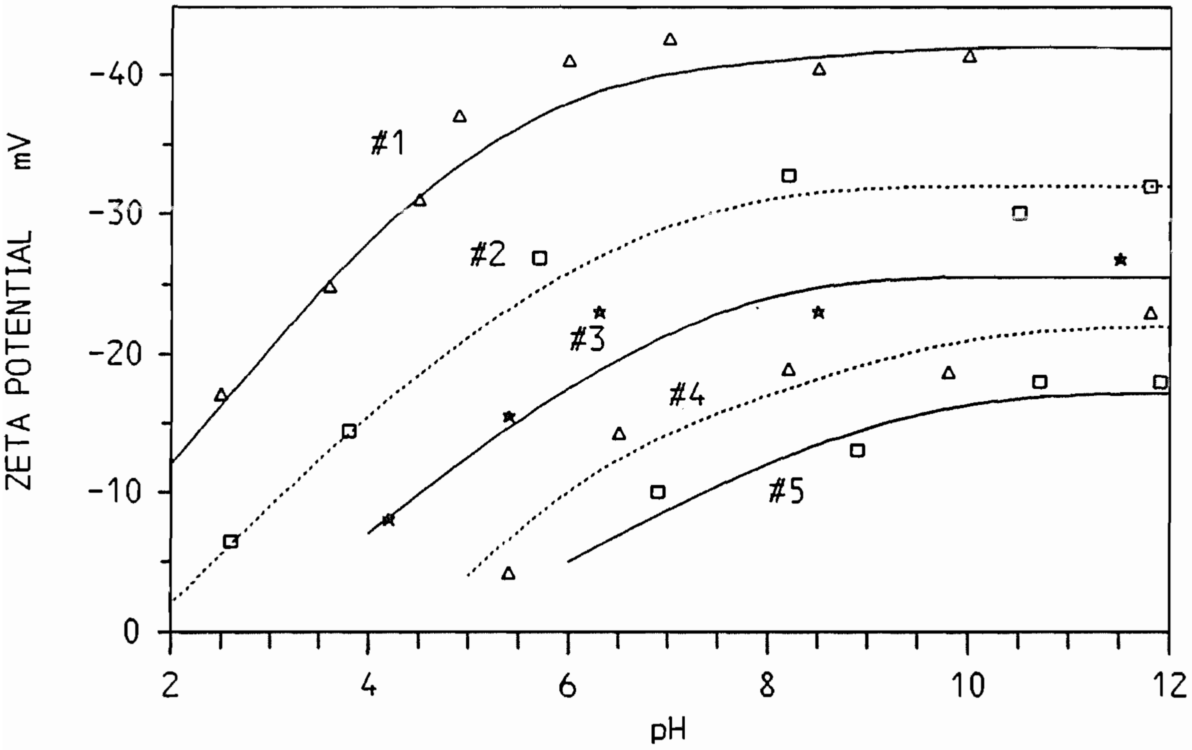

Figure 5.3 Zeta Potentials of Latex Samples as a Function of pH.

preliminary tests showed that good flocculation was achieved in the presence of small amounts of Ca^{2+} at alkaline pH and an ionic strength of 0.3 M (maintained with KCl). It was observed that the flocculated aggregates were approximately 1 cm in diameter, which is of the same order as those found with cane muds (typically 2-5 cm).

Two practical difficulties were encountered in attempting to quantify the extent of flocculation. Firstly, the rate of the reaction was clearly much slower than with cane muds. No doubt this was partly due to the fact that the latex experiments were conducted at ambient temperature whereas even the batch tests with cane muds were performed at 100°C. The lower temperature was more convenient from a practical viewpoint and also meant that the rate of the flocculation reaction was slower than that found with cane muds. Unfortunately, any advantages which may have been gained from these two features were far outweighed by the second problem.

Considerable difficulty was experienced in actually measuring quantitatively either the rate or the extent of aggregation and flocculation. The density of the poly(styrene/itaconic acid) particles was very slightly less than that of the supporting electrolyte. Consequently, the flocculated aggregates did not settle at all under gravity and actually floated to the surface when centrifuged. It was impossible, therefore, to measure the extent of flocculation by similar means and within the same timescale as for cane muds. Direct measurement of the rate of change of turbidity in a conventional spectrophotometer also yielded no useful results.

Limited success was achieved by employing the FICA 42000 Light Scattering Photometer as a variable angle turbidimeter. A novel cell arrangement was constructed (Figure 5.4) to enable the latex to be stirred continuously while simultaneously monitoring the turbidity using a chart recorder attached to the photometer. The end of the needle fitted to the cell cap was carefully bent in an arc of approximately 180° as shown in Figure 5.4. This arrangement allowed reagents (including flocculant) to be added without the risk of interference from extraneous light. It was

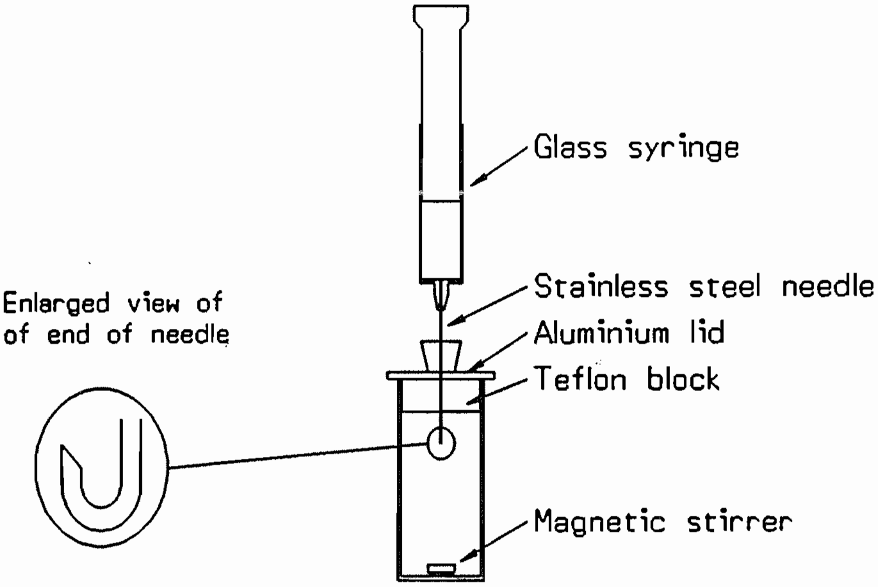

Figure 5.4 Cell for Monitoring Flocculation of Latexes.

found that the scattering angle at which the turbidity was determined made little difference to the results obtained so most tests were made at the 90° scattering angle.

Figure 5.5 shows the results of a typical experiment in which flocculant was added to a sample of latex 1 (Table 5.1). The aqueous phase was 0.30 M KCl containing 3 x 10^{-5} M Al^{3+} at pH 8.0. The flocculant added was Superfloc A125 (26.5 mol % acrylate and 12 x 10^{6}) at the rate of 2.0 mg/L. It must be noted here that the chart recordings obtained after the addition of flocculant exhibited a very high level of noise as large aggregates passed through the light path. Consequently, the data shown in Figure 5.5 for the flocculated sample represent the smooth curve drawn through the chart recording obtained.

It is evident from the slight reduction in turbidity that some coagulation occurred in the reference sample with no added polymer. However, it is also clear that a rapid reaction occurred when the polymer was added. This procedure was employed for a large number of experiments with each of the latex samples described above using a range of polymers and varying concentrations of divalent ions.

In tests using Al^{3+} as the multivalent ion, it proved to be difficult to obtain reproducible, quantitative data on the rates of flocculation. It was found frequently that the measured turbidity varied so erratically that fitting a curve of any type was impossible. However, visual observations at the end of each such experiment confirmed when good flocculation had occurred. Large aggregates were visible and the surrounding liquid was water clear. Obviously, this and similar experimental techniques are unsuitable for situations where large aggregates are formed and where the densities are such that little or no sedimentation occurs.

In these tests, the rate of flocculation was determined in terms of a 'flocculation time' which was defined as the time taken for the turbidity to reach its minimum value. The occurrence of bridging flocculation was characterised by two features - an erratic turbidity recording and a very low final turbidity. In visual observations, the onset of flocculation was readily discernible and the supernatant was generally water clear. 'Flocculation times' of 15 minutes or greater were obtained when there was no visible evidence of flocculation.

The results obtained for latex 1 in 0.30 M KCl with 3 x 10^{-5} M Al^{3+} at several pH values are given Table 5.2 below. The copolymers used were commercial products of the Superfloc range, similar to the A125 referred to in Figure 5.5 above, with molecular weights between 10.8 and 12.2 x 10^{6} . The concentration of added Al^{3+} was above the critical coagulation concentration at all pH vales examined. Consequently, spontaneous coagulation occurred in all tests. However, no flocculation occurred at pH 4 or pH 10, while the rate of flocculation was slightly greater at pH 8 than at pH 6. There was no influence of polymer composition on the rate.

Table 5.2 Flocculation Times for Latex 1 with Al^{3+}

ACRYLATE CONTENT OF POLYMER (mol %)	FLOCCULATION TIME (s)			
	pH 4	pH 6	pH 8	pH 10
27	< 1000	60	45	< 1000
36	< 1000	70	45	< 1000
41	< 1000	50	60	< 1000
47	< 1000	70	45	< 1000

When these tests were repeated with latexes 3 and 5, both of which have lower surface charges, similar results were obtained. The results for latex sample 3, obtained under similar experimental conditions, are given in Table 5.3. No quantitative data were obtained for latex 5 due to the very erratic nature of

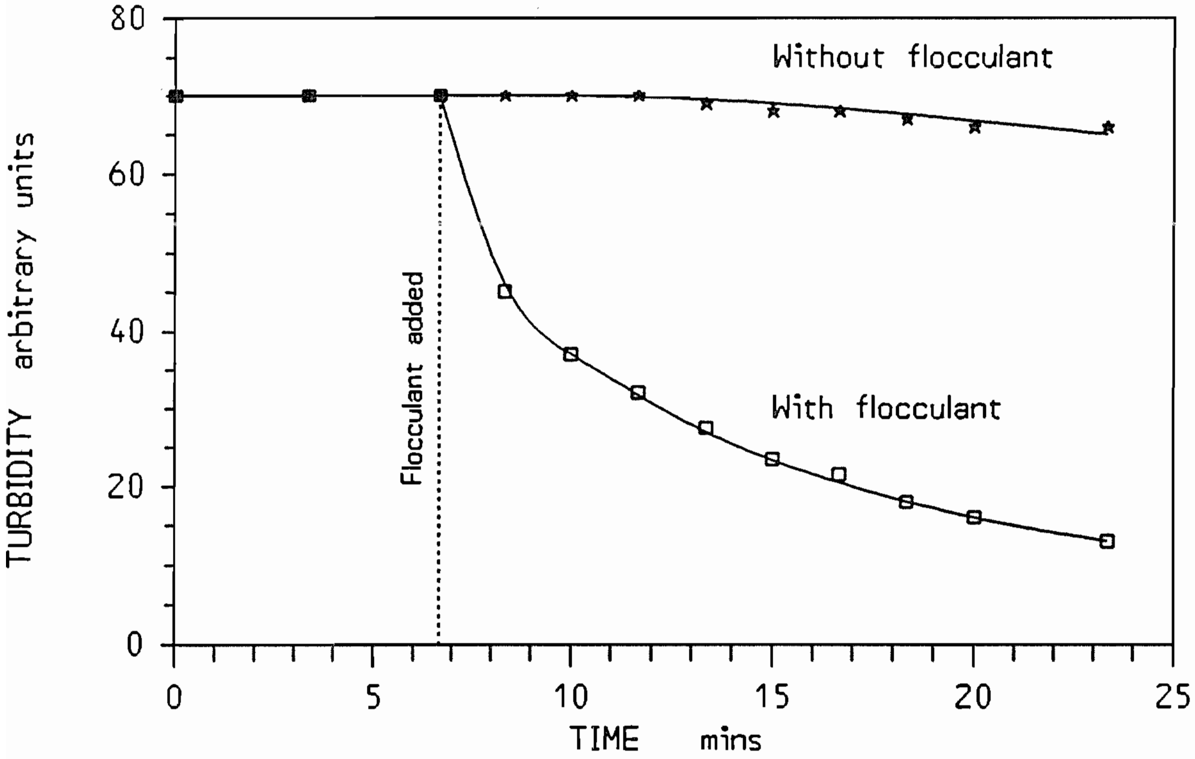

Figure 5.5 Turbidity Changes During Flocculation of Latex #1.

the chart recordings. However, visual observations confirmed that flocculation occurred at pH 6 and 8 with all four polymers. Some flocculation was evident on occasions at pH 4 and 10 but the results were not reproducible.

Table 5.3 Flocculation Times for Latex 3 with Al^{3+}

ACRYLATE CONTENT OF POLYMER (mol %)	FLOCCULATION TIME (s)			
	pH 4	pH 6	pH 8	pH 10
27	< 1000	70	55	< 1000
36	< 1000	60	-	< 1000
41	< 1000	-	65	< 1000
47	< 1000	70	50	< 1000

In experiments using Ca^{2+} instead of Al^{3+}, the size of the aggregates was considerably smaller and there was considerably less noise in the chart recordings of turbidity changes with time. No flocculation occurred at pH 4 even at levels of Ca^{2+} well above the critical coagulation concentration for any latex.

Figure 5.6 shows the results obtained with latex 1 at pH 8, where the critical coagulation concentration was found to be 2.87×10^{-3} M Ca^{2+}. Below this concentration, there was no evidence of flocculation or rapid coagulation as evidenced by the long 'flocculation times'. Since there was no evidence of flocculation, the slight decline in 'flocculation time' with increasing acrylate content of the polymer was assumed to be of no significance. At higher concentrations, flocculation occurred rapidly but again, there was no apparent influence of polymer composition (see Figure 5.6). At pH 10, the critical coagulation

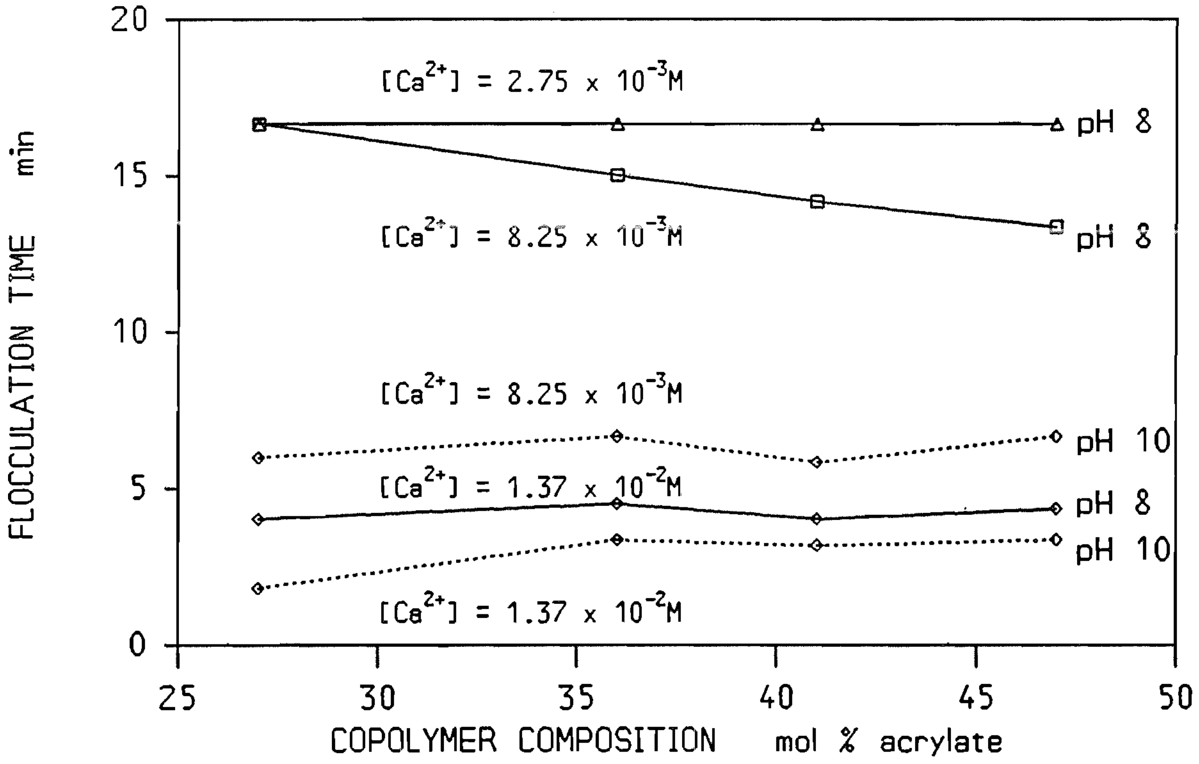

Figure 5.6 Flocculation Rate of Latex #1 with added Ca^{2+}.

appeared to be lower but this was probably due to the formation of a precipitate of $Ca(OH)_2$ which trapped the latex particles as it settled. Under these conditions, flocculation occurred readily (see Figure 5.6).

Since there was no evidence of an optimum polymer composition for flocculation of this latex, only a few visual tests were carried out with other latex samples. These simple tests were sufficient to confirm that the effect of polymer composition was similar at lower surface charges.

A further series of experiments, similar to those above, was carried out with latex 1 at an ionic strength of 1.0 M. The latex exhibited rapid coagulation at pH 4 but was stable at pH 6 and above. This was not surprising in view of the effect of pH on the dissociation of the surface carboxylic acid groups and thus on the zeta potentials (see Figure 5.3). Although, at this ionic strength, the effective range of the electrostatic forces of repulsion between particles is greatly reduced, the particle charge was sufficient to prevent rapid coagulation. In the absence of calcium or other multivalent ions, no flocculation occurred. The results obtained with added Al^{3+} and Ca^{2+} were similar to those described above.

These results indicate that the presence of low concentrations of multivalent ions are essential for the adsorption of the acrylamide/acrylate copolymer. They also indicate that it is necessary to reduce the particle charge to the point where rapid coagulation occurs spontaneously if flocculation is to be effective in scavenging all of the particles. Unfortunately, there was no evidence in any of the experiments of an optimum copolymer composition for flocculation.

5.1.2 OTHER POLYSTYRENE COPOLYMERS

The polystyrene/itaconic acid copolymers discussed above could be flocculated readily and displayed several of the required characteristics described earlier in this chapter. However, the lack of any evidence of a dependence on copolymer composition meant that it was not possible to investigate this phenomenon which is a vital aspect of cane mud flocculation and which was the principal aim of this avenue of work.

It is possible that the effect occurred but could not be detected by any of the experimental procedures employed because of the very small difference in density between the particles and the aqueous phase. Several alternative copolymers were prepared with a view to obtaining particles of higher density. The aim of this phase was to produce a model particle system in which the rate of the flocculation reaction and the rate at which the flocculated aggregates could be removed by simple sedimentation were of the same order as for cane muds.

Initially, a small amount of divinylbenzene (DVB) was added to the styrene/itaconic acid reaction mixture as a crosslinking agent. Several different levels of DVB were added, varying from 0.5 to 5.0 per cent of the total monomer. The most obvious effect of the change was an increase in the size and polydispersity of the resulting latexes. Particle size analyses were unnecessary as many of the particles were visible to the eye and were as large as 0.5 mm. Unfortunately there were also many smaller than 50 μm and microscopic examination revealed a very wide range of particle sizes. When flocculated with several commercial polymers in the presence of added Ca^{2+} as described in the preceding section, the maximum sedimentation rate which could be achieved was 2-3 cm/min. Although this rate was measurable, it was still an order of magnitude below that experienced in cane juices.

A further series of copolymers were prepared using acrylic acid instead of the itaconic acid. The resultant particles were completely unsuitable for many reasons, the principal ones being the extent to which they swelled and the pronounced effect of added electrolytes on the swelling. In fact, two polymers prepared from a monomer mixture in which the mole fraction of acrylic acid was approximately 0.02 did not produce discrete particles but appeared to be a fluffy precipitate of a branched or slightly cross-linked polymer. The addition of 5 per cent DVB resulted in discrete particles of very low charge and broad size distribution.

The third option examined was the replacement of the styrene with its more dense derivative, 4-chlorostyrene. The latex particles obtained showed a pronounced tendency to coagulate during the polymerization reaction. Less than 50 per cent (by volume) of the initial reaction mixture was recovered as a dispersion, the remainder being large lumps of coagulated resin. This was an unexpected result in view of the simplicity of the styrene copolymerizations but it meant that recovery of the latex as stable and discreet individual particles was difficult. Although the experimental difficulties could have been solved, the preliminary flocculation tests again showed that the sedimentation and flocculation rates which could be achieved were still too low.

A summary of the various combinations evaluated and the results achieved are given in Table 5.4.

Table 5.4 Other Copolymer Systems Prepared

COPOLOYMER	TYPICAL SETTLING RATE OF FLOCCULATED LATEX (cm/min)	COMMENTS
Styrene Itaconic acid Divinylbenzene	< 3	Particles very large and polydisperse
Styrene Acrylic acid	< 0.2	Density too low
Styrene Acrylic acid Divinylbenzene	< 1	Polydisperse and surface charge very low.
Chlorostyrene Itaconic acid	< 5	Particles coagulated during polymerization and very difficult to recover.
Chlorostyrene Itaconic acid Divinylbenzene	< 5	Particles coagulated during polymerization and very difficult to recover.

It became apparent that the preparation of a model particle system which met all of the requirements described at the beginning of this chapter would be a major project in itself. The alternative approach was to use a different model system which was suitable only for investigating the adsorption step.

5.2 ION EXCHANGE RESINS

Conventional ion exchange resins have particle sizes which are generally larger than the latex systems discussed above. However, they are readily available commercially in a range of forms, including some which meet at least some of the requirements established above. For example, many weakly basic resins employ carboxylic acids as their functional groups, are available in sizes as small as 50 μm and are sufficiently dense to sediment readily in water. The material selected for experimental work here was 400 mesh analytical grade Biorex 70 cation exchange resin in the sodium form. The exchange capacity of this resin was 10.2 meq/g.

The resin was used only in experiments designed to simulate the polymer adsorption step of the flocculation reaction. No attempts were made to simulate the kinetics of flocculation or even to cause flocculation of the resin particles, although flocculation was expected. The specific experimental procedure was not described in Chapter 2 but was similar to that employed for cane muds. A dispersion of the resin in aqueous solution was mixed rapidly with the required amount of dilute polymer solution and the particles were allowed to settle under gravity. Settling was essentially complete after 10 minutes. The concentration of polymer remaining in the supernatant was then determined using a variation of the filterability test described in Chapter 2. The experimental error in these tests was found to be larger than expected and was estimated to be ± 0.7 ppm.

Experiments were conducted only at pH 8.0 ± 0.2 in 0.3 M KCl with the same four commercial polymers referred to in Table 5.2. The solids concentration was 10 g/L and Ca^{2+}, Mg^{2+} and Al^{3+} were each added at different concentrations. The concentration of added polymer was maintained at 5.0 mg/L. The results are tabulated in Table 5.5 with the amount adsorbed being reported only to the nearest 0.5 ppm due to the magnitude of the experimental error.

Table 5.5 Polymer Adsorption on Ion Exchange Resin

	AMOUNT OF POLYMER ADSORBED (mg/L)			
CONCENTRATION OF ADDED IONS	ACRYLATE CONTENT OF POLYMER (mol %)			
	27	36	41	47
0.30 M KCl	0	0	0	0
+ 2.75×10^{-3} M Ca^{2+}	0	0.5	0	0
+ 8.25×10^{-3} M Ca^{2+}	0	1.0	0.5	0.5
+ 1.37×10^{-2} M Ca^{2+}	1.0	0.5	1.5	1.5
+ 2.75×10^{-3} M Mg^{2+}	0	0	0.5	0
+ 1.37×10^{-2} M Mg^{2+}	0.5	0.5	0	1.5
+ 3.0×10^{-4} M Al^{3+}	0	0	0	0
+ 3.0×10^{-3} M Al^{3+}	3.0	3.0	4.5	2.5

The results suffer somewhat from the large experimental error in the measurement of residual polymer concentration but they do lead to some important conclusions. Firstly, there was no adsorption with KCl only, and little or none in the presence of Mg^{2+} except for the polymer with the highest acrylate content (47 mol %) at the higher concentration of Mg^{2+}. Since there was no visible evidence of flocculation in this experiment, it is possible that the apparently substantial adsorption is an experimental error. Secondly, with Ca^{2+} there was only slight adsorption which increased as the Ca^{2+} concentration increased. Adsorption was much more pronounced with Al^{3+}.

These results are generally in accord with the observations in Chapter 3 on cane mud flocculation. With real cane muds, it is not possible to exclude multivalent ions completely. However in other experiments, not described in Chapter 3, laboratory simulated clarification experiments have been used to demonstrate that no flocculation occurred when the Ca^{2+} normally added as lime was replaced by MgO. Since flocculation cannot occur without polymer adsorption, the absence of flocculation was taken as an indication of the absence of adsorption by the muds.

The general trend of increased adsorption in the sequence $Mg^{2+} < Ca^{2+} < Al^{3+}$ is the same as the trends in both the sizes of these ions and their total specific energies of interaction with carboxylate surfaces[122]. Although the ionic radius may be a contributing factor, the results of the present work indicate that the dissociation constant of the metal ion/ carboxylate complex is the more important parameter. The latter is consistent with the hypothesis that the strength of the polymer adsorption is determined by the multivalent ion which acts to form the ionic bond between the polymer and the particle i.e. the cation bridge. Unfortunately, again, there was no evidence of any influence of copolymer composition on adsorption.

5.3 SUMMARY

The results of the experiments with model particle systems have been unable to confirm unequivocally the mechanism for cane mud flocculation which was proposed on the basis of direct experiments with those muds. Nonetheless, the experiments have yielded useful and interesting data which generally agree with those obtained with cane muds. However, it is clear that particles of this type do not provide an accurate model of the cane mud system and cannot provide absolute confirmation of the proposed mechanism for the flocculation reaction.

CHAPTER 6

CONCLUSION

The work described in this thesis has been directed specifically at an important commercial and industrial application of high molecular weight polyacrylamide flocculants. The principal aims have been to determine the properties of these polymers which make them uniquely suited to the industrial environment, to develop an accurate understanding of the chemistry of their reactions with cane muds and ultimately to apply this knowledge to the benefit of the Australian sugar industry.

6.1 INDUSTRIAL APPLICATION

The results described here have lead to valuable improvements in equipment capacity, operating costs and product quality, all of which are important in helping the industry to maintain its economic viability.

As an understanding of the flocculation reaction has emerged, the selection of the best flocculant for almost any given factory condition has become a routine matter in sugar mills. It is now possible also to optimise factory operating equipment and conditions to ensure the best possible standard of clarification is achieved at all times and at an acceptable cost. It has been possible also to extend the use of polymeric flocculants to include the sedimentation of boiler flyash slurries where similar substantial improvements have been achieved.

Operating procedures and equipment have been modified or redesigned so that the polymer solution is added at the optimum dose and at the most appropriate location to provide rapid mixing for adsorption and aggregate growth while avoiding the excess turbulence which can fracture the aggregates and lead to reduced sedimentation rates and higher turbidities. The capacity of factory clarification equipment has increased while the consumption of polymer has decreased. There has been a marked improvement also in the standard of clarification achieved and this has resulted in valuable improvements in the quality of raw sugar produced.

The knowledge of the properties of the polymers themselves has been employed as the basis for the design of factory equipment for the automatic preparation, storage and dosing of aqueous polymer solutions. This equipment has been thoroughly tested under arduous factory conditions and shown to be the only such equipment which can ensure complete dissolution of polymers of the highest available molecular weight while completely avoiding any of the potential degradation reactions due to thermal, mechanical or chemical effects.

With the steady advance in the understanding of the mechanism of the flocculation reaction and of the properties of the polymers themselves, it has become possible to clearly specify the properties of the polymers best suited to the sugar industry. The ready co-operation of a number of manufacturers in attempting to meet and exceed these specifications has been a feature of this project. The result has been a series of dramatic improvements in the important polymer properties. This has been apparent particularly in the increases in molecular weights of commercial products. The situation has been reached now where several companies manufacture special ranges of products which are used only by the Australian sugar industry, and which are characterised by their very high molecular weights. It seems that other users either have yet to appreciate their value or have not developed equipment which enables them to realise their full potential.

Raw sugar mills have modified their equipment and to enable them to take full advantage of the benefits which can be obtained by the proper use of the highest molecular weight polymers available. Such is their importance to this industry that sugar mills are now completely dependent upon the continuous addition of an appropriate polymer to maintain their operations. Polymer manufacturers, too, have responded by producing improved polymers. The result is that the Australian sugar industry has established a proven international reputation for the exceptionally high quality of their clarification equipment and of the raw sugar which they produce.

6.2 AVENUES FOR FUTURE WORK

This work has answered many questions about the chemistry of the flocculation of cane muds. However, like many other research projects, it has opened several avenues for new or additional research. Foremost among these must be the extension of the principles established here to other process industries who do or could use polymeric flocculants to enhance their operation. There is little doubt that many of them could benefit considerably if they were able to apply even some of these principles.

Within the sugar industry, there remain a number of exciting opportunities for further work. The acrylamide/acrylic acid copolymers are used exclusively at present and are clearly the most effective materials available. One reason for this may well be a historical one. Having been established early as very effective flocculants for many applications, they have been the focus of considerable research and development effort with obvious good results as demonstrated by the ever increasing molecular weights of commercial products.

Whatever the historical effect may be, the polyacrylamides have several other obvious advantages over most other polymers. They are readily soluble in water due to the polarity of the amide and carboxylic acid functional groups. The presence of the ionic monomer also provides an avenue for some control over the distribution of monomers along the molecular chain. In addition, they have a simple saturated carbon backbone with only small functional groups attached. There is little steric hindrance to rotation about the carbon-carbon bonds and the molecule thus remains very flexible.

These observations lead to the intriguing prospect of preparing an even better flocculant. Having identified that the carboxylic acid group is essential as the functional group for polymer adsorption, is it possible to replace the amide with another entity which is sufficiently polar to ensure solubility but is smaller and therefore creates even less steric hindrance, making an even more flexible chain? The most likely prospect is a copolymer of acrylic acid with vinyl alcohol. A comparison of the relative effectiveness of a series of polymers in which the amide was replaced with other polar groups of different sizes would yield useful information on this aspect. The challenge, however, is to prepare polymers which all have similar molecular weights, but whose molecular weights are high enough for them to be effective flocculants.

The influence of different ionic groups on polymer adsorption and flocculation is another area of potential interest. There is evidence from other research work and from considerable industrial experience which demonstrates that there can be a strong effect although there is not even a qualitative explanation for many of the effects observed. It has been shown here that the interaction of the ionized carboxylate groups of the polymer with multivalent cations in solution and the surface of the particles controls the flocculation reaction with cane muds. Unfortunately, it has not been possible to obtain polymers of similar molecular weight containing sulphonates or other anionic functional groups so this aspect has yet to be investigated. Any further work in this area must confront two major tasks. Firstly, it will be essential to have a particle system in which the surface characteristics can be controlled and clearly defined. Secondly, as with the previous case, it will be necessary to prepare polymers of similar, very high molecular weights using a variety of ionic comonomers. Again, simply preparing a series of such polymers of suitably high molecular weight is major challenge.

Another aspect which has been evident throughout this work has been the substantial gulf which exists between the capabilities of the laboratory techniques which are available to characterize the properties of these polymers and the manufacturing technology of the polymer producers. The molecular weights of commercially significant polyelectrolytes generally far exceed the limits to which most analytical procedures have been extended previously. Techniques which are eminently suited to basic research work with low molecular weight polymers have been found to have serious limitations when applied to very high molecular weight, water-soluble polyelectrolytes. Any advances which allow the extension of techniques such as gel chromatography and NMR to the analysis of water soluble polymers of exceptionally high molecular weight will be invaluable in future research.

APPENDIX I

FORTRAN PROGRAMME
FOR PREPARING ZIMM PLOTS OF LIGHT SCATTERING DATA

```

**              ZIMM6
*ONE WORD INTEGERS
*IOCS(PAPER TAPE,TYPEWRITER,1132 PRINTER)
*EXTENDED PRECISION
*LIST SYMBOL TABLE
*LIST SUBROUTINE NAMES
C     ZIMM PLOTS
C
C     CALCULATES ALL POINTS FROM RAW DATA AND
C     PLOTS LINES
C
C     INPUTS - (1)ID
C              (2)VALUES OF K AND AG (GLASS STANDARD)
C              (3)NO OF VALUES OF THETA (N) AND C (M)
C              (4)VALUES OF C STARTING FROM ZERO
C              (5)VALUES OF THETA STARTING FROM
C                 LOWEST ANGLE
C              (6)VALUES OF IH,IV,ITHETA STARTING
C                 FROM LOWEST ANGLE AT ZERO
C                 CONCENTRATION
C
C     FORMATS  (1)20A2
C              (2)I6,F7.2
C              (3)2I2
C              (4)E12.4
C              (5)F6.1
C              (6)F7.2
C
      INTEGER ID(20),PAGE
      REAL C(9),THETA(20),ZANG(9),A(200),CU(20)
      REAL X(200),Y(200),X1(20),SLP(30),INT(30),
      $X2(20),EX1(12),EX2(20),LIMIT(2,30),INT1,INT2
```

```
         REAL CURV(20)
         DATA PAGE,ICP,IPT,I1132/1,4,3/
         DATA LIMIT/60*0.0/
C
C        LOADING MESSAGE
C
         WRITE(ICP,1000)
1000     FORMAT('P/G ZIMM LOADED')
C
C        READ ID
C
         READ(IPT,500)ID
500      FORMAT(20A2)
         WRITE(I1132,300)PAGE,ID
C
C        READ VALUES OF K AND AG
C
         READ(IPT,101)K,AG
101      FORMAT(I6,F7.2)
C
C        READ NO OF VALUES OF C AND THETA
C
         READ(IPT,102)M,N
102      FORMAT(2I2)
C
C        CALCULATE NO OF VALUES OF I,
C        INCLUDING IH,IV ITHETA
C
         NPT=M*(N+2)
C
C        READ VALUES OF C AND CALCULATE VALUES FOR
C        EXTRAPOLATION TO ZERO ANGLE
C
         READ(IPT,103)(C(I),I=1,M)
103      FORMAT(E12.4)
         DO 104 J=2,M
         ZANG(J)=K*C(J)
         I=J-1
104      X2(I)=ZANG(J)
C
```

```
C     READ VALUES OF THETA AND CALCULATE VALUES FOR
C     EXTRAPOLATION TO ZERO CONCENTRATION
C
      READ(IPT,105)(THETA(I),I=1,N
105   FORMAT(F6.1)
      DO 106 I=1,N
      THETA(I)=THETA(I)*3.1416/180
      B=THETA(I)/2
106   X1(I)=SIN(B)*SIN(B)
C
C     READ VALUES OF IH,IV,ITHETA AS A(I)
C
      READ(IPT,107)(A(I),I=1,NPT)
107   FORMAT(F7.2)
C
C     ALL DATA HAVE BEEN READ
C
      ICOUN=1
      DO 200 I=2,M
      WRITE(I1132,108)C(I)
      WRITE(I1132,109)
108   FORMAT(//,2X,'CONCENTRATION=',E12.4)
109   FORMAT(2X,'X COORD',3X,'Y COORD')
      DO 200 J=1,N
C

C     CALCULATE POLARIZATION RATIO AND
C     CABANNES FACTOR
C
      L=I-1
      IL=L*(N+2)+1
      JL=IL+1
      PH=A(IL)-A(1)
      IF(PH)120,120,121
121   PV=A(JL)-A(2)
      RO=PH/PV
      IF(RO-.005)120,120,130
120   CU(J)=1
      GO TO 125
130   Z=1+RO+(1-RO)*COS(THETA(J))*COS(THETA(J))
```

```
      T=(1-7*RO/6)*(1+COS(THETA(J))*COS(THETA(J)))
      CU(J)=Z/T
125   CONTINUE
C
C     CALCULATE X COORDINATE
C
      B=THETA(J)/2
      X(ICOUN)=SIN(B)*SIN(B)+K*C(I)
      KIK=K
C
C     CALCULATE Y COORDINATE
C
      B=THETA(J)
      IL-JL+J
      IJ=J+2
      R=A(IL)-A(IJ)
      R=R/AG
      R=R*SIN(B)/(1+COS(B)*COS(B))
      R=R*0.9*CU(J)*16.3E-06
      Y(ICOUN)=C(I)/R
      WRITE(I1132,201)X(ICOUN),Y(ICOUN)
201   FORMAT(2X,F7.4,E12.4)
200   ICOUN=ICOUN+1
      L=M
      K=N
      M=K
      N=L-1
C
C     CALCULATE AND PRINT VERTICAL REGRESSION LINES
C
      WRITE(I1132,3000)PAGE,ID
3000  FORMAT(1H1,2X,'PAGE',I4,
      $'     ...ZIMM PLOTS...     ',
      $20A2,/,5X,'CONCENTRATION LINES',/)
      PAGE=PAGE+1
C
      DO 60 I=1,N
      K=(I-1)*M
      SXY=0.
      SX=0.0
```

```
      SY=0.0
      SXSQR=0.0
      SYSQR=0.0
      SXCUB=0.0
      SXFOR=0.0
      SXSQY=0.0
C
      DO 50 J=1,M
      L=K+J
      XX=X(L)
      XY=Y(L)
C
      SXY=SXY+XX*XY
      SX=SX+XX
      SY=SY+XY
      SXSQR=SXSQR+XX*XX
      SXCUB=SXCUB+XX**3
      SXFOR=SXFOR+XX**4
      SXSQY=SXSQY+XX*XX*XY
   50 SYSQR=SYSQR+XY*XY
C
C     CALCULATE PARAMETERS OF REGRESSION
C
C
C     CALCULATE SLP
C
      BB=(SY*SXSQR-M*SXSQY)*(SXCUB*M-SXSQR*SX)
      BB=BB-(SXY*M-SX*SY)*(SXSQR*SXSQR-SXFOR*M)
      BC=(SX*SXSQR-M*SXCUB)*(SXCUB*M-SXSQR*SX)
      BC=BC-(SXSQR*M-SX*SX)*(SXSQR*SXSQR-SXFOR*M)
      SLP(I)=BB/BC
C
C     CALCULATE CURV
C
      BS=SLP(I)
      BB=SY*SXSQR-M*SXSQY-BS*(SX*SXSQR-M*SXCUB)
      BC=SXSQR*SXSQR-SXFOR*M
      CURV(I)=BB/BC
C
C     CALCULATE INT
```

```
C
      BCR=CURV(I)
      INT(I)=(SY-BS*SX-BCR*SXSQR)/M
C
      SS1=SYSQR-(SY*SY/M)
      SS2=BS*(SXY-SX*SY/M)+BCR*(SXSQY-SXSQR*SY/M)
      CORR=SS2/SS1
      CORR=SQRT(CORR)
C
C     CALCULATE Y BY EXTRAPOLATION
C
      BIN=INT(I)
      BX=X2(I)
      EX2(I)=BIN+BS*BX+BCR*BX*BX
C
C     DISPLAY RESULTS
C
      WRITE(I1132,3001)I,INT(I),SLP(I),CURV(I)
60    WRITE(I1132,3030)CORR,X2(I),EX2(I)
3001  FORMAT(2X,'LINE',I3,'...Y=',F8.3,'+',F8.3,
      $'*X+',F8.3,'*X**2')
3030  FORMAT(12X,'CORRELATION COEFFICIENT=',F6.3,
      $'EXTRAPOLATION...X=',F6.3,'...Y=',F6.3)
C
C     CALCULATE AND PRINT HORIZONTAL REGRESSION LINES
C
      WRITE(I1132,3002)
3002  FORMAT(//,4X,'ANGLE')
C
      DO 80 I=1,M
      K=I+N+1
      SXY=0.0
      SX=0.0
      SY=0.0
      SXSQR=0.0
      SYSQR=0.0
C
      DO 70 J=1,N
      L=I+(J-1)*M
      XX=X(L)
      XY=Y(L)
```

```
C
        SXY=SXY+XX*XY
        SX=SX+XX
        SY=SY+XY
        SXSQR=SXSQR+XX*XX
70      SYSQR=SYSQR+XY*XY
C
C       CALCULATE PARAMETERS OF REGRESSION
C
        SLP(K)=(SXY-(SX*SY/N))/(SXSQR-(SX*SX)/N)
        INT(K)=SY/N-SLP(K)*SX/N
        CORR=(SXSQR-(SX*SX)/N)*(SYSQR-(SY*SY)/N)
        CORR=(SXY-(SX*SY)/N)/SQRT(CORR)
C
C       CALCULATE Y VALUE BY EXTRAPOLATION
C
        EX1(I)=SLP(K)*X1(I)+INT(K)
C
C       DISPLAY RESULTS
C
80      WRITE(I1132,3010)I,SLP(K),INT(K),CORR,X1(I),EX1(I)
3010    FORMAT(2X,'LINE',I3,'...Y=',F6.3,'*X+',F8.3,
        $'..CORRELATION COEFFICIENT=',F6.3,
        $'..EXTRAPOLATION..X= ',F6.3,'...Y= ',F6.3)
C
C       EXTRAPOLATED LINE - DOWN
C
        SXY=0.0
        SX=0.0
        SY=0.0
        SXSQR=0.0
        SYSQR=0.0
        SXCUB=0.0
        SXFOR=0.0
        SXSQY=0.0
C
        DO 90 I=1,M
        XX=X1(I)
        XY=EX1(I)
C
```

```
      SXY=SXY+XX*XY
      SX=SX+XX
      SY=SY+XY
      SXSQR=SXSQR+XX*XX
      SXCUB=SXCUB+XX**3
      SXFOR=SXFOR+XX**4
      SXSQY=SXSQY+XX*XX*XY
90    SYSQR=SYSQR+XY*XY
C
C     CALCULATE PARAMETERS FOR THIS LINE
C
      BB=(SY*SXSQR-M*SXSQY)*(SXCUB*M-SXSQR*SX)
      BB=BB-(SXY*M-SX*SY)*(SXSQR*SXSQR-SXFOR*M)
      BC=(SX*SXSQR-M*SXCUB)*(SXCUB*M-SXSQR*SX)
      BC=BC-(SXSQR*M-SX*SX)*(SXSQR*SXSQR-SXFOR*M)
      SLP1=BB/BC
C
      BB=SY*SXSQR-M*SXSQY-SLP1*(SX*SXSQR-M*SXCUB)
      CURV1=BB/(SXSQR*SXSQR-SXFOR*M)
C
      INT1=(SY-SLP1*SX-CURV1*SXSQR)/M
C
      SS1=SYSQR-(SY*SY/M)
      SS2=SLP1*(SXY-SX*SY/M)+CURV1*(SXSQY-SXSQR*SY/M)
      CORR=SS2/SS1
      CORR=SQRT(CORR)
C
C     DISPLAY RESULTS
C
      WRITE(I1132,3003)INT1,SLP1,CURV1,CORR
3003  FORMAT(//,2X,'EXTRAPOLATION LINES',//,5X,
      $'CONCENTRATION...Y=',F8.3,'+',F8.3,'*X +',F8.3,
      $'*X**2...CORRELATION COEFFICIENT=',F6.3)
C
C     EXTRAPOLATED LINE - ACROSS
C
      SXY=0.0
      SX=0.0
      SY=0.0
      SXSQR=0.0
```

```
      SYSQR=0.0
C
      DO 100 I=1,N
      XX=X2(I)
      XY=EX2(I)
C
      SXY=SXY+XX*XY
      SX=SX+XX
      SY=SY+XY
      SXSQR=SXSQR+XX*XX
100   SYSQR=SYSQR+XY*XY
C
C     CALCULATE LINE PARAMETERS
C
      SLP2=(SXY-(SX*SY)/N)/(SXSQR-(SX*SX)/N)
      INT2=SY/N-SLP2*SX/N
      CORR=(SXSQR-(SX*SX)/N)*(SYSQR-(SY*SY)/N)
      CORR=(SXY-(SX*SY)/N)/SQRT(CORR)
C
C     DISPLAY RESULTS
C
      WRITE(I1132,3004)SLP2,INT2,CORR
3004  FORMAT(11X,'ANGULAR...Y=',F6.3,'*X + ',
      $F8.3,'...CORRELATION COEFFICIENT =',F6.3)
      WRITE(I1132,3333)KIK
3333  FORMAT(//,15X,'X = SIN(THT/2)**2 + ',I6,'*C')
C
C     PREPARE DATA FOR ZIMMF SUBROUTINE
C
C     CALCULATE NO OF LINES
C
      NL=N+M+2
C
C     SET LIMITS XMIN AND XMAX FOR CONCENTRATION LINES
C
      DO 5050 I=1,N
      IA=I*M
      LIMIT(1,I)=X2(I)
5050  LIMIT(2,I)=X(IA)
      LI=N+1
```

```
      LIMIT(2,LI)=X1(M)
      CURV(LI)=CURV1
C
C     SET LIMITS FOR ANGLE LINES
C
      DO 5055 J=1,M
      JK=N+J+1
      IB=(N-1)*M+J
      LIMIT(1,JK)=X1(J)
5055  LIMIT(2,JK)=X(IB)
C
      JL=M+N+2
      LIMIT(2,JL)=X2(N)
C
C     SLOPES AND INTERCEPTS OF EXTRAPOLATION LINES
C     ENTERED
C
      SLP(LI)=SLP1
      SLP(JL)=SLP2
      INT(LI)=INT1
      INT(JL)=INT2
C
C     CALL SUBROUTINE TO PREPARE POINTS FOR PLTPT
C
      CALL ZIMMF(NL,LIMIT,SLP,INT,CURV,M,N)
C
C     PUNCH TAPE FOR USE WITH PLTPT
C
      WRITE(IPT,4040)
4040  FORMAT('// XEQ PLTPT')
      K=M*N
      WRITE(IPT,4003)(X(I),Y(I),I=1,K)
4003  FORMAT(2F6.3)
C
      WRITE(IPT,4003)(X1(I),EX1(I),I=1,M)
C
      WRITE(IPT,4003)(X2(I),EX2(I),I=1,N)
C
      WRITE(IPT,4004)
4004  FORMAT('99999.')
```

```
C
      WRITE(ICP,1002)ID
1002  FORMAT('POINT TAPE COMPLETED FOR SET',
      $20A2,/,'PUNCH BLANK TAPE AND REMOVE FROM',
      $' PUNCH')
C
      PAUSE
C
      CALL EXIT
      END
```

REFERENCES

1. Bibeau, A.A. and Matejevic, E., J. Colloid Interface Sci., 43, 330 (1973).

2. Vincent, B., Adv. Colloid Interface Sci., 4, 193 (1974).

3. Vold, M.J., J. Colloid Interface Sci., 16, 1 (1961).

4. Langbein, D., J. Adhesion, 1, 237 (1969).

5. Napper, D.H., J. Colloid Interface Sci., 58, 390 (1977).

6. Ruehrwein, R.A. and Ward, D.W., Soil Sci., 73, 485 (1952).

7. La Mer, V.K., Disc. Faraday Soc., 42, 248 (1966).

8. Fleer, G.J., Ph.D. Thesis, Agricultural University, Wageningen, 1971.

9. La Mer, V.K. et al., J. Colloid Interface Sci., 23, 465 (1967).

10. Gregory, J., Trans. Faraday Soc., 65, 2260 (1969).

11. Gregory, J., J. Colloid Interface Sci., 42, 448 (1973).

12. Black, A.P. and Vilaret, M.C., J. Amer. Water Works Assoc., 61, 209 (1969).

13. Iler, R.K., J. Colloid Interface Sci., 37, 364 (1971).

14. Nemeth, R. and Matejevic, E., Kolloid Z., 225, 155 (1968).

15. Sommerauer, A., Sussman, D.L. and Stumm, W., Kolloid Z., 225, 147 (1968).

16. Miller, I.R. and Grahame, D.C., J. Colloid Sci., 16, 23 (1961).

17. Vincent, B., Bysterbosch, B.H. and Lyklema, J., J. Colloid Interface Sci., 37, 171 (1971).

18. Sarkar, N. and Teot, A.S., J. Colloid Interface Sci., 43, 370 (1973).

19. Slater, R.W., Clark, J.P. and Kitchener, J.A., Proc. Brit. Ceram. Soc., 13, 1 (1969).

20. Michaels, A.S., Ind. Eng. Chem., 46, 1485 (1954).

21. Von Smoluchowski, M., Physik A., 17, 557, 585 (1916); Z. Phys. Chem., 92, 129 (1917).

22. Fuchs, M., Z. Phys., 89, 736 (1934).

23. Spielman, L.A., J. Colloid Interface Sci., 33, 562 (1970).

24. Honig, E.P., Roebersen, G.J. and Wiersema, P.H., J. Colloid Interface Sci., 36, 97 (1971).

25. Lips, A., Smart, C. and Willis, E., Trans. Faraday Soc., 67, 2979 (1971).

26. Oster, G., J. Colloid Sci., 15, 512 (1960).

27. Walles, W.E., J. Colloid Interface Sci., 27, 797 (1968).

28. Smellie, R.M. and La Mer, V.K., J. Colloid Sci., 13, 589 (1958).

29. Healy, T.W. and La Mer, V.K., J. Phys. Chem., 66, 1835 (1962).

30. Gregory, J., The Scientifc Basis of Flocculation, Ed. K.J. Ives, Sijthoff and Noordhoff (1978).

31. Clayfield, E.J. and Lumb, E.C., Macromolecules, 1, 133 (1968).

32. Fontana, B.J. and Thomas, J.R., J. Phys. Chem., 65, 480 (1961).

33. Frisch, H.L., Simha, R. and Eirich, F.R., J. Chem. Phys., 21, 365 (1953).

34. Simha, R. and Eirich, F.R., J. Phys. Chem., 57, 584 (1953).

35. Frisch, H.L. and Simha, R., J. Phys. Chem., 58, 507 (1954).

36. Higuchi, W.I., J. Phys. Chem., 65, 487 (1961).

37. Forsman, W.C. and Hughes, R., J. Chem. Phys., 38, 2130 (1963).

38. Silberberg, A., J. Phys. Chem., 66, 1872 (1962).

39. Di Marzio, E.A., J. Chem. Phys., 42, 2101 (1965).

40. Hoeve, C.A., Di Marzio, E.A. and Peyser, P., J. Chem. Phys., 42, 2558 (1965).

41. Hoeve, C.A., J. Polym. Sci., 30, 361 (1970).

42. Silberberg, A., J. Colloid Interface Sci., 38, 217 (1972).

43. Hesselink, J. Th., J. Electroanal. Chem. Interfacial Electrochem., 37, 317 (1972).

44. Passaglia, E. and Stromberg, R.R., Polym. Prepr. Amer. Chem. Soc., Div. Polym. Chem., 5, 508 (1964).

45. Gilliland, E.R. and Gutoff, E.B., J. Appl. Polym. Sci., 3, 26 (1960).

46. Stromberg, R.R., Tutas, D.J. and Passaglia, E., J. Phys. Chem., 69, 3955 (1965).

47. Rowland, F.W. et al., Ind. Eng. Chem., 57, 46 (1965).

48. Fontana, B.J. and Thomas, J.R., J. Phys. Chem., 65, 480 (1961).

49. Fleer, G.J., Koopal, L.K. and Lyklema, J., Kolloid z.z. Polym., 250, 689 (1972).

50. Herd, J.M., Hopkins, A.J. and Howard, C.J., J. Polym. Sci., 34, 211 (1971).

51. Petersen, C. and Kwei, T.K., J. Phys. Chem., 65, 1330 (1961).

52. Howard, G.J. and McConnell, P., J. Phys. Chem., 71, 2981 (1970).

53. Vincent, B., J. Colloid Interface Sci., 42, 270 (1973).

54. Parsegian, V.A. and Ninham, B.W., J. Colloid Interface Sci., 37, 332 (1971).

55. Vincent, B., Adv. Colloid Interface Sci., 4, 193 (1974).

56. Somasundaran, P., Chia, Y.H. and Gorelik, R., Polymer Adsorption and Dispersion Stability, Ed. Goddard, E.D. and Vincent, B., ACS Polymer Symposium Series 240, 1984, 393.

57. Dollimore, D. and Horridge, T.A., Trans. Brit. Ceram. Soc., 70, 191 (1971).

58. Pearse, M.J. and Barnett, J., Filtr. Separation, 17, 460 (1980).

59. Allied Colloids Pty. Ltd., Bradford, England, Private Communication.

60. Mitsui Cyanamid, Japan, Private Communication.

61. Dow Chemical Ltd., U.S.A., Private Communication.

62. Barber, W.A., Acrylamide, American Cyanamid Co., Wayne, N.J. (1957).

63. Collinson, E., Dainton, F.S. and McNaughton, G.S., Trans. Faraday Soc., 53, 489 (1957).

64. Fuoss, R.M. and Strauss, U.P., J. Polymer Sci., 3, 246 (1948).

65. Takahashi, A., Kamei, T. and Kagawa, I., Nippon Kagaku Zasshi, 83, 11, 14 (1962).

66. Sakamoto, R., Nippon Kagaku Zasshi, 83, 386, 512 (1962).

67. Klenina, O.V. and Lebedeva, L.G., Vysokomol. Soedin., Ser. A, 25 (10), 2053 (1983).

68. Strauss, U.P. and Ander, P., J. Phys. Chem., 66, 2235 (1962).

69. Vrij, A. and Overbeek, J. Th., J. Colloid Sci., 17, 570 (1962).

70. Zimm, B.H., J. Chem. Phys., 16, 1099 (1948).

71. Benoit, H., J. Polymer Sci., 11, 507 (1953).

72. Kato, T. et al., Polymer, 25, 218 (1984).

73. Weiss, A.R., Org. Coat., Appl. Polym. Sci. Proc., 48, 864 (1983).

74. Klein, J. and Westerkamp, A., J. Polym. Sci., Polym. Chem. Ed., 19, 707 (1981).

75. Bain, D.R. et al., J. Colloid Interface Sci., 88, 467 (1982).

76. Langley, J., Private Communication.

77. Zurimendi, J.A., Guerrero, S.J. and Leon, V., Polymer, 25, 1314 (1984).

78. Panzer, H.P., Halverson, F. and Lancaster, J.E., Poly. Mater. Sci. Eng., 51, 268 (1984).

79. Inoue, Y., Fukutomi, T. and Chujo, R., Polymer J., 15, 103 (1983).

80. Muller, G., Fenyo, J.C. and Selegny, E., J. Appl. Polym. Sci., 25, 627 (1980).

81. Basedow, A.M., Ebert, K.H. and Hunger, M., Makromol. Chem., 180, 411 (1979).

82. Abdel-Alim, A.H. and Hamielec, A.E., J. Appl. Polym. Sci., 17, 3769 (1973).

83. Saito, T. and Matumura, O., Japan, J. Appl. Phys., 22, 1310 (1983).

84. Bennett, M.C., Internat. Sugar J., 61, 77 (1959).

85. Whayman, E., Unpublished data.

86. Von Smoluchowski, M., Phys. Z., 17, 557 (1916).

87. Bennett, M.C. and Ragnauth, J.M., Internat. Sugar J., 62, 13 (1960).

88. Briggs Bonneville, A., Sugar, 48, 36 (1953).

89. Sockhill, B.D., Proc. Qld. Soc. Sugar Cane Technol., 22, 259 (1955).

90. Hale, D.J. and Whayman, E., Proc. Qld. Soc. Sugar Cane Technol., 37, 243 (1970).

91. U.S. F. & D.A., 21 CFR 173.5 (1984).

92. Higuchi, M. and Senju, R., Polymer J., 3, 370 (1972).

93. Kenyeres, J.S. and Ursu, V., J. Polym. Sci., Polymer Chem Ed., 18 (1), 275 (1980).

94. Norris, M.V., Encyclopedia of Industrial Chemical Analysis, 4, 168.

95. Fenyo, J.C., Laine, J.P. and Muller, G., J. Polym. Sci., Polymer Chem. Ed., 17, 193 (1979).

96. Quantitative Inorganic Analysis, Ed. A.I. Vogel, Longmans, 1951, 482.

97. A.S.T.M. Method D1013-70.

98. Terayama, H., J. Polymer. Sci., 8, 243 (1952).

99. Williams, D.J.A. and Ottewill, R.H., Kolloid z.z. Polym., 243, 141 (1971).

100. Principles of Polymer Chemistry, Ed. P.J. Flory, Cornell University Press, New York, 1953.

101. Huggins, M.L., J. Amer. Chem. Soc., 64, 2716 (1942).

102. Simha, R., J. Appl. Phys., 23, 1020 (1952).

103. Cheng, P.Y. and Schachman, H.K., J. Polymer Sci., 16, 19 (1955).

104. Crees, O.L. et al., Proc. Qld. Soc. Sugar Cane Technol., 40, 239 (1973).

105. Lord Rayleigh, Phil. Mag., 41, 447 (1871).

106. Lord Rayleigh, Proc. Royal Soc., A84, 25 (1910).

107. Lord Rayleigh, Proc. Royal Soc., A90, 219 (1914).

108. Lord Rayleigh, Proc. Royal Soc., A94, 296 (1918).

109. Debye, P., Ann. Physik, 46, 809 (1915).

110. Smoluchowski, M., Phil. Mag., 23, 165 (1912).

111. Einstein, A., Ann. Physik, 33, 1275 (1910).

112. Debye, P. J. Appl. Phys., 15, 338 (1944).

113. Guinier, A., Ann. Physik, 12, 161 (1939).

114. Zernike, F., Arch. Neerl. Sci., III A, 74 (1918).

115. Kirkwood, J.G. and Goldberg, R.J., J. Chem. Phys., 18, 54 (1954).

116. Cassara, E.F. and Eisenberg, H., J. Phys. Chem., 64, 753 (1960).

117. Mysels, K.J., J. Colloid Sci., 10, 507 (1955).

118. Cabannes, J., La diffusion moleculaire de la lumiere, Presses Universitaires de France, Paris (1929).

119. King, L.V., Proc. Royal Soc., A104, 333 (1923).

120. Coumou, D.J., J. Colloid Sci., 15, 408 (1960).

121. Brinton, C.C. and Lauffer, M.A., 'Electrophoresis: Theory, Practice and Applications', ed. Bier, M., Academic Press (1959).

122. 'Interfacial Phenomena', Davies, J.T. and Rideal, E.K., Academic Press (1961).

123. Slater, R.W. and Kitchener, J.A., Disc. Faraday Soc., 42, 267 (1966).

124. Linke, W.F. and Booth, R.D., Trans. Amer. Inst. Min. Metal. Eng., 217, 364 (1969).

125. Attia, Y.A. and Rubio, J., Br. Polym. J., 7, 135 (1975).

126. Crummett, W.B. and Hummel, R.A., J. Amer. Water Works Assoc., 55, 209 (1963).

127. Black, A.P., Birkner, F.B. and Morgan, J.J., J. Amer. Water Works Assoc., 57, 1547 (1965).

128. Domasch, K., Wasserwirtschaft-Wassertechnik, 33, (11), 380 (1983).

129. Packham, R.F., Proc. Soc. Water Treatment, 16, 88 (1967).

130. Laboratory Manual for Queensland Sugar Mills, 5th Edition, Bureau of Sugar Experiment Stations, Brisbane, 1970.

131. Hen, J., J. Colloid Interface Sci., 49 (3), 425 (1974).

132. Homola, A. and James, R.O., J. Colloid Interface Sci., 59 (1), 123 (1977).

133. Stone-Masui, J. and Watillon, A., J. Colloid Interface Sci., 52 (3), 479 (1975).

134. Labib, M.E. and Robertson, A.A., J. Colloid Interface Sci., 77 (1), 151 (1980).

135. Harding, I.H. and Healy, T.W., J. Colloid Interface Sci., 89 (1), 185 (1982).

136. Hearn, J., Ottewill, R.H. and Shaw, J.N., Brit. Polymer J., 2, 117 (1970).

137. Crees, O.L., B.Sc. (Hons) Thesis, James Cook University, 1971.

138. Hidi, P., Proc. Inter. Soc. Sugar Cane Tech., 13, 1736 (1968).

139. Bennett, M.C. and Ragnauth, J.M., Inter. Sugar J. 62, 13 (1960).

140. Bennett, M.C., Inter. Sugar J., 61, 77 (1959).

141. Van Wazer, J., Phosphorus and its compounds, Interscience, N.Y. (1958).

142. Foster D.H., unpublished data.

143. Kynch, G.J., Trans. Farsday Soc., 48, 166 (1952).

144. Solid-Liquid Separation, ed. L. Svarovsky, Butterworths (1981) p248.

145. Thomas, W.M., Encycl. Polym. Sci. Technol., ed. Mark, H.F. et. al, Interscience, N.Y., 1, 182 (1964).

146. Riess, G. and Callot, P., Fractionation of Synthetic Polymers, ed. L.H. Tung, Marcel Dekker, New York, 1977.

147. Bain, D.R., Cafe, M.C., Robb, I.D. and Williams, P.A., J. Colloid Interface Sci., 88 (2), 467 (1982).

148. Klein, J and Westerkamp, A., J. Polym. Sci., Polymer Chem Ed., 19, 707 (1981).

149. Crees, O.L., M.Sc. Thesis , Univ. of Bristol, 1974.

150. Tanford, C. The Physical Chemistry of Macromolecules, Wiley, New York, 1961.

151. Gundert, F. and Wolf, B.A., Makromd. Chem., 187, 2969 (1986).

152. Halverson, F., Lancaster, J.E. and O'Connor, M.N., Macromolecules, 18 (6), 1/39 (1985).

153. Panzer, H.P., Halverson, F. and Lancaster, J.E., Polymer Mater. Sci. Eng., 51, 268 (1984).

154. Randall, J.C., Polymer Sequence Determination, Academic Press, N.Y., 1977.

155. Encyclopedia of Polymer Sciences and Technology ed. H.F. Mark, N.G. Gaylord and N.M. Bikales, Wiley, New York, 1964.